A THREE-DIMENSIONAL STUDY OF PILLAR STRESSES IN MINES WITH IRREGULAR MINING BOUNDARIES

by

B. B. Dhar

ABSTRACT

This study is concerned with the prediction of pillar stresses with irregular room and pillar geometry in elastic ground. A three-dimensional analytical approach based on mine simulation by models has been developed.

An electrolytic tank is used as an analogue to calculate the elastic displacements due to excavations. The analogue has provided a prediction of displacements which can be related to stresses.

The calculated pillar stresses show that it is possible to predict the variation of pillar loading: with location of the pillar within the mining zone, with the variation of the pillar height, with the variation of the pillar breadth, with the variation of the elastic properties of the pillar rock with respect to wall rock and, above all, with the extraction ratio.

The results obtained are compared with other analytical approaches and field measurements.

The model study has been further extended to analyse the abutment stresses induced by varying the geometry of the mining outline.

A THREE-DIMENSIONAL STUDY OF PILLAR STRESSES IN MINES

A THREE-DIMENSIONAL STUDY OF PILLAR STRESSES IN MINES WITH IRREGULAR MINING BOUNDARIES

A THREE-DIMENSIONAL STUDY OF PILLAR STRESSES IN MINES WITH IRREGULAR MINING BOUNDARIES

by

B. B. Dhar

A thesis submitted to the Faculty of Graduate Studies and Research in partial fulfillment of the requirements for the degree of Doctor of Philosophy.

Department of Mining Engineering
and Applied Geophysics
McGill University
Montreal Canada.

February 1970

PREFACE

This thesis is concerned with scientific theory and broadening of the analytical base in certain practical problems, facing a Mining Engineer. This broadening of the analytical base has made it possible to design a pillar support, based on rational coefficients, derived from three-dimensional test work. With minor exceptions earlier studies (9,10) of this nature were limited to two-dimensions.

Rock mechanics develops from extending the analytical methods of soil mechanics into the range of the mathematical theory of elasticity. Perfect elasticity is a theoretical condition. Rocks and rock masses comply with very wide strength standards and thus wider variations in elastic behaviour are to be expected than will be apparent with materials meeting standard requirements. This limitation applies less with strength of materials procedures and others which relate to materials having a closer approximation to elastic behaviour.

Generally, while accepting this limitation, there is sufficient elasticity in rocks and rock masses to permit their study in that context. The electrolytic tank is a tool in this process.

The original contribution in this work in the field of rock mechanics, is related to the design of pillars. Pillar design procedure usually consists of three steps: the determination of the pillar loading (average pillar stresses), the determination of the pillar strength and the influence of these two elements on the sequence of mine operation.

This thesis claims the development of a three-dimensional analysis to predict pillar stresses within irregular mining boundaries. The approach is based on mine models, using an electrical analogue. The method is valid for both horizontal and inclined tabular orebodies.

The thesis consists of: the development of an analytical solution for predicting pillar loads, the theory and the construction of the electrical analogue, and the analysis of the predicted data. The comparison of this data with in situ measurements of pillar loadings and two-dimensional analytical data establish the validity of the procedures developed.

ACKNOWLEDGEMENTS

The author wishes to express his great appreciation to the Director of this research project, Professor D.F. Coates, for his invaluable criticism, suggestions and encouragement throughout the progress of this project. He is also indebted to Professors F.T.M. White, Chairman of the Department of Mining Engineering and Applied Geophysics, and Professor J.E. Schwellnus for their interest in the problem and numerous suggestions.

He is particularly grateful to Professor R.G.K. Morrison for assistance in the arranging of data and the preparation of the thesis.

Professor J.E. Udd of this Department and Mr. S.K. Mahajan, a graduate student in the Department of Geology were helpful in many ways.

Mr. W.D. Ortlepp of East Rand Proprietary Mines, Ltd., Transvall, South Africa, provided valuable information regarding the electrical analogue.

Mr. W.J. Doig, Technican, Department of Geology (formerly with Mining Department) was most helpful with his constant cooperation in the design and construction of the electrical analogue.

The National Research Council of Canada and the Department of Energy, Mines and Resources, Ottawa provided financial assistance and the latter permitted the use of their electronic equipment.

Finally, I must acknowledge the patience and understanding of my wife, who was a power of strength during the preparation of this work.

CONTENTS

NOTATIONS

A_T - area of walls adjacent to the entire mining zone

A_p - area of the pillar parallel to the walls

B - breadth of the pillar (average)

E - modulus of linear deformation of the wall rock

E_p - modulus of linear deformation pillar rock

EA - total excavated area in a reef plane

h - semi-height of a pillar (H/2)

H - height of pillar

H' - mean height between top and bottom electrodes

i - dip of the deposit with the horizontal

k - S_t/S_o or σ_h/σ_v (ratio between horizontal and vertical field stress)

ℓ - semi-span of the mining zone ($L/2$)

L - breadth of the mining zone (or total span of the mining zone)

psi - pounds per square inch

P - a pillar load

R - extraction ratio (wall area excavated/over total wall area)

S - scale factor (Mine/model)

S_h - field stress in the horizontal direction

S_t - field stress parallel to the seam or reef and normal to strike

S_v - field stress in the vertical direction

S_o - field stress normal to the seam or reef

S_p - average pillar stress on walls (ΣP/area of the walls tributary to the pillar)

S_x - field stress in the x-direction(or parallel to strike of the seam or reef)

S_y - field stress in the y-direction

S_z - field stress in the z-direction

TA - tributary area

V_1 - applied voltage to the bottom electrode of the tank

V - measured voltage in the working area of the top electrode

Z - depth of the horizontal seam or reef below the surface

x,y,z - the rectangular coordinate system of the mine

X_1, Y_1, Z_1 - the rectangular coordinate system of the tank

μ - Poisson's ratio of the wall rock

μ_p - Poisson's ratio of the pillar rock

σ_p - pillar stress (P/A_p)

σ'_p - σ_p/S_o

$\bar{\sigma}_p$ - average pillar stress ($\Sigma P/\Sigma A_p$)

$\Delta\sigma_p$ - increase in the pillar stress due to mining

$\Delta\sigma'_p$ - $\Delta\sigma_p/S_o$

σ_1 - major principal stress

σ_2 - intermediate principal stress

σ_3 - minor principal stress

ΔEA - an element of excavated area in a reef plane

δ' - reverse displacement (or deflection) due to the average pillar pressure

δ_p - net displacement of the pillar

$\Delta\delta_p$ - increase in the pillar displacement

δ_e - displacement (or deflection) of the walls due to excavation

δ'_p - local penetration of the pillar due to the increase in the pillar stress, $\Delta\sigma_p$

δ_r - displacement (or deflection) of the pillar due to release of side constraint due to mining

δ_z - the convergence (or normal closure)

δ_m - the maximum normal closure (i.e. width between hanging wall and footwall)

δ_u, δ_v - the ride (horizontal) components in the x and y directions respectively due to the normal closure

δ_w - the (vertical) component of the normal closure along z-axis, normal to the walls

$\delta_{wx}, \delta_{ux}, \delta_{vx}$ - displacement components due to RIDE in x-direction (in inclined deposits)

$\delta_{wy}, \delta_{uy}, \delta_{vy}$ - displacement components due to RIDE in y-direction (in inclined deposits)

$\delta_W, \delta_U, \delta_V$ - the net displacement components in z,x and y directions respectively due to normal closure and the Ride in x and y directions respectively

$\emptyset$ - the position factor in a three-dimensional case

I - the shape factor of pillar in a three-dimensional case.

LIST OF ILLUSTRATIONS

INTRODUCTION

Since prehistoric times pillars of ore in place have constituted a logical and usually effective method of support. Problems arise with such support due to the loading of the pillars and the ability of the pillars to carry the load.

Pillars are described by Morrison, as ground subjected to significant superimposed stress fields. If abutments are regarded as one extreme in this spectrum, then pillars can be thought of as being rock structures isolated on two, three or four sides and acute angled projections into the stoping area. For present purposes the dimensions of pillars are defined as follows; length and breadth are respectively the greatest and least dimensions in the plane of the lode. Width, thickness or height is the dimension from hanging to footwall or roof to floor (75).

In the case of structures where geometry of the opening can be simply defined mathematically, a theoretical treatment of both strength and stress is possible. In metal mining the geometry is often complex. In such cases the design procedure might be based on laboratory testing of the material concerned and analogue testing for stress analysis. Experience has demonstrated the effective use of such approaches in other complex fields of structural mechanics.

In recent years substantial progress has been made in the study of loading and strength of pillars in plastic ground, such as salt and potash (1,2). Here it would appear that measurements can be extrapolated to give reasonably predictable estimates of closure on a time basis. In harder, brittle rocks the situation is less satisfactory. Research is concentrating on the problem but, for the time being, it must be conceded that science has not yet displaced empiricism.

Varying degrees of elasticity are present in the rock substance of the harder rocks and thus elasticity can be considered applicable to the rock mass. This permits the use of the mathematical theory of elasticity in problems connected with the mining of many types of mineral deposits. However, it might not be available to describe the stress displacements in a rock mass that is fractured. Also the theory disregards the possible time dependency of stress and displacements.

The design of pillars requires, at least, a theoretical value for the stress concentrations that actually occur in the rock mass. Such values, in a large measure have been established by both laboratory and field tests.

Stress analysis and the testing of rocks for design purposes also requires some knowledge of strength parameters. This unfortunately is difficult to obtain as it involves relating the strength of the rock substance to that of the rock mass (77) with

its complex structural features. An important aspect to be considered in the case of pillars, used for support, is the determination of the total load rather than the detailed stress distribution. This implies that the average stress may be a more significant parameter for pillar failure than the stress concentration at the surface of the pillar.

Furthermore, the pillar displacements should be a function of load (average stress) to a larger extent than of the stress concentrations. The displacements of the pillar should have a close relationship to the range of stability for the pillar.

Bearing in mind the structural distinction between the substance and the mass a new hypothesis for pillar loading has been advanced by Coates (10). It is based on the assumption that the pillar displacement is a function of average stress rather than the effect of stress concentrations near the surface of the openings.

Coates' approach has inspired the present work which extends his two-dimensional hypothesis to three-dimensions and includes the effects of irregular mining boundaries.

In field theory (steady state), heat flow, electricity and elasticity all conform with Laplace's equation. Utilizing the analogy of potential in electricity and displacement in elasticity, we can obtain a measure of displacement between two points in a model by measuring the potential. The electrolyte tank, concerned

with displacements, has been developed as an analogue for the mathematics of elasticity. To extend the research of earlier investigations such a tank has been erected and used in this study. The tank provides results in three-dimensions when most other methods are confined to two.

CHAPTER I

THE STATE OF PRESENT KNOWLEDGE

The pillar loading problem, in mining, has been investigated by various authors in the past. Such studies however, have concentrated on coal pillars, probably because the room-and-pillar mining practice is most common in the coal industry. These studies have suggested that the average loads the pillars could carry were related to the crushing strength of a specimen of coal with the width to height ratio of the pillar.

An early expression to calculate the average load (psi) that a coal pillar in a flat seam can support is given below (3)

$$S = C\sqrt{W/T}$$

where S is the average load that can be safely supported, C is the laboratory crushing strength (psi) of a sample having a width to height ratio of 1.0 and adjusted by a suitable factor of safety (4 to 6 normally used for anthracite mining), W the least dimension of pillar in the plane of the seam (in feet) and T, the height of the pillar in feet.

Greenwald, Howarth and Hartmann (4) give a relationship between strength of square pillars and the square-root of their ratios of lateral dimension to height. This relationship was expressed mathematically as,

$$S = K\sqrt{R}$$

where S is the crushing strength, K is a constant and R is the ratio of the lateral dimension to height. The factor K was calculated in the field on a cubical test pillar by measuring the crushing strength S. The value of K thus obtained was used to calculate the crushing strength of other pillars in the mine. Their study was further extended (5) to develop a general equation applicable to all the square pillars in the Pittsburgh coal bed and such other beds as may have similar physical characteristics. The expression is

$$S = 2800 \frac{\sqrt{W}}{\sqrt[6]{h^5}}$$

where W is the width and h is the height of the pillar (wall to wall), both in inches. Such an expression gives the strength of the coal bed only and does not take into consideration the strength of the roof or floor of the seam.

Later, based on laboratory experiments on coal specimens and the field study of coal pillars supporting loads for upto 40 years, an equation was suggested by Holland and Gaddy (7) to calculate the ultimate strength of coal pillars. The equation is

$$S = \frac{K\sqrt{L}}{T}$$

where S is the ultimate strength of coal pillar in psi, K is the coefficient depending on coal bed, L is the least breadth of the pillar in inches and T is the thickness of the pillar in inches. This study was extended and discussed by Holland (8). He also suggested that the actual pillar size to be used to support the load depends on

loading conditions which will influence the strength of the pillars. Besides this his finding was, that as the breadth of the pillar is increased there is a little decrease in the maximum stress but a significant change in the stress distribution in the pillar.

Salamon (71) has recently suggested a method for designing bord and pillar workings based on a statistically derived pillar strength formula. His formula, given below, for calculating the strength of coal pillars is based on pillars that are square in the plane of the seam,

$$\text{Strength} = 1320 \frac{w^{0.46}}{h^{0.66}}$$

where, w is the width of the pillar and h is the height of the pillar, both in feet.

The results of these calculations have been given in a nomogram. The method is applicable to South African mines.

All the expressions thus far are based on the strength of the pillar.

The formula given below suggested by Steart (6) introduces the so-called tributary concept for estimating the stress in coal pillars,

$$P = 160 \, D \times A/a$$

where P is the stress in pillars per square foot, D is the depth of the coal seam in feet and A is the area in square feet enclosed with bords (centre to centre) and a is the area of the coal pillars in square feet. The factor of 160 in the above expression was selected as a pressure of 160 pounds per square foot, per foot depth in the South African Coal Seams.

Experimental Approach: Duvall's (9) method also depends upon the tributary area. It was designed to calculate the average pillar stress in horizontal deposits under a vertical compressive load. For a long mining zone, which is a two dimensional case, the average pillar stress is given by the following equation,

$$\frac{\sigma_p}{S_o} = \frac{1}{1-R} \qquad (1\text{-}1)$$

where, σ_p is the average pillar stress, S_o is the field stress normal to the deposit and R, the extraction ratio. The percentage recovery in terms of the breadth of the opening B_o, and breadth of the pillar B is equal to $[B_o/(B_o+B)] \times 100$. Therefore,

$$\frac{\sigma_p}{S_o} = \frac{100}{100 - [B_o/(B_o+B)] \times 100} \qquad (1\text{-}1(a))$$

Equation (1-1(a)) in terms of N, the number of pillars, can also be written as (10):

$$\frac{\sigma_p}{S_o} = \frac{R}{1-R} \frac{N}{N+1} + 1 \qquad (1\text{-}1(b))$$

when $N \rightarrow \infty$

$$\frac{\sigma_p}{S_o} \rightarrow \frac{1}{1-R}$$

However, when N is small, Equation (1-1(b)) gives an answer that is not seriously in error with respect to theory. It has therefore been suggested by Coates (10) that the formula be expressed in the following form,

$$\frac{\Delta\sigma_p}{S_o} = \frac{R}{(1-R)(1+1/N)}$$

and

$$\frac{\sigma_p}{S_o} = \frac{\Delta\sigma_p}{S_o} + 1 \qquad (1\text{-}1(c))$$

and be referred to as the Tributary area (TA) method.

This method generally disregards the effect of geometry such as the span or the breadth of the mining zone with respect to its depth, for horizontal workings, or the height and the location of the pillar within the mining zone. Neither does it provide for the actual field stress, in particular the magnitude of the component parallel to the breadth of the mining zone, nor for a difference in the modulus of deformation of the pillar rock relative to that of the wall rock. It may thus be said that such an approach was the first simple approximation for calculating average pillar loads in horizontal deposits worked on room and pillar geometry.

Other workers (11,12,13) have attempted to relate pillar loads to certain geometrical factors and rock properties. Denkhaus (14) reviewing the pillar loading problem has shown that the only general analytical expression for predicting pillar loading was based on Tributary Area. This was further confirmed by Coates (10) in 1965.

Photoelastic studies have been conducted by various authors (9,15,16). These have confirmed the expected stress distributions wherever comparison was possible. An interesting study (17) was made on gelatine model pillars, where the dip of the seam varied

from 0 degrees to 90 degrees. Such a study was used to calculate the average normal and tangential stresses by simple approximations.

Field Measurements: The stress measurements in the field have been of great interest in recent years, a variety of methods have been studied and progress has been made in stress measuring techniques. Methods have been designed to measure the magnitude of such stresses. The problem is complicated by the heterogeneity of the rock mass and results are still short of universal acceptability.

Obert (18,19), Potts (57), May (58), Hast (59), Obert, et.al. (61,72), Jeager (62) etc. have studied various types of stress measuring instruments and their use.

Leeman (63) has reviewed most of the techniques available to date. He also has developed a borehole strain gauge device which can be used for borehole depths upto 200-300 feet.

An early attempt to measure the pillar stresses in the field was made by Obert (18,19), based on measuring the velocity of sound through the pillars. The velocities thus obtained were compared with the velocities obtained on small samples of the rock from the pillars. However, it was found that the readings obtained from any two pairs of holes in the pillars and the average velocity obtained on the test specimens at zero stress were all equal, within the range of experimental error. These results indicated that the stress difference were not of sufficient magnitude to be measured by this technique.

Mohr (20) attempted to measure pillar stresses in a potash mine by cementing two unidirectional electrical resistance strain gauges at right angles to each other at the end of a borehole. The end of the borehole was then stress relieved by overcoring. The change in the strain resulting from overcoring was assumed to be a measure of normal stress at that point. This method was used in pillars at a depth of 429 meters and two sets of measurements made, one set of measurements produced an average vertical stress of 142 ksc and the horizontal stress of 102 ksc and the other set of readings produced a vertical and horizontal stress of 96 ksc and 59 ksc respectively. Another set of readings in a pillar at a depth of 498 meters, using the same method produced a vertical stress of 96 ksc and a horizontal stress of 45 ksc.

These observations of pillar measurements (20) seem to be of questionable value, as it can be seen that the calculated overburden stress in the second and third set of observations above must have been 103 ksc and 120 ksc respectively, which is greater than the measured stress of 96 ksc. However, at that time the techniques of measuring field stresses were quite new and since then much progress has been made.

A borehole deformation meter was used (21) in measuring stresses in coal pillars. Pillar strain measurements have been made (22) during the pillar recovery operation; also the effect of cave-line approaching towards instrumented pillars was studied. The latter study showed that the vertical strain decreased as the cave-line was nearing the

instrumented stations. Thus the span of working has an effect on pillar strain.

Pillar stress measurements were recently made in a uranium mine (40) using a borehole deformation meter developed by the U.S. Bureau of Mines (61). Such a study showed no correlation between the pillar stresses and depth but a rough correlation existed between the breadth of the pillars and the pillar stresses. However, the phenomenon of discing was observed in same boreholes which is attributed to the high stress concentrations.

Later, at the same mine, pillar stresses were measured (64) using the so called Strain Cell containing electrical resistance strain gauges (63). Both these methods showed the same general variation between the major and minor principle stresses, which is a good indication of the reliability of the two instruments.

Analytical Approach: It seems that approaches to pillar loading have been mostly empirical. A comprehensive theory for the prediction of pillar loads has been advanced by Coates (10). He predicts the increase in pillar stress from the net displacements at the pillars, as a result of mining. This includes most of the geometrical properties such as the location of the pillar within the mining zone, the normal and tangential components of field stresses, the height and the breadth of the pillar and deformation properties of the material, both pillar rock and the wall rock. Such a result is more comprehensive than is possible with the tributary area method. However, it is essentially a two dimensional approach and as such it disregards the effect of variation of geometry in the third direction.

Coates' theory was developed by establishing the displacement equations for a long, broad opening in an infinite elastic medium. The general solution depends upon the derivation of the equations initially for the individual displacement components.

Based on these displacement components and the related material properties, a hypothesis has been put forward for predicting pillar stresses. The equation thus established predicts the increase in pillar stresses due to mining. This equation for long and deep mining zones is given below for ready reference, and will in future be referred to as the Coates' Hypothesis.

$$\frac{\Delta\sigma_p}{S_o} = \frac{2R-((kh'(1-\mu)(\sqrt{1-x^2})) + h') - \mu_p(k\,h'E/E_p)}{h'E/E_p + \pi(1-R)(1-1/N)(1+ h/\sqrt{1-x^2})/2 + Rb\ (1-\mu)\pi} \qquad (1\text{-}2)$$

where $\Delta\sigma_p$ = the increase in pillar stress resulting from mining

R = extraction ratio (wall area excavated/total wall area)

S_o = field stress component normal to the vein or seam

S_t = field stress component parallel to the dip of the vein

$k = S_t/S_o$

h = semi-height of the pillar = H/2

ℓ = semi-span of the mining zone = L/2

$h' = h/\ell$

μ = Poisson's ratio of the wall rock

μ_p = Poisson's ratio of the pillar rock

E = modulus of deformation (linear) of the wall rock

E_p = modulus of deformation (linear) of the pillar rock

x' = linear displacement in the x direction

$x = x'/\ell$

N = number of pillars

B = average breadth of the pillars

$b = B/\ell$

The empirically modified form of Equation (1-2) in terms of the plane strain (23) is given below.

$$\frac{\Delta\sigma_p}{S_o} = \frac{2R(1-x/5+h') - kh'(1-W-W_p n)}{h'n+1.8(1-R)(1+1/N)(1+h'/(1-x/5))+2R\ b(1-W)/\pi} \qquad (1\text{-}2(a))$$

where

k = S_t/S_o, the ratio of transverse to normal field stress,

W = $\mu/(1-\mu)$, and μ is the Poisson's ratio of the wall rock

W_p = is the same parameter for wall rock

n = M/M_p and $M = E/(1-\mu^2)$, with E being the modulus of deformation of the wall rock and M_p being same parameter for pillar rock,

other terms are as in Equation (1-2).

A similar expression was derived for shallow mining zones (10,23).

Coates' hypothesis, when compared with laboratory investigations, field observations and with the tributary area theory appears to be the most reliable two-dimensional approach. However, an underground pillar layout represents a three dimensional problem. The present study has been undertaken to find an analytical solution in three dimensions for pillar loading within irregular mining boundaries.

Analytical and Experimental Study of Abutment Stresses: Earlier stress measurements (59) have shown the stress concentration in the abutment zones. Analytically the stresses in depth beyond the opening have been calculated and plotted (65) based on the simple analogy of a stoping cross-section and an ellipse. Later in 1966 (66) the stresses in depth were calculated and plotted by simulating cross-sections with ovaloidal openings.

A recent review of the stresses in depth around ovaloidal and elliptical openings has been provided (67) for a wide range of variables. This study is two-dimensional but provides good insight on the so called abutment stress problem.

Such studies have shown that the stress concentrations beyond the surface of the opening fall rapidly till they approach the field value. A similar observation was made in 1898 by Kirsch (68) while studying the openings of circular cross-section.

The present study concerns itself with the prediction of pillar and abutment stresses (in a tabular orebody) based on a three-dimensional approach. In this study measurements of stresses in the field are examined for their confirmation of or deviation from the values predicted by this approach. The geology of the areas pose some difficulties in simulating the actual field conditions.

CHAPTER II

The Three-Dimensional Method

Introduction: Any mining opening for the purpose of stress measurements, represents a three-dimensional problem. For the present study a typical room and pillar geometry will be considered.

In the previous review, theoretical and empirical studies regarding pillar loading are confined to the two-dimensional approach. Problems dealing with the stress distribution around multiple three-dimensional openings have not been treated theoretically because of mathematical complexity. Even very little information is available from the three-dimensional photoelastic model studies.

It has been established theoretically and experimentally that with increasing extraction the average pillar loading approaches the maximum until at high extraction ratios the average stress approximates the maximum stress (72). The limiting condition is usually the strength of the pillar.

Thus the problem that must be solved in connection with pillars is the determination of total load any pillar has to sustain in the course of mining. The analysis of pillar load, therefore, should be based on the three-dimensional concept.

The problem of predicting pillar loads for a three-dimensional case can be achieved, by modifying the existing two-dimensional solutions with data obtained from model studies.

Based on the assumption that the structural conditions are uniform pillar loads depend mainly upon two fundamental factors - the pre-mining stress and the geometry of the openings.

This study is confined to conditions analogous to a tabular orebody in an infinite elastic medium. Normal displacements must be determined that reflect the effect of mining in the whole reef plane.

The components of wall displacements as described by Coates (10) are:

1. The inward movement due to the excavation of the ground, which is equivalent to applying a stress inwards on the walls. Let this inward movement be denoted by "δ_e" .

2. The average reverse displacement as a result of increase in the pillar stress. Let this be denoted by "δ' ".

3. The displacement that results from eliminating the side constraint on the pillar due to mining. Let this be denoted by "δ_r".

4. The local penetration of the pillars that results from the concentration of the average wall pressure. Let this be denoted by "δ'_p".

These components of displacement have been derived (10) for the two-dimensional case. To extend them for the three-dimensional case requires several adjustments, including the determination of the position factor, $\emptyset$, which in turn is related to the normal displacement, δ_w.

The factor $\emptyset$, is a function of the dimensions of the mining zone in the reef plane and δ_w, is the component of the normal closure along z-axis and normal to the walls.

These adjustments and the derivation of the position factor, $\emptyset$, to establish a general solution for predicting pillar loads are as follows.

Displacement of walls due to Excavation: The vertical displacement of walls, δ_e, in a long mining zone has been established (10) in terms of the internal traction, S'_i, for a two-dimensional case (Figure 2-1(a)).

$$\delta_e = \frac{2 S'_i \ell \sqrt{1-x^2}}{E} \qquad (2\text{-}1)$$

where ℓ is the semi-span of the mining zone, E is the modulus of elasticity and x is the dimensionless ratio of x'/ℓ, where x' is distance from the centre of the mining zone in x-direction.

Equation (2-1) can be extended to a three-dimensional case by introducing $\emptyset$, a position factor. The position factor is a function of the dimensions of the mining zone in the reef plane. Therefore,

$$\delta_e = \frac{2 S'_i \ell}{E/(1-\mu^2)} \emptyset \qquad (2\text{-}1(a))$$

where in a three-dimensional case, ℓ is equivalent to the semi-span for the plane strain solution (i.e. $E \rightarrow E/(1-\mu^2)$).

The internal traction, $S'_i = S_o A_o / A_T = S_o R$, where A_o is the wall area exposed by mining, A_T is the total wall area adjacent to the mining zone, S_o is the normal component of the field stress and R is the extraction ratio. Substituting for S'_i in Equation (2-1(a)), we have

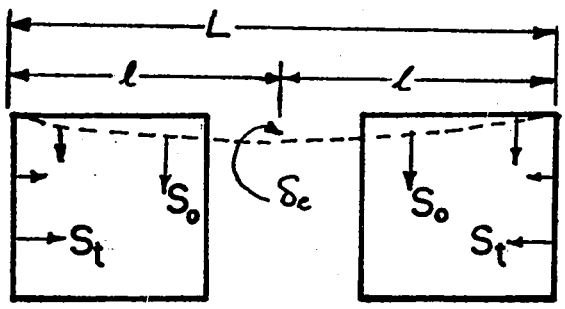

(a) DISPLACEMENT OF WALLS DUE TO EXCAVATION

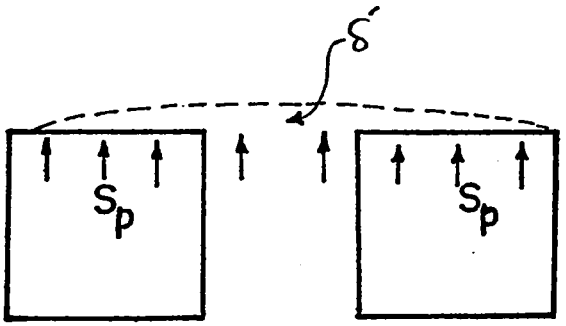

(b) REVERSE DISPLACEMENT OF WALLS DUE TO AVERAGE PRESSURE Sp

FIGURE 2-1

$$\delta_e = \frac{2R\, S_o\, \ell}{E/(1-\mu^2)}\ \phi \qquad (2\text{-}1(b))$$

Thus, δ_e, the vertical displacement due to excavation can be calculated for a three-dimensional case by using Equation (2-1(b)) provided, the position factor, ϕ, is known. For 100 percent extraction Equation (2-1(b)) would become:

$$\delta'_e = \frac{2\, S_o\, \ell}{E/(1-\mu^2)}\ \phi \qquad (2\text{-}1(c))$$

where δ'_e is the vertical displacement as a result of 100 percent extraction.

Determination of the position factors, ϕ :

The total normal displacement, δ_w, for 100 percent extraction is equal to the sum of the displacement produced by the excavation and the original displacement due to the pre-existing normal field stress, i.e.

$$\delta_w = \delta'_e + \delta_o \qquad (2\text{-}2)$$

where, δ'_e is the displacement due to 100 percent extraction and δ_o is the displacement due to the pre-existing normal field stress.

The displacement component δ'_e for a three-dimensional case can be obtained from the Equation (2-1(c)) earlier developed, while δ_o will be given by the following expression

$$\delta_o = \left\{ S_o - \mu S_t - \mu^2 (S_o + S_t) \right\} \frac{h}{E_p} \qquad (2\text{-}2(a))$$

where S_t is the field stress component parallel to the seam or stope and normal to the strike, h is the semi-height of the pillar and E_p is the modulus of deformation of the pillar rock.

Substituting for δ'_e and δ_o in Equation (2-2), we have,

$$\delta_w = \frac{2 S_o \ell}{E/(1-\mu^2)} \phi + \left\{ S_o - \mu S_t - \mu^2 (S_o + S_t) \right\} \frac{h}{E_p}$$

or

$$\phi = \left[\delta_w - \left\{ S_o - \mu S_t - \mu^2 (S_o + S_t) \right\} \frac{h}{E_p} \right] \frac{E/(1-\mu^2)}{2 S_o \ell} \qquad (2\text{-}3)$$

Therefore, the expression for δ_e (Equation (2-1(b)) will reduce to the following form after substituting for ϕ, the position factor.

$$\delta_e = \frac{2R S_o \ell}{E/(1-\mu^2)} \left[\delta_w - \left\{ S_o - \mu S_t - \mu^2 (S_o + S_t) \right\} \frac{h}{E_p} \right] \frac{E/(1-\mu^2)}{2 S_o \ell}$$

$$= R \left[\delta_w - \left\{ S_o - \mu S_t - \mu^2 (S_o + S_t) \right\} \frac{h}{E_p} \right] \qquad (2\text{-}1(d))$$

or

$$\delta_e = R \delta_w - \frac{R S_o h}{E_p} \left\{ 1 - \mu \frac{S_t}{S_o} - \mu^2 (1 + S_t/S_o) \right\}$$

Reverse Displacement of walls as a result of increase in pillar stress:

The resulting displacement of walls due to excavation causes an increase in the pillar stress and thereby produces an average pressure, S_p, over the area tributary to the pillar, Figure 2-1(b). The resulting displacement due to this pressure in the reverse of the excavation case. For a two-dimensional case the reverse displacement, δ', is given by the following expression:

$$\delta' = \frac{2\, S_p \ell \sqrt{1-x}}{E/(1-\mu^2)} \qquad (2\text{-}4)$$

For a three-dimensional case, Equation (2-4) can be extended in the same manner as for the excavation case, simply by introducing the position factor, ϕ, and replacing S_p by S''_i a function of pillar stress. Therefore, it follows that

$$\delta' = \frac{2\, S''_i \ell}{E/(1-\mu^2)}\, \phi \qquad (2\text{-}4(a))$$

where, S''_i is equal to the sum of the pillar loads divided by the sum of the individual tributary areas (that is the wall area occupied by pillar plus that of the average adjacent opening). That is,

$$S''_i = \frac{\Sigma \Delta P}{A_T} .$$

The average increment in pillar stress, $\overline{\Delta\sigma}_p$, is the sum of the pillar loads (or pillar pressure, S_p, multiplied by the sum of tributary areas) divided by the sum of the pillar loads parallel to walls. Therefore, we have

$$\frac{\Sigma\Delta P}{A_T} = \overline{\Delta\sigma}_p \frac{\Sigma\Delta A_p}{A_T}$$

$$= \overline{\Delta\sigma}_p (1-R)$$

For a two-dimensional case the increment in pillar stress, $\Delta\sigma_p$, has been related to the average increment pillar stress, $\overline{\Delta\sigma}_p$(10,25) as follows:

$$\overline{\Delta\sigma}_p = \frac{\pi}{4} \frac{\Delta\sigma_p}{\sqrt{1-x^2}}$$

Therefore $$\frac{\Sigma\Delta P}{A_T} = \frac{\pi}{4} \frac{\Delta\sigma_p}{\sqrt{1-x^2}} (1-R)$$

and $$\left(\frac{x'}{\ell}\right)^2 + \left(\frac{\delta_{w(x)}}{\delta_{w(c)}}\right)^2 = 1$$

or

$$\frac{\delta_{w(x)}}{\delta_{w(c)}} = \sqrt{1-\left(\frac{x'}{\ell}\right)^2} = \sqrt{1-x^2} \quad \text{where} \quad x = x'/\ell$$

where $\delta_{w(x)}$ is the normal displacement at the point under reference and $\delta_{w(c)}$ is the same at the centre. The point defined by x in a two-dimensional case can be replaced by the coordinates x and y, a rectangular opening in the plane of the reef.

Assuming the displacement surface is ellipsoidal, $\delta_{w(x,y)}$ would be related as follows:

$$\delta_{w(x,y)} = \delta_{w(c)} \sqrt{1-x^2} \sqrt{1-y^2} \quad .$$

Thus as was done in two-dimensional solution (10), the average increment in pillar stress, $\overline{\Delta\sigma}_p$, can be related to the individual values,

$\Delta\sigma_p$, by a summation or integration of the above function, which produces the equation

$$\Delta\sigma_p = \left(\frac{\pi}{4}\right)^2 \frac{(1-R)\ \Delta\sigma_p}{\sqrt{1-x^2}\sqrt{1-y^2}}$$

or

$$\frac{\Sigma\Delta P}{A_T} = \left(\frac{\pi}{4}\right)^2 \frac{(1-R)\ \Delta\sigma_p}{\sqrt{1-x^2}\sqrt{1-y^2}} \quad .$$

The position factor $\sqrt{1-x^2}$ and $\sqrt{1-y^2}$ will be the same as ϕ, thus

$$\frac{\Sigma\Delta P}{A_T} = \left(\frac{\pi}{4}\right)^2 \frac{(1-R)\ \Delta\sigma_p}{\phi} \quad .$$

Substituting for $S''_i \left(= \frac{\Sigma\Delta P}{A_T}\right)$ in Equation (2-4(a)) the expression for δ' is

$$\delta' = 2\left(\frac{\pi}{4}\right)^2 \frac{(1-R)\ \Delta\sigma_p}{\phi}\ \phi\ \frac{\ell}{E}\ (1-\mu^2)$$

or

$$\delta' = \frac{2\pi^2}{16}\ (1-R)\ \Delta\sigma_p\ \frac{\ell}{E}\ (1-\mu^2) \qquad (2\text{-}4(b))$$

In view of the term $\sqrt{1-x^2}\ .\ \sqrt{1-y^2}$ cancelling in Equation (2-4(b)) it is not unreasonable to assume that the parameter ϕ (which would equal $\sqrt{1-x^2}\ .\ \sqrt{1-y^2}$ for a rectangular plan) would also cancel for an irregular plan and that the constant would have substantially the same value of $\pi^2/16$. The determination of the factor ℓ in Equation (2-4(b)) will complete the solution for δ' in a three-dimensional case.

It has been shown (10) that the maximum normal displacement at the centre of the opening is related as follows:

$$\delta_{w(c)} = \frac{3\, S_o \ell}{E/(1-\mu^2)} - \frac{S_t\, h}{E/(1-\mu^2)}$$

the above expression is in terms of the plain strain and $\delta_{w(c)}$ is the maximum normal displacement at the centre.

$$\text{i.e.} \qquad \ell = \left[\delta_{w(c)} + \frac{S_t h(1-\mu^2)}{E} \right] \frac{E}{3\, S_o(1-\mu^2)} \,. \qquad (2\text{-}5)$$

Substituting for ℓ in Equation (2-4(b)) we have the final expression for δ',

$$\delta' = \frac{2\pi^2}{16} (1-R)\, \Delta\sigma_p \frac{(1-\mu^2)}{E} \left[\delta_{w(c)} + \frac{S_t h(1-\mu^2)}{E} \right] \frac{E}{3\, S_o(1-\mu^2)} \qquad (2\text{-}4(c))$$

$$= \frac{\pi^2}{24} (1-R)\, \frac{\Delta\sigma_p}{S_o} \left[\delta_{w(c)} + \frac{S_t(1-\mu^2)\, h}{E} \right]$$

Displacement of the pillar resulting from release of side constraint due to mining: Figure 2-2(a) shows the displacement of the pillar as a result of the release of side constraint. The appropriate expression to calculate δ_r in the two-dimensional case has been established (10) and is given below:

$$\delta_r = \frac{\mu_p\, S_t}{E_p}\, h \qquad (2\text{-}6)$$

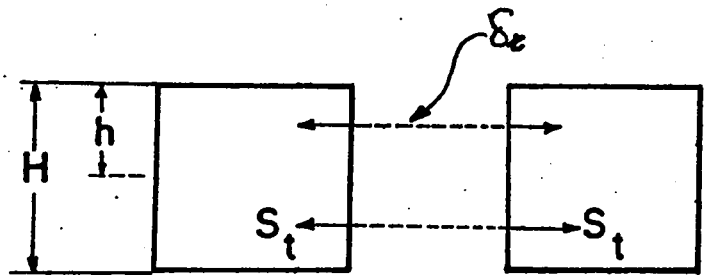

(a) DISPLACEMENT OF THE PILLAR DUE TO RELEASE OF SIDE CONSTRAINT

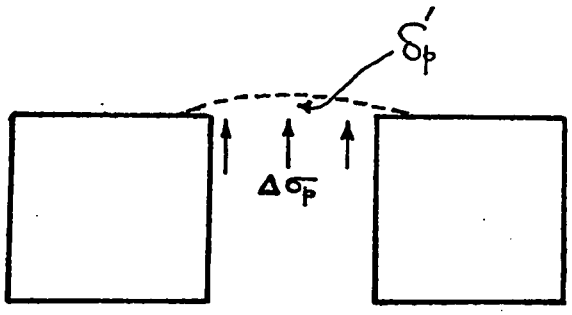

(b) LOCAL PENETRATION OF PILLAR DUE TO $\Delta\sigma_p$

FIGURE 2-2

where μ_p and E_p are Poisson's ratio and the modulus of deformation of pillar rock respectively; S_t the field stress component parallel to the seam or stope and normal to the strike, and h is the mid-height of the pillar.

The expression given by Equation (2-6) can be extended to the whole reef plane as the pillar is free to relax on all exposed sides. Let the component of the field stress in the strike direction be S_x, then the expression for δ_r, for a three-dimensional case will be:

$$\delta_r = \frac{\mu_p S_t h}{E_p} + \frac{\mu_p S_x h}{E_p}$$

$$= \mu_p \left[S_t + S_x \right] \frac{h}{E_p} \qquad (2\text{-}6(a))$$

S_t and S_x may be regarded as the components of pre-mining stress parallel to the dip of the orebody and parallel to the strike of the orebody respectively.

Local Penetration of the Pillars into walls: The local penetration, δ'_p, of the pillars into the wall rock is the result of the concentration of stress, $\Delta\sigma_p$, at the pillars. In other words, the local penetration is in excess of the general reverse deflection δ'. Figures 2-1(b) and 2-2(b) explain the difference.

Based on the existing solution for the relative penetration, on the edge of a semi-infinite plate (24) due to a uniform pressure, a solution for the two-dimensional case has been derived (10) for the maximum local penetration of a pillar due to the excess of $\Delta\sigma_p$, the concentrated stress, over the average pressure S_p, and is given by the following expression,

$$\delta'_p = \frac{\Delta\sigma_p - S_p}{\pi E} B(1-\mu) \qquad (2\text{-}7)$$

where, B is the width of the loaded zone (10).

The average pressure S_p, in the above expression for the total span of the mining zone, $L(= 2\ell)$, will be equal to $\Sigma[\Delta\sigma_p B]/L$. Therefore, we have

$$\delta'_p = \left[\Delta\sigma_p - \frac{\Sigma[\Delta\sigma_p B]}{L}\right] \frac{B}{\pi E}(1-\mu)$$

$$= \left[\Delta\sigma_p - \Delta\sigma_p \frac{\Sigma B}{L}\right] \frac{B}{\pi E}(1-\mu) \qquad (2\text{-}7(a)$$

$$= \Delta\sigma_p \left[1 - \frac{\Sigma B}{L}\right] \frac{B}{\pi E}(1-\mu)$$

But $\Sigma B/L = (1-R)$, where R is the extraction ratio (wall area excavated over total wall area).

Therefore,

$$\delta'_p = \Delta\sigma_p [1-1+R] \frac{B}{\pi E}(1-\mu) \qquad (2\text{-}7(b))$$

$$= \Delta\sigma_p R \frac{B}{\pi E}(1-\mu)$$

For the three-dimensional solution Equation (2-7(b)) must include shape factor, I, and B must be the minimum dimension of the pillar in the plane of the orebody, that is

$$\delta'_p = \frac{\Delta\sigma_p RB(1-\mu)}{\pi E} I \qquad (2\text{-}7(c))$$

where I will vary from 1.0 for an infinitely long pillar to 0.56 for a square pillar (76). In view of δ'_p being small compared to $\Delta\delta_p$ and δ', and has only small influence on computed pillar stresses (23), it seems practical to simplify the terms to:

$$\delta'_p = \frac{0.2\ \Delta\sigma_p\ RB}{E} \qquad (2\text{-}7(d))$$

which means assuming average values of $\mu = 0.2$ and $I = 0.71$ will be good enough for an engineering solution (particularly considering the difficulty of determining μ of the rock mass).

The Net Displacement of the Pillars:

The net displacement, δ_p, of the pillar will be equal to the algebraic sum of all the effects produced by the pre-mining stresses and by the mining itself.

The effects produced by mining on the displacement of the pillar have been analysed by Coates (10) in terms of the total stress being equal to the increase plus the original field stress. It means that the increment of the pillar displacement, $\Delta\delta_p$, is related to the increase in the pillar stress, $\Delta\sigma_p$. Mathematically it can be expressed as:

$$\Delta\delta_p = \frac{\Delta PH/2}{A_p E_p} \qquad (2\text{-}8)$$

Since $H/2 = h$, the semi-height of the pillar and $\Delta P/A_p$ (load/area) $= \Delta\sigma_p$, the increase in the pillar stress, we have

$$\Delta\delta_p = \frac{\Delta\sigma_p h}{E_p} \qquad (2\text{-}8(a))$$

where ΔP is the increase in the pillar load and A_p is the horizontal cross-sectional area of the pillar.

The increase in pillar displacement, $\Delta\delta_p$, is also related to the various components of displacement and is equal to the algebraic sum of the individual components, i.e.

$$\Delta\delta_p = \delta_e - \delta' - \delta_r - \delta'_p \qquad (2\text{-}9)$$

These components of displacement for a three-dimensional solution have been derived earlier.

Derivation of the formula for Pillar loading:

The net increase in the pillar displacement can be obtained by substituting Equations(2-1(d)), (2-4(c)), (2-6(a)) and (2-7(d)) into Equation (2-9) :

$$\Delta\delta_p = \left[R\delta_w - \frac{RhS_o}{E_p}\left\{1-\mu\ \frac{S_t}{S_o} - \mu^2\ (1+\frac{S_t}{S_o})\right\}\right] - \left[\frac{\pi^2}{24}\ (1-R)\ \frac{\Delta\sigma_p}{S_o}\left\{\delta_{w(c)} + \right.\right.$$

$$\left.\left. + \frac{S_t(1-\mu^2)\ h}{E}\right\}\right] - \left[\mu_p(S_t + S_x)\ \frac{h}{E_p}\right] - \left[\frac{0.2\ \Delta\sigma_p\ RB}{E}\right], \quad (2\text{-}10)$$

From Equation (2-8(a)) we have,

$$\Delta\delta_p = \frac{\Delta\sigma_p\ h}{E_p}\ .$$

Therefore,

$$\frac{\Delta\sigma_p\ h}{E_p} = \left[R\ \delta_w - \frac{R\ h\ S_o}{E_p}\left\{1-\mu\ \frac{S_t}{S_o} - \mu^2\ (1+\frac{S_t}{S_o})\right\}\right] - \left[\frac{\pi^2}{24}\ (1-R)\ \frac{\Delta\sigma_p}{S_o}\right.$$

$$\left.\left\{\delta_{w(c)} + \frac{S_t(1-\mu^2)\ h}{E}\right\}\right] - \left[\mu_p(S_t + S_x)\ \frac{h}{E_p}\right] - \left[\frac{0.2\ \Delta\sigma_p\ RB}{E}\right],$$

or

(2-11)

$$\frac{\Delta\sigma_p h}{E_p} + \left[\frac{\pi^2}{24}\ (1-R)\ \frac{\Delta\sigma_p}{S_o}\left\{\delta_{w(c)} + \frac{S_t(1-\mu^2)h}{E}\right\}\right] + \left[\frac{0.2\ \Delta\sigma_p\ RB}{E}\right]$$

$$= \left[R\ \delta_w - \frac{RhS_o}{E_p}\left\{1-\mu\ \frac{S_t}{S_o} - \mu^2\ (1+\frac{S_t}{S_o})\right\}\right] - \left[\mu_p(S_t + S_x)\ \frac{h}{E_p}\right],$$

or

$$\frac{\Delta\sigma_p}{S_o}\left[\frac{h\,S_o}{E_p} + \frac{\pi^2}{24}(1-R)\left\{\delta_{w(c)} + \frac{S_t(1-\mu^2)h}{E}\right\} + \frac{0.2\ RBS_o}{E}\right]$$

$$= \left[R\,\delta_w - \frac{h\,S_o}{E_p}\left[\left\{1-\mu\,\frac{S_t}{S_o} - \mu^2\left(1+\frac{S_t}{S_o}\right)\right\}R + \left(\frac{S_t}{S_o} + \frac{S_x}{S_o}\right)\mu_p\right]\right]$$

$$\frac{\Delta\sigma_p}{S_o} = \left[\frac{R\,\delta_w - \frac{h\,S_o}{E_p}\left[\left\{1-\mu\,\frac{S_t}{S_o} - \mu^2\left(1+\frac{S_t}{S_o}\right)\right\}R + \left(\frac{S_t}{S_o} + \frac{S_x}{S_o}\right)\mu_p\right]}{\frac{\pi^2}{24}(1-R)\delta_{w(c)} + \frac{h\,S_o}{E_p}\left\{1 + \frac{S_t(1-\mu^2)\,E_p}{S_o\,E}(1-R)\,\frac{\pi^2}{24}\right\} + \frac{0.2\ RBS_o}{E}}\right]$$

(2-12)

Then

$$\frac{\sigma_p}{S_o} = \frac{\Delta\sigma_p}{S_o} + 1 \qquad (2\text{-}12(a))$$

In the above expression (Equation (2-12)) the parameters δ_w and $\delta_{w(c)}$ are to be determined experimentally for 100 percent extraction (using an electrical analogue). The other parameters are obtained from the mine and the laboratory tests of the rock mass in order to complete the solution.

Determination of the total normal displacement, δ_w:

The displacement components in the solid rock surrounding the mine excavations can be obtained experimentally, using the solution developed by Salamon (26,28). Such a solution is based on dividing the excavated area into small elementary areas, normally referred to as face elements (26). They are integrated to give the total mined area.

The face element principle has been explained in detail elsewhere (26), however, a brief explanation is given in Appendix A-I. The elementary displacement component, $\Delta\delta_w$, (say at a point $P(x_o,y_o,z_o)$) in the direction of z-axis and normal to the reef plane in the solid rock and induced by a face element, ΔEA, the excavated area, located in the reef, plane ($z = o$) defined by the coordinates (x_1,y_1) has been derived (26,28) in terms of the convergence, $\delta_z(x_1,y_1)$, the Poisson's ratio of the rock mass and is given by the following equation,

$$\Delta\delta_w = \frac{\delta_z \, \Delta EA(x_1,y_1)}{8\pi\,(1-\mu)} \, z_o \left[\frac{2(2-\mu)\, z_o^2 + (1-2\mu)r^2}{(r^2 + z_o^2)^{5/2}} \right] \qquad (2\text{-}13)$$

where, $r^2 = (x_o-x_1)^2 + (y_o-y_1)^2$. Diagrammatically the principle is explained in Figure A-1 (see Appendix A-I).

Thus the total displacement, δ_w, at the point P in the solid rock will be equal to the sum of all the elementary displacements or in other words taking the integral of the whole mining region, collectively referred to as EA. Therefore,

$$\delta_w = \frac{\delta_z}{8\pi(1-\mu)} \iint_{EA} z_o \left[\frac{2(2-\mu)z_o^2 + (1-2\mu)r^2}{(r^2 + z_o^2)^{5/2}} \right] dx_1 dy_1 \qquad (2\text{-}14)$$

The convergence distribution, given by $\delta_z(x_1,y_1)$ has been calculated in terms of function Ω (a solution of Laplaces equation), the elastic constants E and μ and the normal component, S_o of the field stress (see Appendix A-II) and is given by the following expression,

$$\delta_z = 4(1-\mu) \frac{S_o}{E} \Omega (x_1, y_1, 0) \qquad (2\text{-}15)$$

Substituting for δ_z in Equation (2-14) we have

$$\delta_w = \frac{4(1-\mu^2) S_o}{8\pi(1-\mu)E} \iint_{EA} \Omega (x_1,y_1) z_o \left[\frac{2(2-\mu)z_o^2 + (1-2\mu)r^2}{(r^2 + z_o^2)^{5/2}} \right] dx_1 dy_1$$

or

$$\frac{(1+\mu)S_o}{2\pi E} \iint_{EA} \Omega (x_1,y_1) z_o \left[\frac{2(2-\mu)z_o^2 + (1-2\mu)r^2}{(r^2 + z_o)^{5/2}} \right] dx_1 dy_1 \qquad (2\text{-}16)$$

The experimental determination of the function, Ω , in terms of the potential, V, using an electrical analogue has been discussed in detail elsewhere (29) and summarised in Appendix A-II. Based on this analogy, Equation (2-16) can be expressed in terms of the potential V and the required formula in the simplest form (31) is

$$\delta_w = N S_o \iint_{EA} V(x_1,y_1) \quad z_o \left[\frac{2(2-\mu)z_o^2 + (1-2\mu)r^2}{(r^2 + z_o)^{5/2}} \right] dx_1 dy_1 \qquad (2\text{-}17)$$

where $N = \frac{(1+\mu)}{2\pi E V_1} H' =$ constant

V_1 = the applied voltage to the bottom electrode

E = modulus of elasticity of the rock mass

μ = Poisson's ratio of the rock mass

$r^2 = (x_o - x_1)^2 + (y_o - y_1)^2$

H' = distance between the top and bottom electrode at the centre.

and S_o = the normal component of field stress.

The above integral may be evaluated by dividing the plane into a grid of small squares and performing the following simple summation:

$$\delta_w = N S_o \Sigma V \{\bar{K}\} \qquad (2\text{-}18)$$

where V and $\bar{K}$ are the values at the centre of the square grid (for details please see Appendix B-1).

The electrical analogue and its related features will be discussed later, however, a diagrammatic sketch is given in Figure 2-3. Figure 2-3(b) is a section through the analogue with information regarding Equation (2-17).

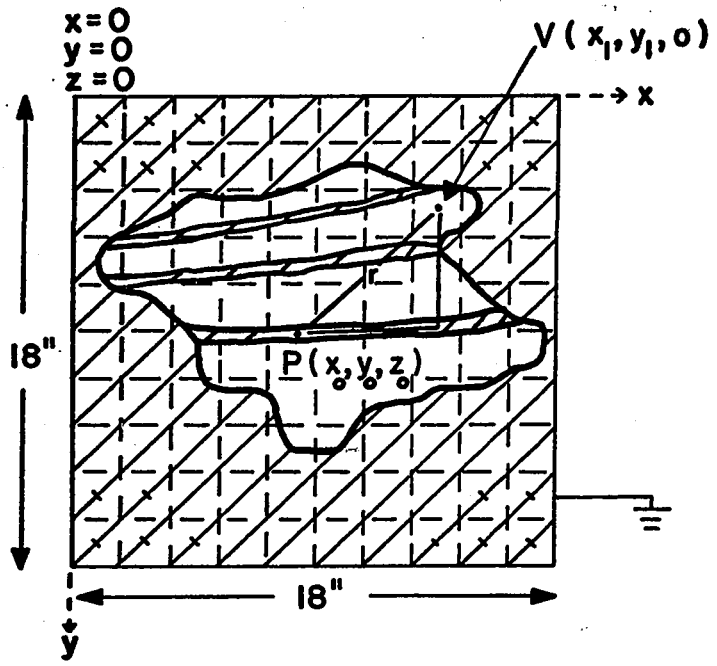

(a) ENLARGED VIEW OF THE WORKING AREA

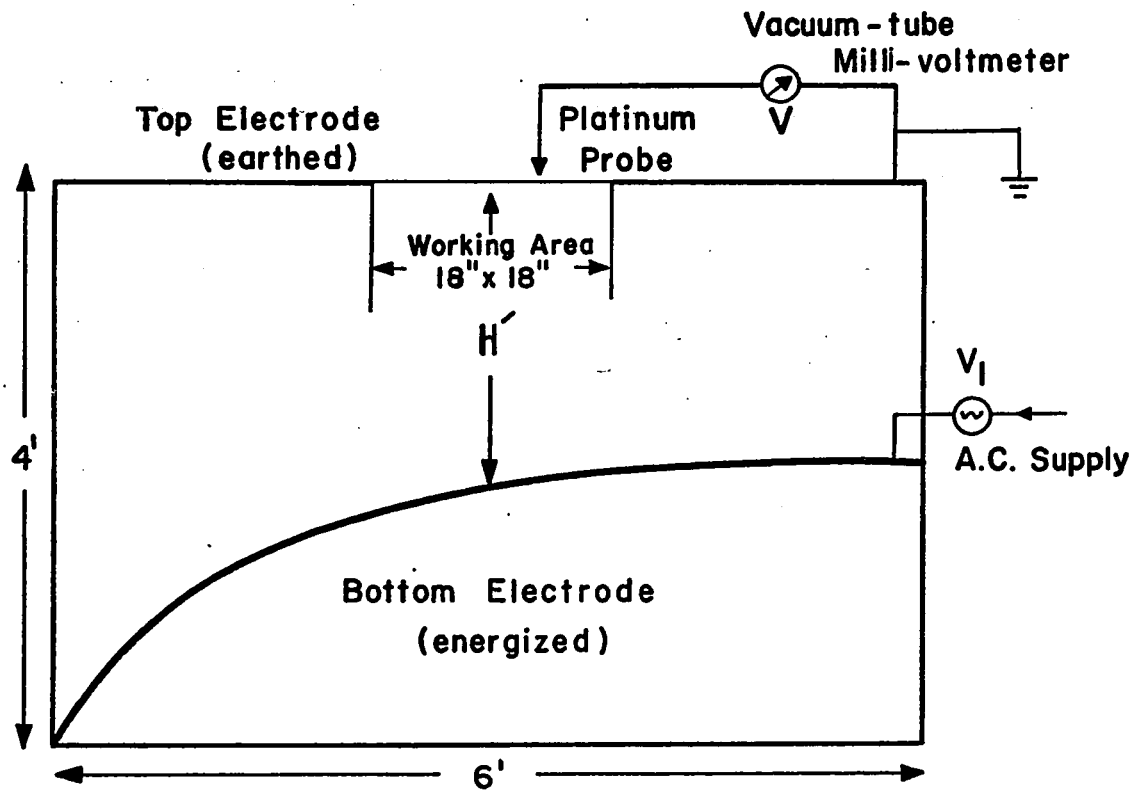

(b) SECTIONAL VIEW THROUGH THE ANALOGUE

FIGURE 2-3

It may be mentioned here that H' in Equation (2-17) has the same value everywhere when simulating horizontal deposits.

Figure 2-3(a) shows the working area of the analogue with a modelled (mining) outline to be simulated. The maximum size of the working area 18 inches by 18 inches is divided into a square grid of 0.2 inches apart. The shaded area in the Figure 2-3(a) is the conductive portion which forms a part of the top earthed electrode.

An IBM 360/75 computer was used to evaluate the integral (Equation (2-17)), using the summation form of Equation (2-18).

CHAPTER III

THE ELECTRICAL ANALOGUE THEORY

The elastic closure, δ_z, can be expressed in terms of the harmonic function Ω i.e. $\delta_z = - C \Omega$ (see Appendix A-II) provided,

$$\nabla^2 \Omega = 0$$

where

$$\nabla^2 = \frac{\partial^2}{\partial x^2} + \frac{\partial^2}{\partial y^2} + \frac{\partial^2}{\partial z^2} \qquad (3\text{-}1)$$

and the function conforms with the appropriate boundary conditions.

The essential feature of an analogue is not the numerical correspondance between element values but rather the fact that for each dependent variable and all derivatives of one system, the corresponding function in the second system can be predicted.

Partial Differential equations characterizing the field problems:

The engineering problem involves the study of excitations, responses and the system parameters. The excitation and response values are generally expressed in terms of variables which are dependent on time and position within the field. These dependent variables are identified 1) as "across" variables and 2) as "through" variables.

1. An "across" variable is the one that relates the condition at a point within the field to that of some other field point or an arbitrary reference point. The instrument that records the "across" variable must be applied simultaneously at the separated points, and this

value actually represents the difference in value between the two points. Voltage drop is the "across" variable, measured in electrical circuits, and is normally referred to as the potential difference.

The term velocity of a point has a meaning only if it is referred to some other point, moving or stationary. Therefore velocity is an example of an "across" variable.

2. The second variable, known as "through" variable is the same everywhere within a component and does not require the specification of two points of measurement. For example, in electrical circuits the current existing in a conductor can be measured at any point along the conductor and is recognized as a "through" variable. However, the magnitude and direction of the current must be determined. Similarly in dynamics, force is an example of a"through" variable and it possesses both magnitude and direction.

In mathematical terminology the "across" variable is the difference between the scalar potentials at two points in the field, while the "through" variable is a vector.

The essential principles which account for the analogous nature of field problems are known as the principles of conservation and continuity, and these may be stated in simple terms as follows: as excitation introduces some physical quantity to the system (i.e. the field), at any time within the field this total quantity must be equal to the net amount added or subtracted by excitation plus the amount initially present within the system itself; in addition, the

continuity principle requires that the through variable must emanate from a source, internal or external excitation, and return to the same or some other source.

Laplace's Equation in an Electrical System: Laplace's equation expresses the mathematical formulation of potential theory and is very useful in describing steady state conditions in most of the areas of the physical world. It holds good for one, two and three-dimensional systems.

Three Dimensional System

Figure 3-1(a) shows a three-dimensional electrical system, which is composed of a rectangular solid box made of a conductive material, having a uniform resistivity (e.g. graphite). Constant voltages are applied to the three sides of the solid for excitation. Figure 3-1(b) illustrates a small cube within the solid as a differential element. The voltage gradient across each face is first expressed in terms of the current and resistance parameter,

$$\left(\frac{\partial v}{\partial x}\right)_1 = -\frac{i_1 R}{\Delta y\, \Delta z}, \qquad \left(\frac{\partial v}{\partial x}\right)_2 = -\frac{i_2 R}{\Delta y\, \Delta z}$$

$$\left(\frac{\partial v}{\partial y}\right)_3 = -\frac{i_3 R}{\Delta x\, \Delta z}, \qquad \left(\frac{\partial v}{\partial y}\right)_4 = -\frac{i_4 R}{\Delta x\, \Delta z} \qquad (3\text{-}2)$$

$$\left(\frac{\partial v}{\partial z}\right)_5 = -\frac{i_5 R}{\Delta x\, \Delta y}, \qquad \left(\frac{\partial v}{\partial z}\right)_6 = -\frac{i_6 R}{\Delta x\, \Delta y}$$

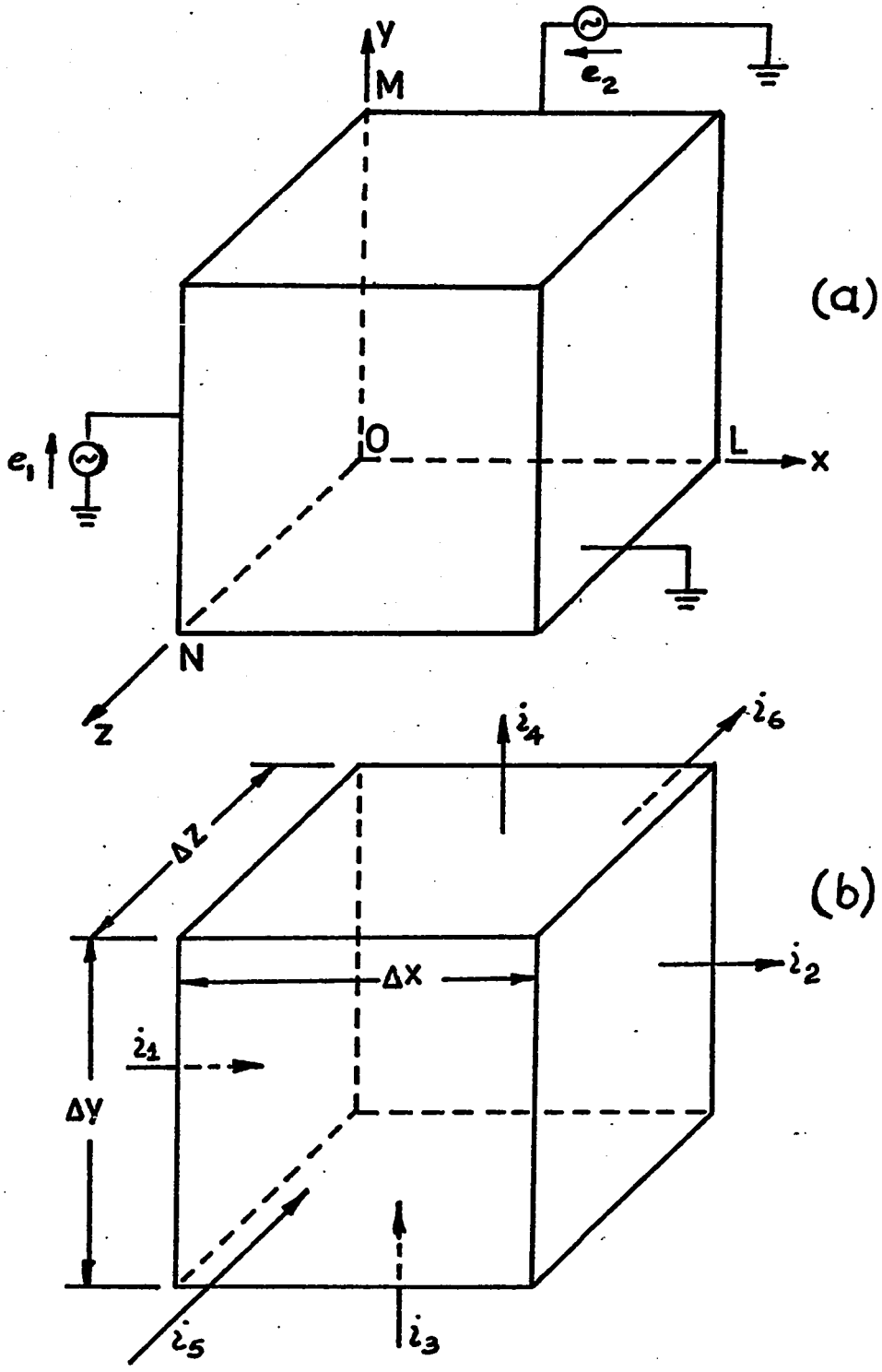

THREE DIMENSIONAL ELECTRICAL SYSTEM

FIGURE 3-1

where R may be considered the resistance between opposite faces of a unit cube. The rate of change of gradients thus can be expressed as:

$$\frac{\partial^2 v}{\partial x^2} = \frac{\left(\frac{\partial v}{\partial x}\right)_2 - \left(\frac{\partial v}{\partial x}\right)_1}{\Delta x} \qquad \Delta x \to 0$$

$$\frac{\partial^2 v}{\partial y^2} = \frac{\left(\frac{\partial v}{\partial y}\right)_4 - \left(\frac{\partial v}{\partial y}\right)_3}{\Delta y} \qquad \Delta y \to 0 \qquad (3\text{-}3)$$

$$\frac{\partial^2 v}{\partial z^2} = \frac{\left(\frac{\partial v}{\partial z}\right)_6 - \left(\frac{\partial v}{\partial z}\right)_5}{\Delta z} \qquad \Delta z \to 0$$

Adding the three components of Equation (3-3) and substituting for the voltage gradients from Equation (3-2), we have

$$\frac{\partial^2 v}{\partial x^2} + \frac{\partial^2 v}{\partial z^2} + \frac{\partial^2 v}{\partial z^2} = -\frac{i_2 R}{\Delta x \Delta y \Delta z} + \frac{i_1 R}{\Delta x \Delta y \Delta z} - \frac{i_4 R}{\Delta x \Delta y \Delta z} \qquad (3\text{-}4)$$

$$+ \frac{i_3 R}{\Delta x \Delta y \Delta z} - \frac{i_6 R}{\Delta x \Delta y \Delta z} + \frac{i_5 R}{\Delta x \Delta y \Delta z}$$

$$\Delta x \to 0, \quad \Delta y \to 0, \quad \Delta z \to 0$$

or $$\frac{\partial^2 v}{\partial x^2} + \frac{\partial^2 v}{\partial y^2} + \frac{\partial^2 v}{\partial z^2} = \frac{R}{\Delta x \Delta y \Delta z}(i_1 - i_2 + i_3 - i_4 + i_5 - i_6) \qquad (3\text{-}5)$$

Since there can be no accumulation of electrical charge within the differential element, the net current into the element must be zero, i.e.

$$i_1 - i_2 + i_3 - i_4 + i_5 - i_6 = 0 \qquad (3\text{-}6)$$

Therefore, Equation (3-5) becomes

$$\frac{\partial^2 v}{\partial x^2} + \frac{\partial^2 v}{\partial y^2} + \frac{\partial^2 v}{\partial z^2} = 0 \qquad (3\text{-}7)$$

and the appropriate boundary conditions at the six faces of the cube will be

at $x = 0$, $0 < y < M$, $0 < z < N$ $\quad v = e_1$,

at $0 < x < L$, $y = M$, $0 < z < N$ $\quad v = e_2$

at $x = L$, $0 < y < M$, $0 < z < N$ $\quad v = 0$,

at $0 < x < L$, $0 < y < M$, $z = 0$ $\quad \frac{\partial v}{\partial z} = 0$

$$\text{at} \quad \begin{matrix} 0 < x < L \\ y = 0 \\ 0 < z < N \end{matrix} \quad \frac{\partial v}{\partial y} = 0 \;, \quad \text{at} \quad \begin{matrix} 0 < x < L \\ 0 < y < M \\ z = N \end{matrix} \quad \frac{\partial v}{\partial z} = 0 \tag{3-8}$$

This is known as Laplace's equation in a three-dimensional system. The general expression is achieved by introducing the Laplacian Operator ∇^2 which merely signifies the "sum of the second derivatives with respect to all the cartesian space variables of interest". Finally, regardless of the dimensions, Laplace's equation becomes

$$\nabla^2 v = 0 \tag{3-9}$$

A significant feature of Equations (3-7) is that the resistance parameter of the field does not appear in the expression. It shows that the voltage distribution within the field is independent of the magnitude of resistivity. Besides this, the expression makes it clear that whatever the shape of the conductor (i.e. one, two or three dimensional) through which a steady current flows, the potential V must satisfy the Equation (3-9). This is true everywhere except at points where there is either a source or sink of current. However, Equation (3-9) alone does not determine the solution of any problem because it expresses only one of the conditions which V must satisfy. In any particular problem there are boundary conditions which must be satisfied. Any solution of Laplace's equation which also satisfies the boundary conditions constitutes the unique solution of the given problem.

Boundary Conditions defining the function , Ω :

Referring to Equation (3-1), we have the boundary conditions defining the function Ω. These conditions are:

a) $\delta_z = 0$ where there is no excavation,

b) $\delta_z = \delta_m$ where the hanging wall and footwall are effectively in contact,

c) the induced normal stress S_o, has a constant value, where the closure is not complete, and

d) the induced displacements approach zero at great distances away from the excavations.

Since the above boundary conditions hold good for both horizontal and inclined deposits, $\partial\Omega/dZ$ will not have a constant value as in case of horizontal deposits, because the depth Z has a constant value, Z_o, only at the origin . Thus at any other point on the reef plane the depth from the surface will be $Z_o + y \sin i$, where $y \sin i$ is the vertical component due to the dip of the orebody. The coordinate y is the linear distance along the dip and i is the dip of the deposit.

When i is equal to zero, the term $y \sin i$ automatically reduces to zero which is the case in a horizontal deposit.

The boundary conditions defining the function Ω can now be written in a general form as follows:

at the reef plane

$$\left.\begin{aligned} \Omega\big|_{z=o} &= 0 && \text{outside the excavated area, EA,} \\ \Omega\big|_{z=o} &= -\,\Omega_o && \text{within the excavated area where closure is complete,} \\ \frac{\partial\Omega}{\partial z}\Big|_{z=o} &= 1+\sin i && \text{within the excavated area, where closure is not complete,} \end{aligned}\right\} \quad (3\text{-}10)$$

and at infinity

$$\Omega\big|_{z=\infty} = 0$$

In Equation (3-10), the differential $\frac{\partial\Omega}{\partial z}$ can be written as

$$\frac{\partial\Omega}{\partial z} = 1 + y\ B/L_2$$

where L_2 is a representative linear dimension in the mine

and

$$B = \frac{L_2}{Z_o} \sin i \qquad (3\text{-}11)$$

On the basis of the relationship developed (29) between the normal closure and the function Ω, we have

$$\delta_z(x,y) = -\,C\,\Omega(x,y,0) \qquad (3\text{-}12)$$

and

$$\Omega_o = \frac{\delta_m}{C}$$

where δ_m is the maximum value of δ_z. The coefficient C for homogeneous isotropic conditions has been determined (29) and is equal to $-4(1-\mu^2)S_o/E$.

Therefore, we have

$$\delta_z = \frac{4(1-\mu^2)S_o}{E} \Omega \qquad (3\text{-}13)$$

which in turn means that the closure is proportional to the magnitude of the function Ω.

It has been shown earlier that the potential, V, associated with steady state current flowing in a homogeneous continuous medium satisfy the Laplace equation. Thus it may be said that the functions Ω and V, both are the solutions of the same basic equation. Now if two functions defining the problem are identical, an electrical tank can be constructed for the experimental determination of the function, Ω for the simulation of mine openings.

This analogy between the function , Ω, and the potential, V, has been established (29) and summarised in Appendix A-II.

CHAPTER IV

THE ELECTROLYTIC TANK

General: Electrolytes were utilized as early as 1875 by Adams (32) to study the forms of equipotential curves, surfaces and lines of electric forces. Heep (33) was the first to discuss some of the design features of an electrolytic tank while studying the potential measurements.

In general, the electrolytic tank is a conductive liquid analogue, whose principle with the boundary conditions, is explained in Appendix A-II.

The tank consists of two basic units, the electrolyte and the electrodes. Both units are housed in a non-conductive container. This container should be large compared to the scale model of the boundary configuration of the field under study or a conformal transformation thereof.

In addition to these basic units the other components necessary for such a study are the source of excitation and the sensing equipment. All these units are discussed below in some detail.

THE COMPONENTS AND THE OPERATION OF THE TANK:

Electrolytes:

For a satisfactory solution of Laplace's equation by a conductive liquid analogue system, the conductive liquid must have the following properties (34).

1. The liquid must be purely resistive, with no electrical reactance.

2. The resistivity of the liquid must be uniform throughout.

3. The resistivity must be large compared to the resistivity of electrodes and small compared to the input resistance of the sensing device.

4. The resistivity must show a linear relationship between voltage and current over the entire operating range.

5. There should not be any chemical reaction between the electrodes and the electrolyte.

6. The surface tension should be small to avoid the formation of a meniscus at the boundaries and at the probe tip.

7. The surface of this liquid must be free of dirt, films, and other foreign matter.

8. The rate of evaporation at room temperature must be slow.

Water from the mains has been suggested (33) as a good electrolyte. It has been found that it is unnecessary to add any thing to this water since the conductivity is already high enough. A higher conductivity could even be harmful, because of the transition resistance which occurs on the surface of the electrodes due to impurities or polarization. Sander and Yates (35) have made studies on different combinations of electrodes and electrolytes at different temperatures. However, many investigators have reported satisfactory results using ordinary tap water as the electrolyte. Unsatisfactory

results with tap water have been noted also, but the divergence of opinion at this point is mainly due to the variation in the composition of tap water from place to place. This observation was made by the author on Montreal (Quebec) water, which has a high conductivity. An alternative was to use distilled water, but this was discarded because large quantities of distilled water are not easily available and distilled water does not stay pure when stored in a large tank for a long time.

Another suitable alternative was deionized water. Tap water can be easily deionized by using suitable ion exchange resins. The principle of ion exchange (36) can be defined as "a reversible exchange of ions between a solid and a liquid in which there is no substantial change in the structure of the solid". In this definition the solid is the ion-exchange material or resin particle. This principle is explained below with the help of reactions involved in such a phenomenon.

Ion Exchange Reactions: The reaction below is an example of ion-exchange phenomenon, which can be understood if we recognize that only compounds which yield soluble ions in solution are subjected to ion-exchange reactions.

$$NaCl + AgNO_3 \rightleftharpoons AgCl + NaNO_3$$

This reaction shows that the sodium ions of the sodium chloride molecule can be exchanged for the silver ion of the silver nitrate molecules.

Similarly the sodium form of a cation resin, will exchange the mobile sodium ions from the resin with the silver ions from solution. A reaction to show such a phenomenon can be written as:

$$RSO_3^+Na^+ + AgNO_3^- \rightleftharpoons RSO_3^+Ag^+ + NaNO_3^-$$

where R indicates the organic portion of the resin and SO_3 is the immobile portion of the ion active group. Since ion-exchange reactions are reversible, contacting a resin in the silver form with $NaNO_3$ would proceed as follows:

$$RSO_3Ag + NaNO_3 \rightleftharpoons RSO_3Na + AgNO_3 \quad .$$

This reaction or the reverse of the preceding reaction is known as regeneration. These resins are sold under the patent names of their respective companies. The four major types of ion-exchange resins in commercial use are, strong-and weak-acid (cation) resins and strong- and weak-base (anion) resins. J. T. Baker Chemical Company, Philipsburg, N.J., sells them under the patent name of "Dowex", and Fisher Scientific Company, Fairlawn, N.J., under "Rexyn".

To decrease the conductivity or increase the resistance of the electrolyte (water in our case), the water has to be treated with two resins, one which will absorb the cations and the other anions. Different ways have been suggested (36) for such a treatment.

1. The water is passed through a column of resins, in which case the acid and base resins can be mixed before hand.
2. Two beds of acid and base resins can be separated by a glass wool filter.
3. The water is passed through a bed of resins contained in a tank at higher elevation, to which water can be pumped and the outlet connected to the tank.
4. The most suitable method for large quantities of water is to dump the two resins in a tank of water and let it settle for a few days.

The presence of resins in the tank which ultimately are going to settle down to the bottom, does not interfere with the operation as the resins are inactive in an electrical field. The added advantage of this system is that if any polarization with the passage of time takes place, the ions will be absorbed by the resins present in the tank. Care must be taken that about 10-15 percent extra resins are added to the tank.

It has been observed by the author that with the passage of time, at room temperature the evaporation losses are quite high. To keep the level of electrolyte constant in the tank, a small column of one inch diameter filled with resins is supplied with water from the mains. This slow supply of deionized water keeps the level of the electrolyte constant. This column of resins can be used for a couple of months to supply deionized water. Once a change in the colour of resins is noted, the column has to be washed and refilled with resins.

The resins used by the author are:

1. Rexyn 101 (H), Ionic Form H^+, 16-50 mesh.
2. Rexyn 201 (OH) Ionic Form OH^-, 16-50 mesh.

With the above treatment of ordinary water, the electrolyte was quite satisfactory.

Electrodes:

The electrodes must have the following properties:

1. The electrical resistivity must be small, in other words, the resistivity of the electrodes must be negligible relative to that of electrolyte.
2. Electrode material must not react chemically with the electrolyte.
3. Electrodes must present a smooth, well defined surface.
4. They must be of a material which can be readily shaped and cleaned.

Einstein (37) has given a list of the different combinations of electrodes and electrolytes with the merits of each combination. It appears that platinum is the best material, but where electrodes with large surface areas are required, since platinum is expensive, the next best material is graphite coated electrodes. Surfaces of brass or copper are sprayed with commercially available graphite jell and then baked at approximately 200°c. This results in a smooth, liquid-resistant layer. Coating very large sheets of electrodes, say 4' x 4' or bigger, by graphite is still not possible because of the limiting

size of furnaces for baking. An alternative is etched brass or copper sheets. The combination of copper and water, or brass and water, are fairly good for general purposes. Brass sheets have an additional advantage over copper because they can maintain the desired curvature easily. In the construction of the electric tank analogue for this work, the bottom electrode is of brass (owing to the required curvature) and the top electrode is of copper.

Excitation:

In the case of a conductive-liquid analogue, the electrical excitation is in the form of constant voltages applied to the electrodes. Since in measuring the potentials it is only necessary to compare the relative voltage in the liquid, the absolute value and the sign of voltage on the electrodes is unimportant. Thus, a potential at a point in the liquid means the relative potential, that is, the ratio of the voltage of the probe to the voltage of electrode with the highest potential, both calculated with respect to an electrode of zero potential. An alternating voltage may thus be used and is even preferable because the electrolyte is not decomposed if a sufficiently high frequency is used. On the other hand, when a direct current voltage source is employed, polarization-type electrochemical phenomena occur almost immediately at the electrodes, resulting in gaseous layers around the electrode surfaces. This gaseous layer forms a region of high resistivity and distorts the potential field. Thus an A.C. generator is normally preferred for the supply voltage. Einstein (37) has shown the variation of electrode surface components with frequency and temperature, and the merits of some electrode-electrolyte combimation. His results show that the value

of the surface impedence falls with increasing frequency. The increase is slow above 1000-2000 cycles per second, and the relative disadvantages of working the circuits at high frequencies soon outweigh the resulting reduction of polarization. A suitable operating frequency is 1000-1500 cycles per second.

His study on concentration and temperature show that it is advantageous to operate the electrolytic tank at high temperatures. However, if the tank is operated at any temperature other than room temperature serious errors due to thermal convection currents within the electrolyte are difficult to avoid.

Sensing Device:

Sensing is done by a probe suitable for the simulation. It is necessary to use a very fine probe submerged to a minimum depth in order to reduce the miniscus error at the tips. Sander and Yates (35) have discussed in detail the design requirements for probes. The probe impedence has been further discussed by Burfoot (38) on the basis of work done by Sander and Yates (35), and Einstein (37).

To reduce probe errors to a minimum, Sander and Yates (35) used a thin walled capillary tube, 1/16 inch in diameter and approximately 1/4 inch in length, which is inserted into the electrolyte to a depth of approximately 1/8 inch. The upper end of the capillary tube opens into the electrolyte in which electrical contact is made by means of platinum foil. In this way, the potential within the tank is sensed without introducing a metal probe. But, in such

an arrangement placing a relatively large insulator in the field causes perturbations. For surface probes the best probe arrangement is to fix a thin platinum wire in a thin insulating tube, sealed with insulating fluid, which keeps the length of the tip fixed. The insulated probe then can easily be put into the hole of the top electrode touching the water surface. Since in our case the potentials had to be measured at the surface of the electrolytic tank through a series of holes, as will be discussed later, such an arrangement was found suitable and convenient to handle. A platinum tip of 0.01 inches diameter is strong enough to keep its shape and does not bend as the exposed tip is only 1/8 inch long. Distortions of the potential field due to the introduction of the probe are also best avoided by making the probe as small as practical.

When the electrode system and the dimensions of the tank are of the order of feet and only the surface of the electrolyte is traversed by the probe, errors from this source may be considered negligible (34).

TANK CONSTRUCTION:

General: The analogue used to simulate field problems in mining should be such that the central portion of the top electrode, referred to as the working area,must be as large as possible. This reduces the errors caused by the finite dimension of the point of the probe and by the rise of liquid surface at the electrodes. The large size

of the working area also provides the potentiograms of large size which makes them more accurate. Besides this the loss of details in models is reduced if the scale factor to be used is small.

The dimensions of the working area cannot be too large compared to the size of the tank in both depth and area. Salamen, et,al (29) have given the theoretical analysis for minimum cylindrical tank dimensions. The finite dimensions of the tank will introduce errors which can be divided into two components, δ_1 due to finite depth and δ_2 due to finite radius.

Assuming that the measured value of potential in the working area is V and the theoretical value is V_1, then by introducing errors δ_1 and δ_2, the measured value will be equal to the sum of errors plus the theoretical value. It has been shown (29) that when the ratio between the tank depth and the radius of working area is equal to or greater than 2.5, the magnitude of the error introduced by δ_1 is less than one percent. Also when the ratio between the radius of the tank and the working area is equal to or greater than 2.25, the percentage of error introduced by δ_2 is less than one percent.

Based on these assumptions the tank for the present study was designed as a square tank with dimensions that keep errors below one percent.

The Body of the Tank: The tank consists of a frame, within which

a plywood box 6 feet by 6 feet and 4 feet depth is built as shown in Figure 4-1. The inside of the plywood box was coated with two coats of epoxy resin and allowed to dry for three days. A lining of woven glass fibre was then placed inside the box, coated with the same resin and allowed to dry for two days. To ensure complete water-proofing two additional coats of epoxy resin were applied and allowed to dry for one week.

To make sure that there was no conductivity from inside to outside of the tank, frequent checks were made with an ohmmeter.

The Top Electrode: The top electrode consists of 0.018 inch thick copper sheet braced with 0.187 inch thick aluminium sheet. In place of this combination a thick sheet of copper would be quite satisfactory but the cost involved in using thick sheets of copper is substantial. The bracing of the copper sheet by aluminium sheet was necessary to avoid any bending in the electrode. The preference for aluminium as bracing material over other material was because of its light weight.

The two metallic plates were joined with a thin layer of Faymore 869 Adhesive, which was allowed to cure for a period of five days under a uniform pressure. At the end of the curing period the two plates are more or less one solid piece.

The top electrode was further cross braced with 3 inch by 2 1/2 inch by 1/4 inch aluminium I-sections and 2 inch by 2 inch by 1/4 inch angles. The overall dimensions of the top electrode are 5 feet-10.8 inch by 5 feet -10.8 inch with a cut-out portion of 18 inch by 18 inch at

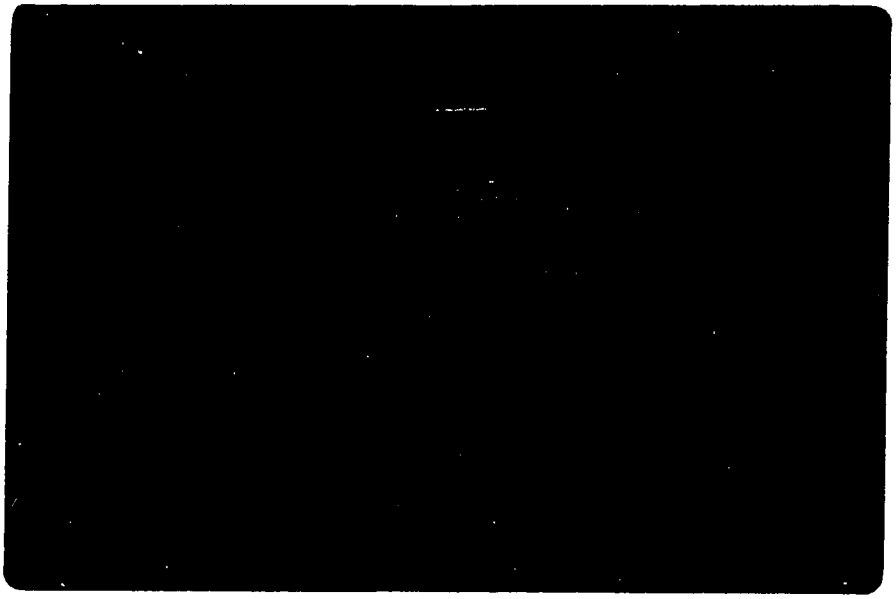

THE ELECTROLYTIC TANK

FIGURE 4 - 1

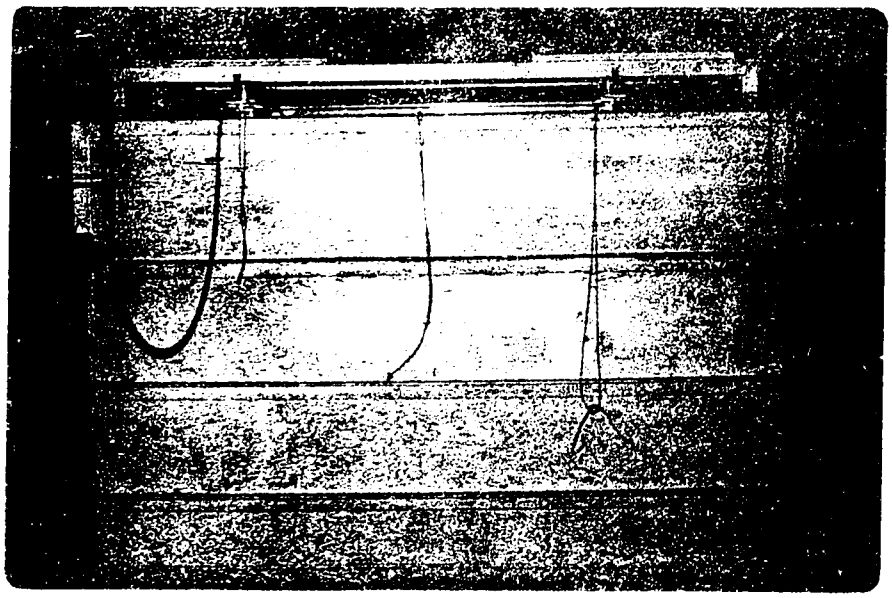

THE ELECTROLYTIC TANK

FIGURE 4 - 1

the centre, known as the working area. Figure 4-2 shows the top electrode in position. The suspension of the electrode within the tank by four levelling screws as shown in Figure 4-2 is necessary as it should be in contact with the electrolyte only.

Figure 4-3 is a detailed drawing showing the complete suspension arrangement. Four 1/2 inch threaded holes are drilled into the extended ends of the angle aluminium through which pass 4-1/2 inch brass screws. The brass screws fit into the holes drilled in the top edge of the frame housing the tank. These holes are insulated with Teflon washers as shown. Such an arrangement allows a vertical movement of about 2 1/2 inches within the tank if the overall length of the brass screws is 4 inches.

In the central cut-out portion of the top electrode a non-conductive victor board cut to the square shape of 18 inches is fitted. A systematic pattern of holes is drilled in the victor board to support the probe at the correct depth. This board will be referred to in future as the model plate. The model plate is carried by clamps on the shoulders of the cut-out area (Figure 4-4), these clamps are adjusted in such a way that the lower surface of the model plate stays flush with the copper surface of the top electrode. The shoulder clamps at the same time maintain the electrical continuity between the conductive portion of the model plate and the top electrode.

The Bottom Electrode: The bottom electrode consists of a plain sheet of brass 0.040 inches thick 5 feet -10.5 inches square, suspended by eight non-conductive ropes, four on each side. These ropes

A PHOTOGRAPH OF THE ELECTROLYTIC TANK SHOWING
THE TOP ELECTRODE

FIGURE 4 - 2

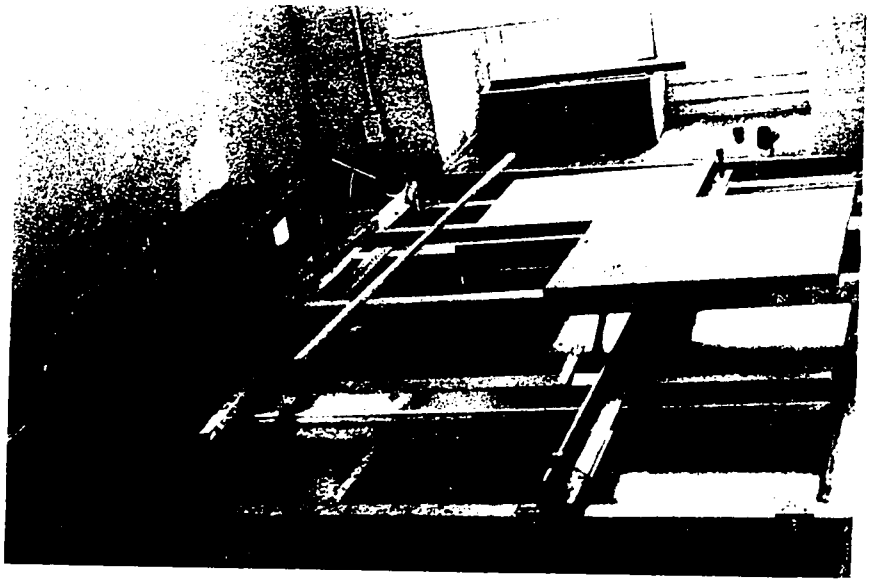

A PHOTOGRAPH OF THE ELECTROLYTIC TANK SHOWING
THE TOP ELECTRODE

FIGURE 4 - 2

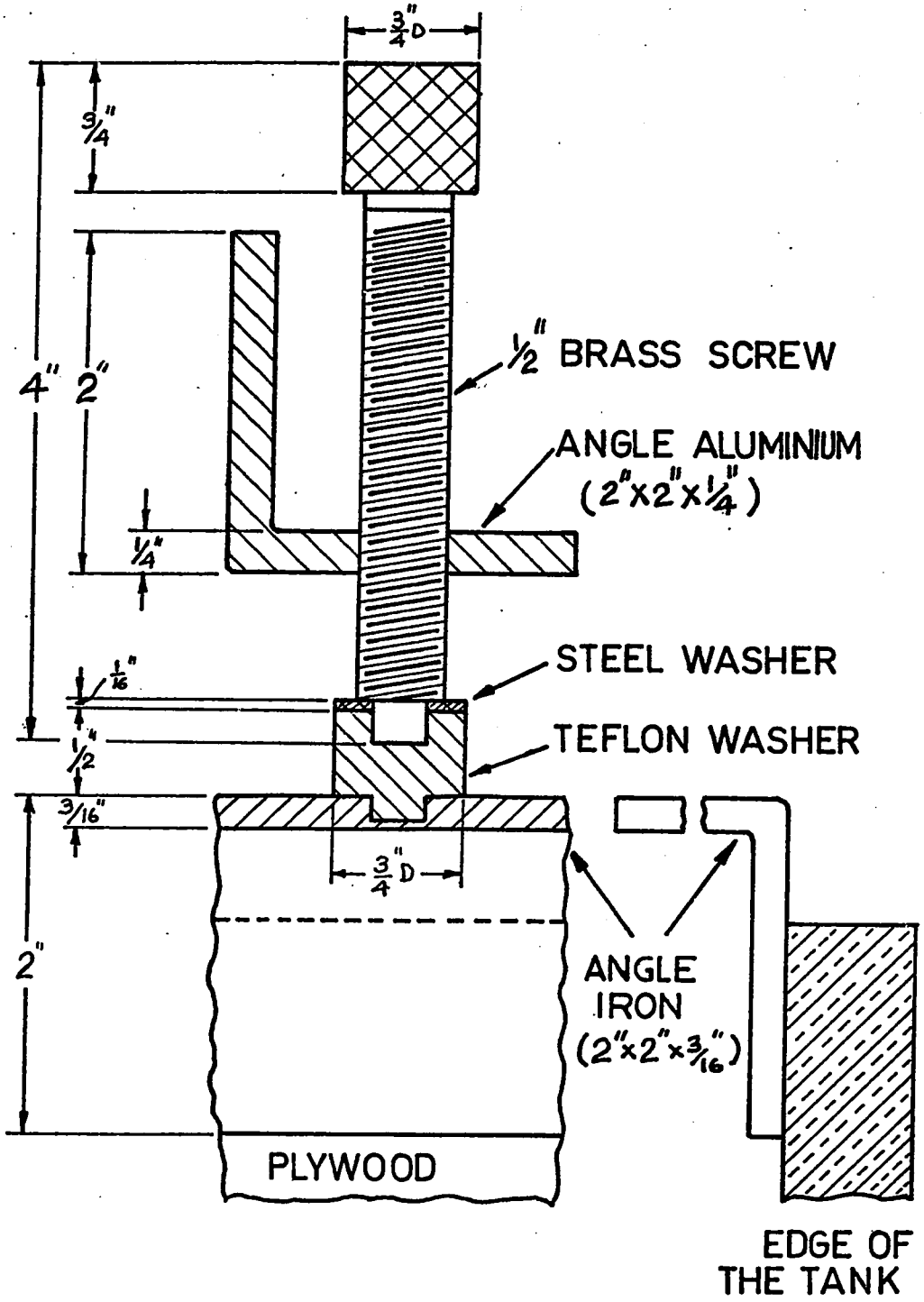

DETAILED DRAWING SHOWING THE SUSPENSION ARRANGEMENT OF THE TOP ELECTRODE

FIGURE 4-3

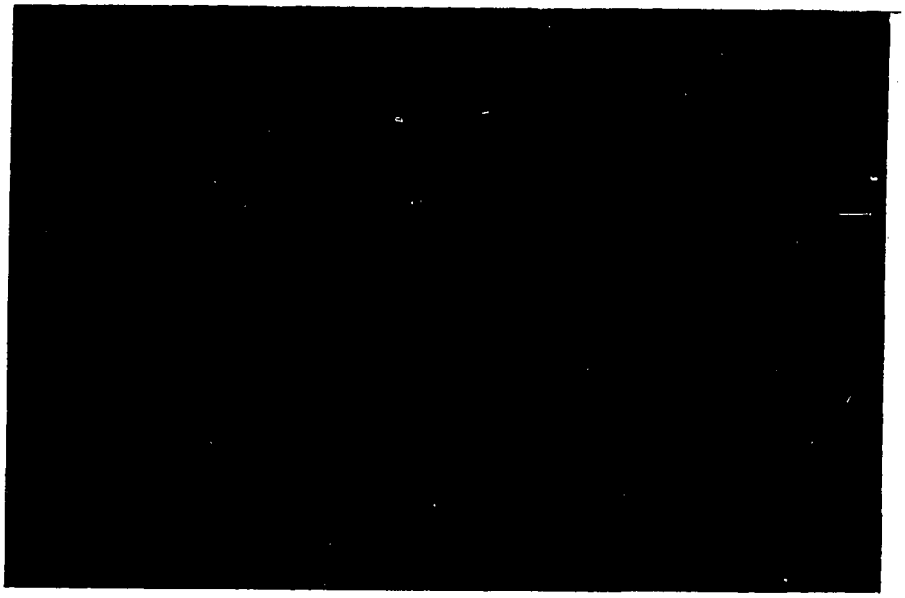

A PHOTOGRAPH OF THE ELECTROLYTIC TANK SHOWING THE MODEL PLATE IN THE WORKING AREA OF THE TOP ELECTRODE

FIGURE 4 - 4

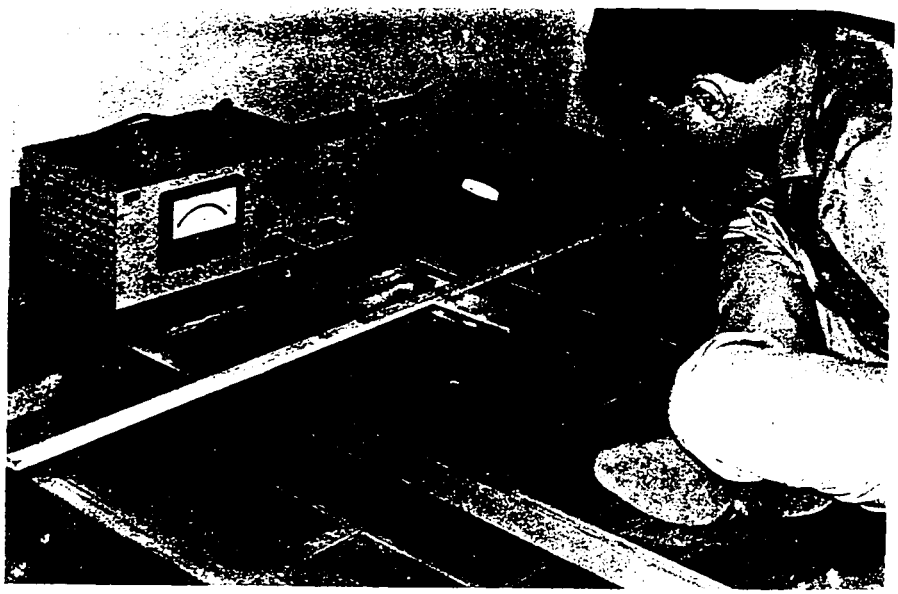

A PHOTOGRAPH OF THE ELECTROLYTIC TANK SHOWING THE MODEL PLATE IN THE WORKING AREA OF THE TOP ELECTRODE

FIGURE 4 - 4

can be clamped to the edge of the tank which allows the bottom electrode to rest flat on the bottom of the tank or in a desired precalculated curvature. Figure 4-1 shows the four ropes of the bottom electrode. It may be noticed that the length is different in each case, which shows that the bottom electrode in this model was not flat but curved.

The suspension hooks of the bottome electrode are attached to the ends of the 5 wooden, 1 inch square cross pieces. These cross-pieces are fitted to the brass sheet on the lower surface facing the bottom of the tank. To avoid any interferance with the curvature of the electrode, the cross-pieces are fixed in such a way as to maintain curvature which is an added advantage of using brass as the bottom electrode.

CHAPTER V

MODEL STUDIES OF PILLAR STRESSES

General: The previous chapters have shown that within irregular mining boundaries, the increase in pillar stresses can be calculated analytically by using the three-dimensional approach, provided the terms δ_w and $\delta_{w(c)}$ in Equation (2-12) can be determined. It was also shown (Appendices A-I and A-II) that by simulating the mine outlines on an electrical analogue, δ_w and $\delta_{w(c)}$ can be determined.

The electrical analogue, (electrolytic tank) its construction and related features have all been explained in detail.

MODEL PREPARATION:

To ensure that the experiment to be performed on the analogue is subjected to the least experimental error, it is necessary to calibrate the whole array. The closure distribution can be determined by a theoretical solution for a parallel sided longwall stope and for an isolated circular stope (29). These theoretical distributions are compared with the experimental value obtained from the tank. Both these openings were simulated with the tank, and the agreement between theory and experiment was within ± 5 percent.

It was decided after several trials that the frequency of the system will be maintained at 1000 cycles per second and supply voltage to the tank at 9 volts.

The actual preparation of the mine model for the study is described below step by step.

1. A mine plane of the mine workings is first reduced to a scale to fit into the model plate of 18 inch by 18 inch. Since the observations are all in the reef plane, the mine plan for inclined workings must be reduced to accomodate for the dip. The dip reduction can be achieved either by a dip-reduction pantograph or by rabatting.

2. The next step is to transfer this outline to the model plate. This is done on the lower surface of the model plate by marking the stoped out portion after properly centering the whole plan on the plate. The unmined ground such as abutments, isolated pillars and dikes are the areas which are then covered with masking tape. Figure 5-1 shows the model plate with the Nordic mine outline.

3. The masked portion of the plate is then coated with conductive silver paint. The electrical continuity is checked throughout the masked area with a sensitive ohmmeter. Since the conductive portion of the model plate is now a part of the top electrode, it will have the same potential. The non-conductive portion of the model plate represents the stoped out area. When the top electrode is brought in contact with surface of the electrolyte by the help of four levelling screws, the exposed electrolyte surface through the non-conductive portion of the model plate is the area where the potential measurements are made. The model plate is pre-drilled with a

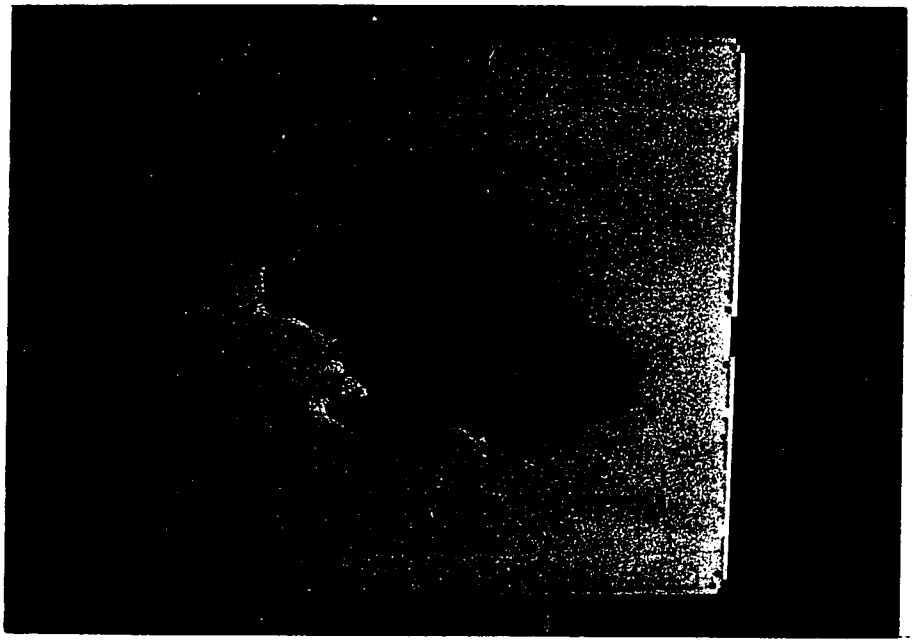

A SIMULATED MINE MODEL OF NORDIC MINE (DIKES REMOVED)

FIGURE 5 - 1

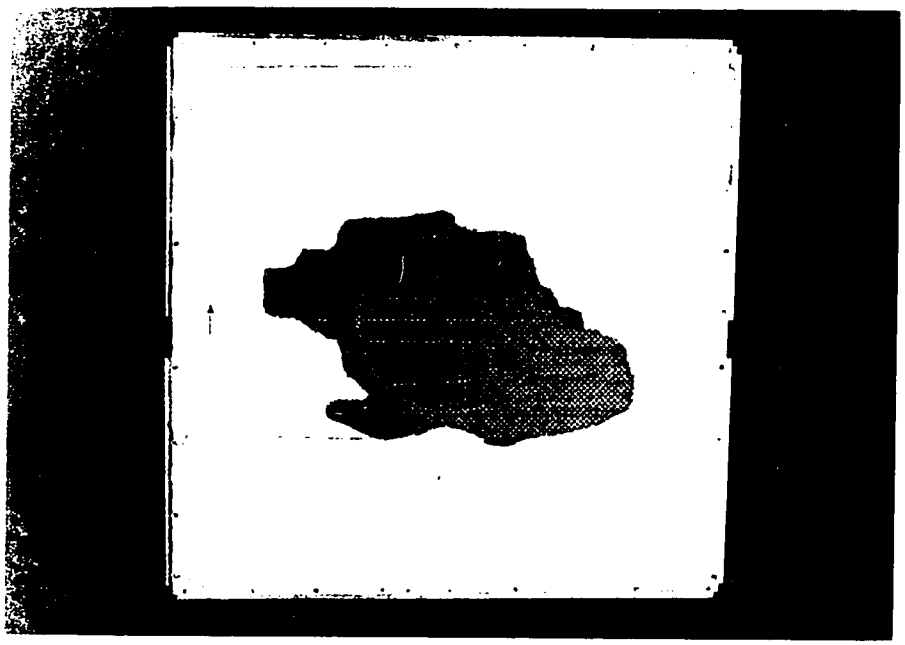

A SIMULATED MINE MODEL OF NORDIC MINE (DIKES REMOVED)

FIGURE 5 - 1

systematic pattern of holes to make a square grid. Through these holes the voltages on the exposed water surface are measured by the help of a probe and a high input independence vacuum tube millivoltmeter. Figure 4-4 shows such an arrangement.

4. After the model has been made and placed in the working area of the top electrode, the next step is to ensure the proper curvature of the bottom electrode. For horizontal deposits the bottom electrode is flat. Simulating inclined deposits the curvature of the bottom electrode is defined by $H_1(Y_1)$, Equation (A-27). $H_1(Y_1)$ at the centre of the model is the mean depth, used to calculate the analogue constant (see Appendix B-I).

Next the bottom electrode is energised by 9 volts of alternating current at 1000 cycles per second with a variable frequency generator and a power amplifier. The top electrode including the silvered portion of the model plate is earthed.

MINE MODELS FOR PILLAR STRESS ANALYSIS:

Nordic Mine of Rio Algom Mines Ltd., Elliot Lake, Ontario:

This mine is an example of a tabular orebody with a fairly uniform dip. This mine has two advantages, it has been used by others (39) for predicting pillar stresses on the basis of a two-dimensional deflection hypothesis, and the field measurements of some pillar stresses are also available (40) for comparison purposes.

General Geology: The regional geology of the area has been explained in detail elsewhere (41,42,43). For present purposes a brief description follows.

Nordic uranium orebody occurs within a succession of pre-cambrian sediments of the Huronian formation. A major unconformity exists between the Huronian and the pre-Huronian rocks. The formations belonging to the former group are gently folded with slight metamorphism, whereas the rocks of the latter group have been subjected to a high degree of folding and metamorphism.

This major contact has been exposed in the form of a broad Z-shaped structure (see Figure 5-2) by erosion and the northern part of this represents a synclinal fold with the Huronian sediments plunging moderately to the west. The southern part represents an anticline where the Huronian rocks have been eroded and the pre-Huronian basement exposed.

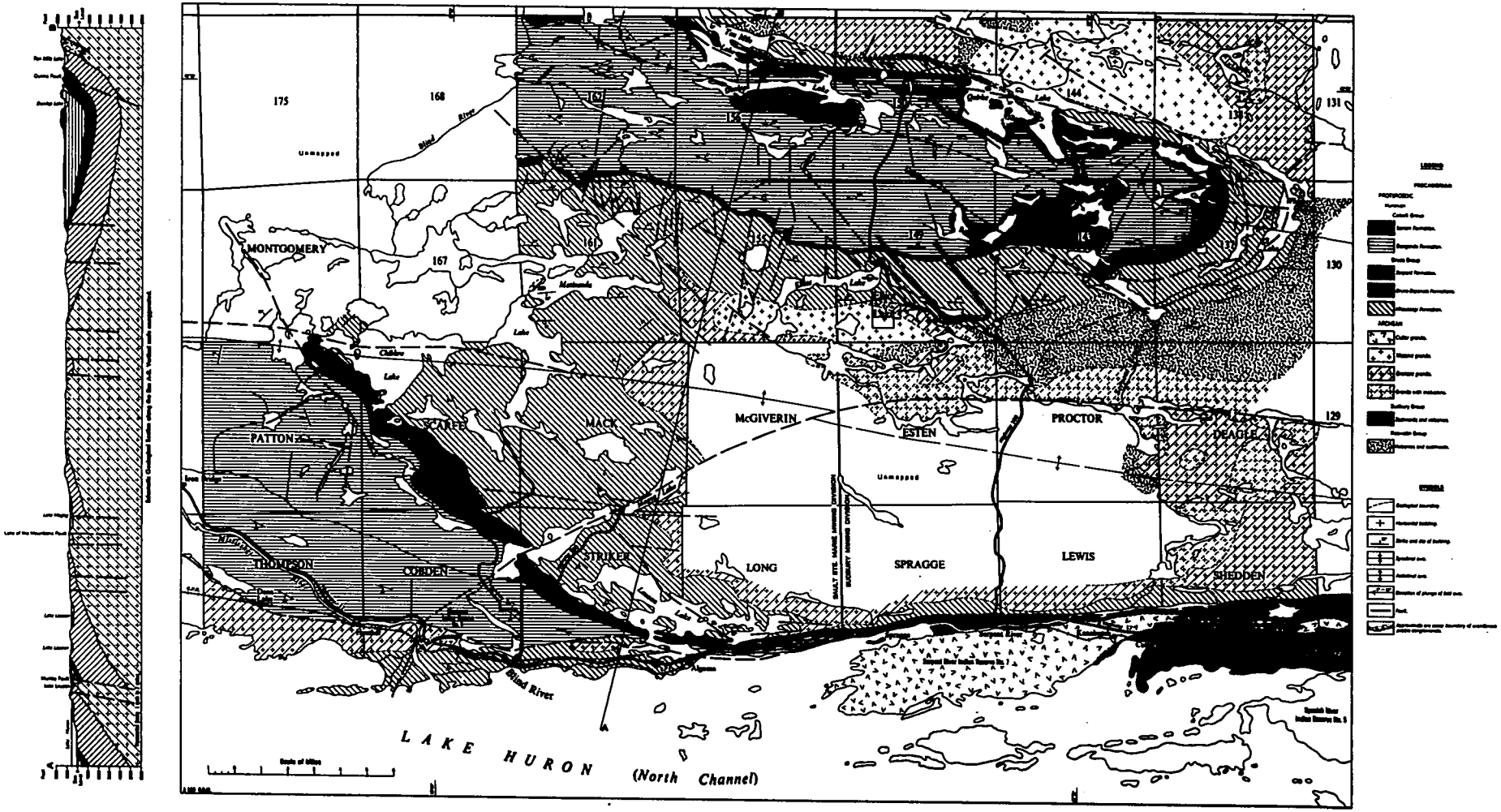

A SKETCH MAP SHOWING THE GEOLOGY OF THE BLIND RIVER AREA, DISTRICT OF ALGOMA, ONTARIO (REF.43)

FIGURE 5 - 2

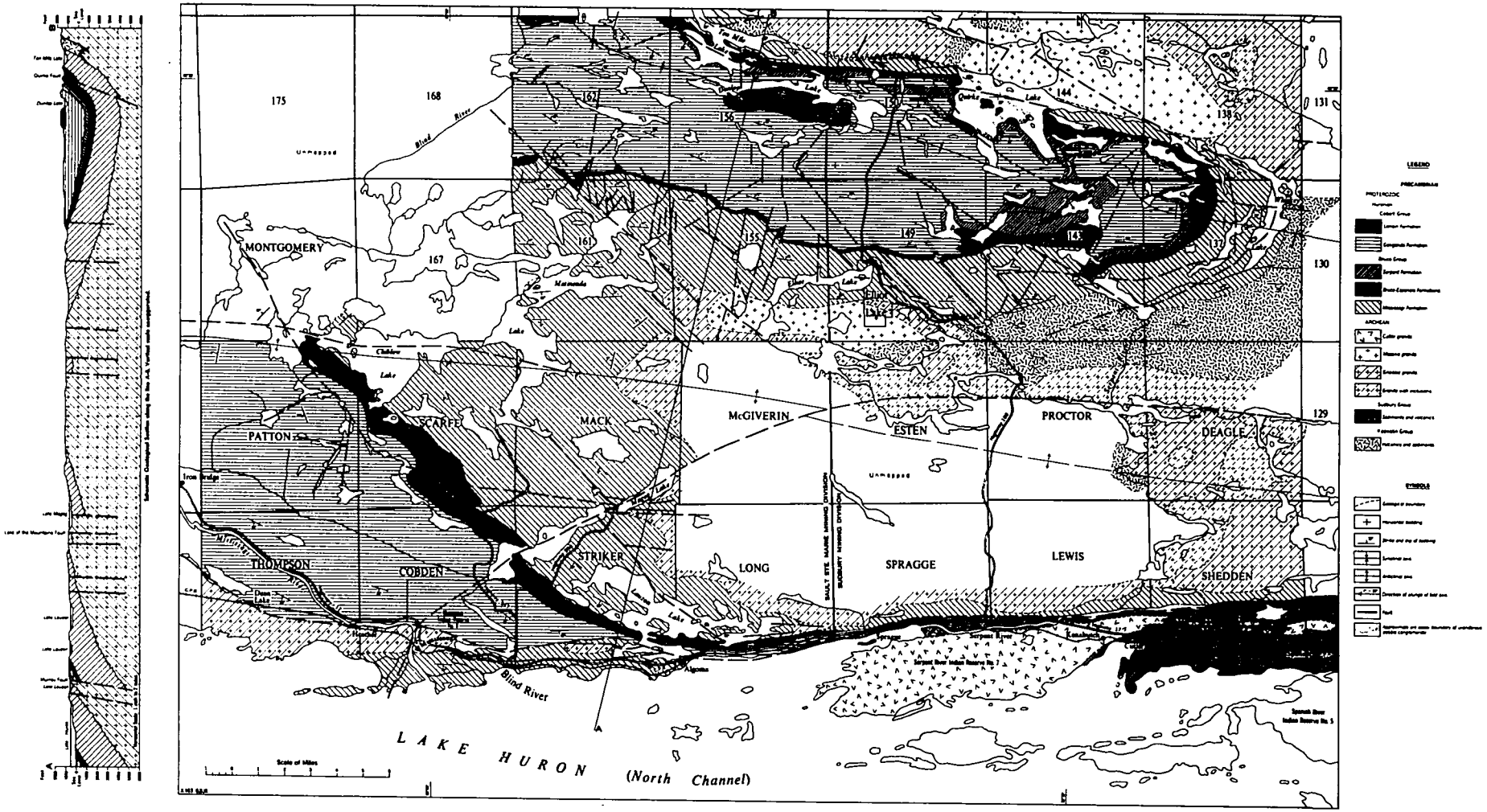

A SKETCH MAP SHOWING THE GEOLOGY OF THE BLIND RIVER AREA, DISTRICT OF ALGOMA, ONTARIO (REF.43)

FIGURE 5 - 2

The two potential ore zones are found in quartz-pebble conglometrates in the synclinal area. The mine is on the south limb of the syncline (43).

The formation is cut by several east-west diabase dikes, dipping almost vertically. Diabase sills also appear in the succession. Faults are present regionally, with strikes in the north-west and north-east directions. There is a main east-west fault. The movement has generally been the south side up and to the west.

Structural Geology: The regional folding in the region is believed to be the result of regional compression in a north-south direction. Relaxation of this compression possibly accounts for some of the east-west steep angle faults, which were subsequently introduced by diabase dikes (41,42).

The two predominant faults, in the east and west areas respectively are nearly vertical, striking N 80°E and N 80°W respectively. These are normal faults with displacements from an inch to a foot on the north side.

Fractures strike nearly east-west, and usually are normal to the reef but some have a vertical dip. They occur in groups and seldom seem to extend for more than 75 feet.

A few fractures, striking N 75°E, may be associated with minor faults further east (42).

The orebody here dips between 10 and 23 degrees to the north with an east-west strike (42).

The test area in the mine (9W9 to 1109 stopes) seems to be relatively free from faults . To the east, the predominant direction of near-vertical faults is N 80°E. To the west it is about N 80°W. These are normal faults usually with downward displacement on the north side by a few inches to a few feet (42).

The Orebody: The orebody occurs in closely packed conglomerates with quartzite and small amounts of microcline (42).

The orebody in the mine area lies close to the Archean basement at the out crops and is about 30 feet above the basement in the test area, gradually increasing to about 50 feet to the northwest. Above the orebody lies upto 500 feet of medium to coarse-grained quartizite. On the whole, it is massive and nearly monolithic. It is overlain by about 30 feet of greenstone conglomerate followed by 50-100 feet of argillite (42).

Four nearly vertical diabase dikes 50-80 feet thick cut the Huronian in the east-west direction (42). Figure 5-3 is the plan of the mine showing the mining boundary, the test locations and the three dikes cutting the orebody in east-west direction.

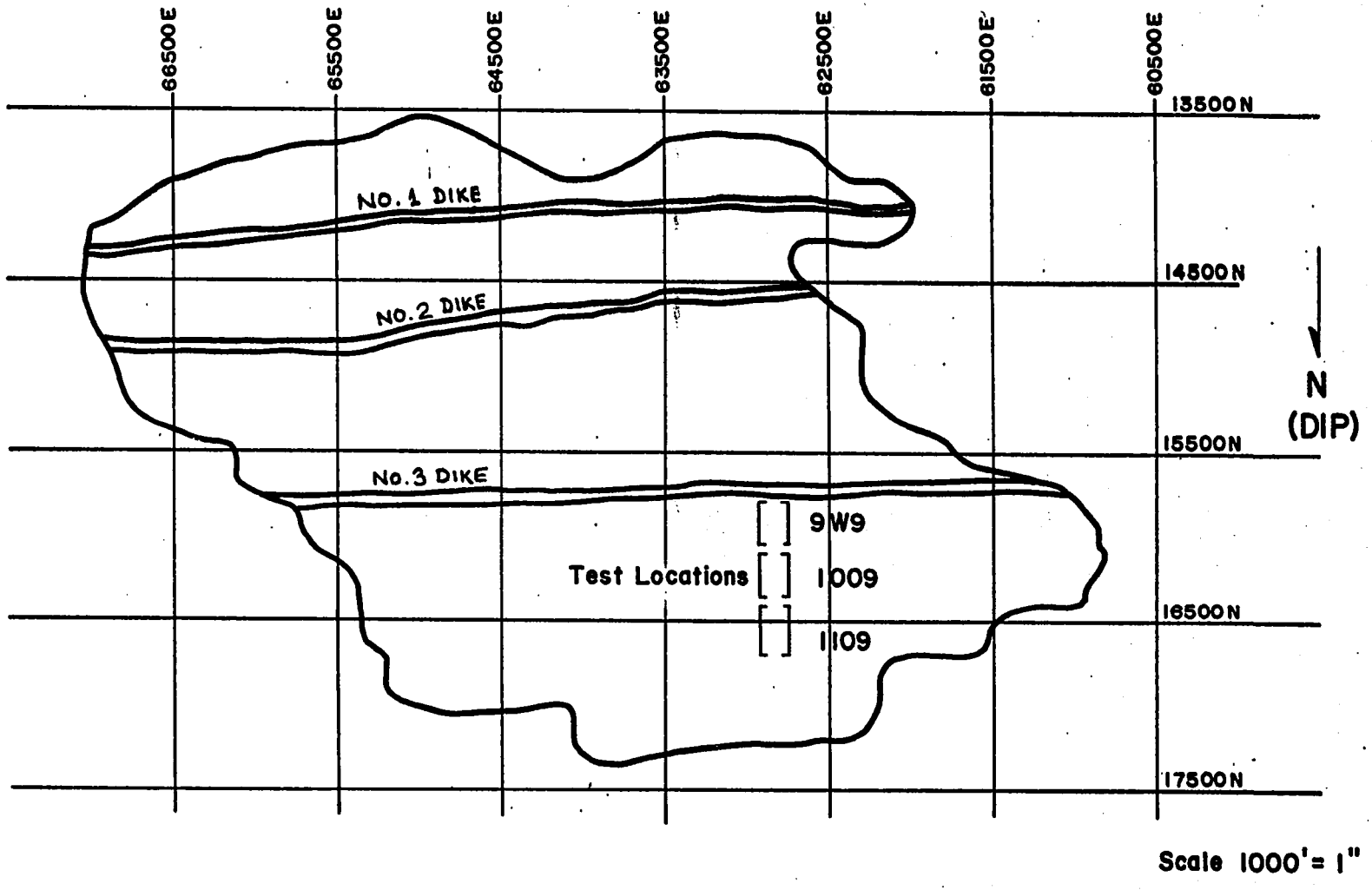

DIP REDUCED MINE PLAN OF NORDIC MINE
(SHOWING 1965 OUTLINE OF WORKINS AND DIKES)

FIGURE 5-3

Mining Method: The mining is a conventional room and pillar operation. A section of the workings is shown in Figure 5-4. (This area has been used for the measurements, in the field and the locations of drill holes are indicated by the respective numbers in three stopes, such as 9-1R, 10-1L, 11-1C etc.) Haulages are driven on strike, stopes are between 200 to 350 feet length. Raises are carried up-dip to leave a central pillar 10 foot wide, between two stopes each 65 feet on strike mined to a width (height) varying from 7 to 14 feet. A crown pillar about 15 feet in breadth is nominally left between the top of the rooms and the haulage-way above.

Field Measurements of the Pillar Stresses:

Method of Measurement : The in-situ stress measurements in the pillars in this mine have been obtained using the borehole deformation meter developed by the Unites States Bureau of Mines (61). This technique consists of drilling an EX hole (1.5 inches in diameter) into the rock. The deformation meter is then inserted into the hole which, in effect acts as a feeler gauge. As the rock surrounding the hole is in compression due to the stresses in the ground, the hole is actually drilled into the rock when it is in a deformed state (61). The stress in the rock is then relieved by overcoring the hole with a 6-inch bit. As the stress is relieved the rock expands, which increases the diameter of the EX hole . The deformation meter then measures this increase in diameter in the specific directions. The measuring element is a beryllium copper cantilever on which four resistance gauges are mounted and

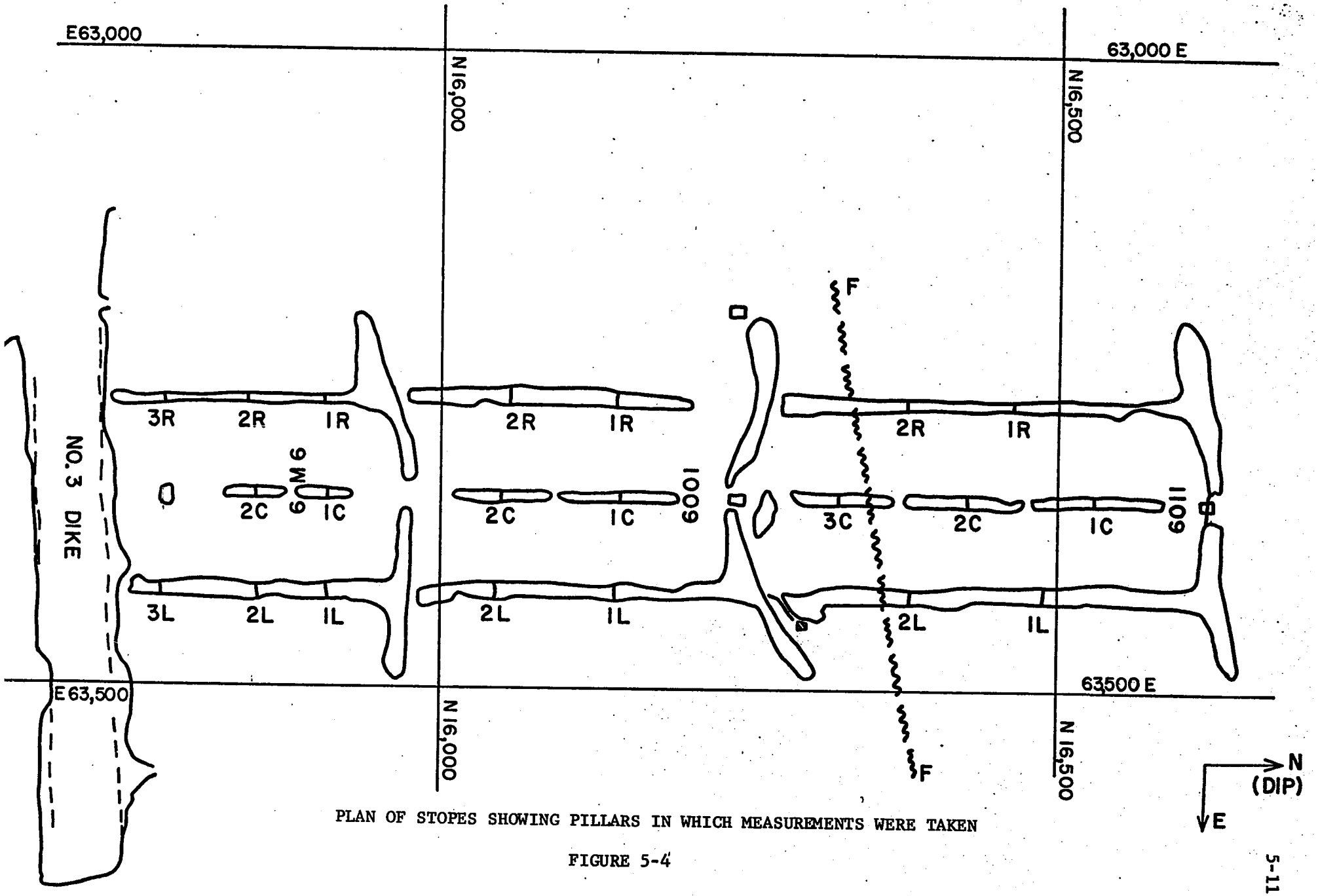

PLAN OF STOPES SHOWING PILLARS IN WHICH MEASUREMENTS WERE TAKEN

FIGURE 5-4

connected to form a Wheatstone bridge. The cantilever also produces the force required to keep the position in contact with the side walls of the borehole.

From the measured increase in the diameter of the EX hole, resulting from the release of the surrounding stress by overcoring, it is possible to calculate the stresses acting in the plane perpendicular to the axis of the hole. The deformation is dependent on the amount of stress being relieved and the modulus of deformation of the rock.

The drilling operation is carried out with a skid-mounted machine with a hydraulic head, powered by two-cylinder, four stroke piston type compressed air motor (40). A short length of 6-inch core is first taken from the rock face to get past the surface fracture zone. The hole is then centered for EX core barrel by placing guides and then drilled about 10 feet ahead of the 6-inch core face.

The deformation meter is initially placed in the EX hole at the desired orientation 6 to 9 inches from the collar. The cable connecting the meter inside the hole and the strain indicating device outside is brought out through the drill rods. The difference between the initial reading and the final reading during the overcoring operation is a measure of the amount of deformation or expansion of the EX hole.

After overcoring one position, the 6 inch core is broken off, the end of the hole withdrawn and marked for location of the deformation

measurement.. However, in some cases the measurements are lost owing to the premature breaking of the core during the overcoring operation. This is believed to be a result of weekly cemented joint planes or from the discing and fracturing (40).

The Results: The results of the pillar stress measurements in this mine are given in Table 5-1. These measurements have been made at the locations shown in Figure 5-4. The breadth of the pillars in this area varied from 8 to 15 feet. The depth below the surface to the measuring holes varied from 850 to 1010 feet. The major principle stresses (measured) varied from 7500 psi to 15600 psi (40).

The measurements at locations 9-1R, 9-2C and 11-1R could not be obtained as a result of discing during overcoring. This is believed to be an indication of higher stresses at these locations. The major principal stress was neither vertical nor normal to the plane of the ore but was inclined up-dip at an angle of about 30^{o} to the orebody. This inclination shows that shear stresses exist on planes parallel to the walls. However, the magnitude of these stresses is relatively low. It is probable that most significant pillar stresses are those normal to the hanging and footwalls. These values vary from 5480 psi to 13700 psi with possibly higher values at locations where discing occurred (40).

TABLE 5-1

Average Pillar Stresses from Field Measurements (40)

B = breadth of pillar

z = depth from ground surface

σ_p = stress normal to walls in pillar

No.	B(ft.)	z(ft.)	σ_p (psi)
9-1R	9.4	870	-
9-2R	8.3	860	8,200
9-3R	7.7	850	10,360
9-1L	14.5	870	7,700
9-2L	8.7	860	7,630
9-3L	10.7	850	13,700
9-1C	10.7	870	5,480
9-2C	8.8	860	-
10-1R	10.2	910	7,270
10-2R	15.2	890	8,010
10-1L	14.8	910	6,840
10-2L	14.2	890	6,340
10-1C	8.7	910	12,260
10-2C	9.7	890	8,150
11-1R	8.3	1000	-
11-2R	13.6	980	10,460
11-1L	13.6	1000	9.190
11-2L	10.7	980	10,580
11-1C	8.2	1010	10,210
11-2C	11.2	990	9,320
11-3C	10.3	960	10,230

Predicted Pillar Stresses:

The model study for Nordic mine is based on the mine plan (Figure 5-3) mapped in 1965 (42). The parameters and the constants of the mine used for this study are discussed below.

The field stress measurements at Nordic have been made at sites 900 feet to 1100 feet away from the active mining zones (40). The representative nature of these observations has been discussed by Coates (39), and he has suggested a k-factor (i.e. $S_t/S_o = k$) of 3.36. These observations have shown that the horizontal components of field stress are greater than the vertical. It has been suggested (39) also that the gravitational stress should be used for the vertical field stress. For all calculation made in this study the ratio between S_t and S_o and S_x and S_o has been taken as 3.36 due to lack of data to the contrary.

The centre of the mine model is defined by the intersection of 15500 N and 64000 E grid lines, (approximately on the seventh level). The depth of this point from the surface is about 725 feet, which gives a gravity load of 840 psi. The normal component of the field stress, S_o, is based on the gravity load of 840 psi, a k-factor of 3.36 and an average dip of 14 degrees. This gives a value of 950 psi for S_o.

The elastic moduli selected are a result of a review of various laboratory tests conducted (43,44,45,46) on the pillar and wall rock of Nordic Mine. The values thus selected are 12×10^6 psi and 0.18 for the Modulus of Elasticity and Poissons Ratio, respectively, for both wall and pillar rocks.

Other constants are average dip of the orebody 14 degrees, average height of the pillar 8 feet and the average breadth of the pillar 10 feet.

The normal displacements calculated from the model are at the locations where the pillar stresses have been measured in the field, as shown in Figure 5-4. The mine coordinates of these locations had to be transferred to the tank coordinates with a linear scale reduction. The scale factor, S, used was 6000.

It may again be mentioned here that Equation (2-12) developed for predicting pillar stresses is a function of the variable δ_w, the displacement as a result of 100 percent extraction, $\delta_{w(c)}$ the displacement at the centre of the total mining zone. In other words, it may be said that for determining pillar stresses, within irregular mining outlines, with a three-dimensional approach the analogue provides us with only two variables δ_w for each point of reference and $\delta_{w(c)}$. The other terms in Equation (2-12) are constant for a (mine) model. The desired curvature of the bottom electrode to simulate dip of the orebody is obtained from Equation (A-27).

Thus knowing the size of the pillars, the percentage extraction ratio (R), the elastic properties of the wall rock and pillar rock, the normal and horizontal components of the field stresses together with δ_w and $\delta_{w(c)}$, Equation (2-12) can be used to predict the pillar stresses.

The pillar stresses predicted by Equation (2-12) are based on 86 percent extraction and not 84 percent as used earlier (39). The figure of 86 percent was the result of a thorough planimeter survey of the mine plane by the author. These results are the data in Table 5-2.

TABLE No. 5-2

Predicted Pillar Stresses

S_o = 950 psi, k = 3.36, $E = E_p = 12.0 \times 10^6$ psi, $\mu = \mu_p = 0.18$

h = 4.0 ft., B = 10.0 ft., R = 0.86, $\delta_{w(centre)}$ = 27.299 m m

No.	δ_w(m m)	σ_p(psi)
9-1R	18.450	9,598
9-2R	16.271	8,568
9-3R	12.348	6,713
9-1C	18.288	9,522
9-2C	15.532	8,219
9-1L	24.156	12,297
9-2L	18.741	9,736
9-3L	13.118	7,077
10-1R	23.479	11,977
10-2R	22.987	11,744
10-1C	25.634	12,996
10-2C	24.713	12,560
10-1L	26.402	13,378
10-2L	25.011	12,701
11-1R	18.068	9,418
11-2R	18.768	9,749
11-1C	18.665	9,700
11-2C	19.897	10,274
11-3C	21.902	11,231
11-1L	20.324	10,485
11-2L	21.868	11,215

DISCUSSION OF RESULTS:

Figures 5-5, 5-6 and 5-7 show the comparison along the sectional lines passing through the right rib, central and left rib pillars (see Figure 5-4) of the predicted and measured values of these stresses. These locations are spread along three stopes 9W9, 1009 and 1109. By the study of these figures it is apparent that there is some agreement between predicted and measured pillar stresses at most of the locations.

The measured values in Figures 5-5 and 5-7 are very similar in general trend while the measured values in Figure 5-6 show entirely a different trend. On the other hand the predicted values in all the three diagrams are relatively similar in trend. The average of measured values in 9W9 stope (8857 psi) and 1109 stope (9998 psi) show a reasonable agreement with the predicted averages of 8341 psi and 10296 psi for 9W9 stope and 1109 stope respectively. The predicted values in 1009 stope are higher than the measured values although location 10-1C shows a close agreement.

The best agreement between predicted and measured values are found in Figure 5-6, the central section of the test area.

On examining the structural features in the three stopes the following observations may be noted.

1. The plan of 9W9 (Figure 5-8) shows the distribution of joints or fracture lines that could be observed in the roof of the stope. In addition number 3 dike forms the southern boundary of the stope.

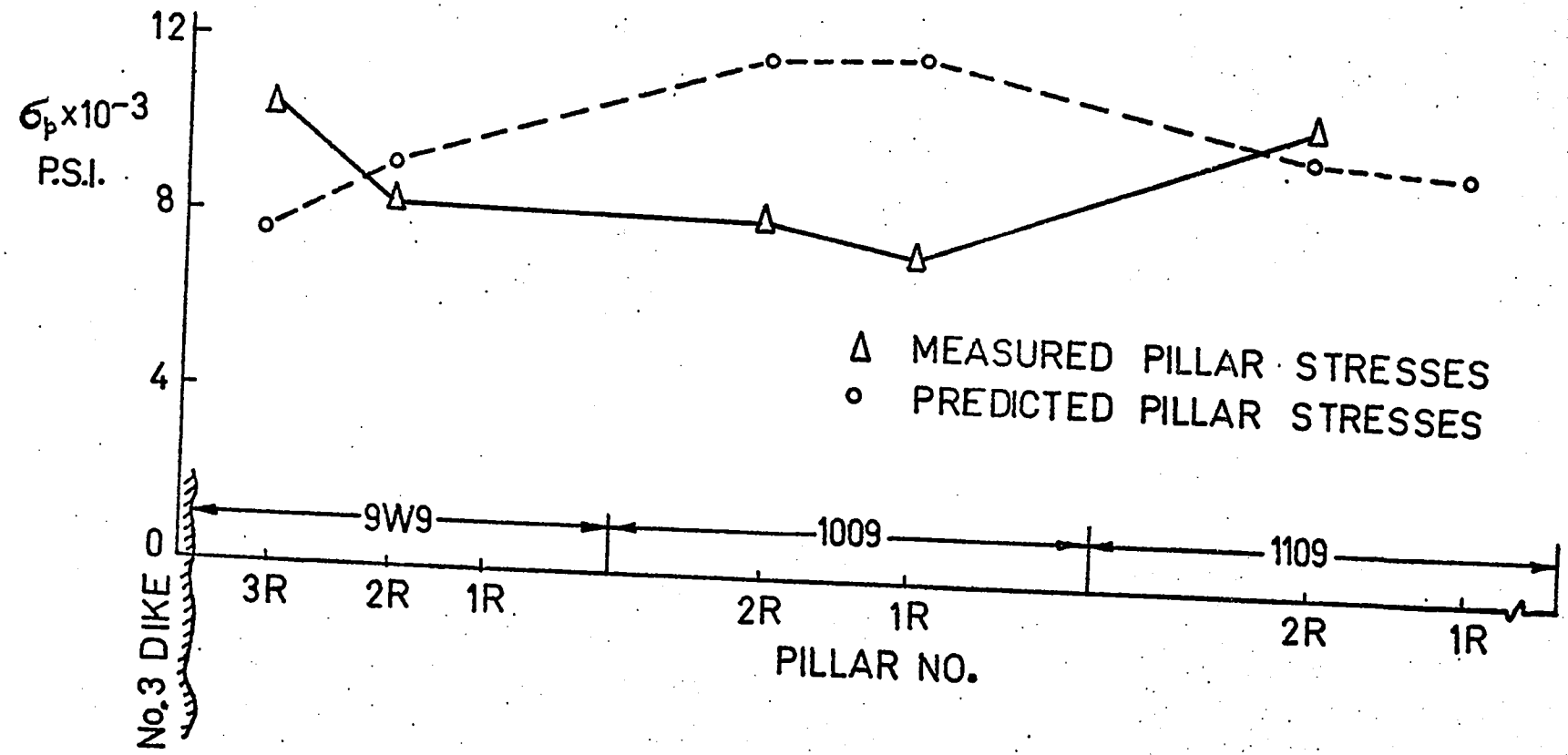

COMPARISION BETWEEN THE MEASURED AND THE PREDICTED PILLAR STRESSES THROUGH THE RIGHT RIB PILLARS

FIGURE 5-5

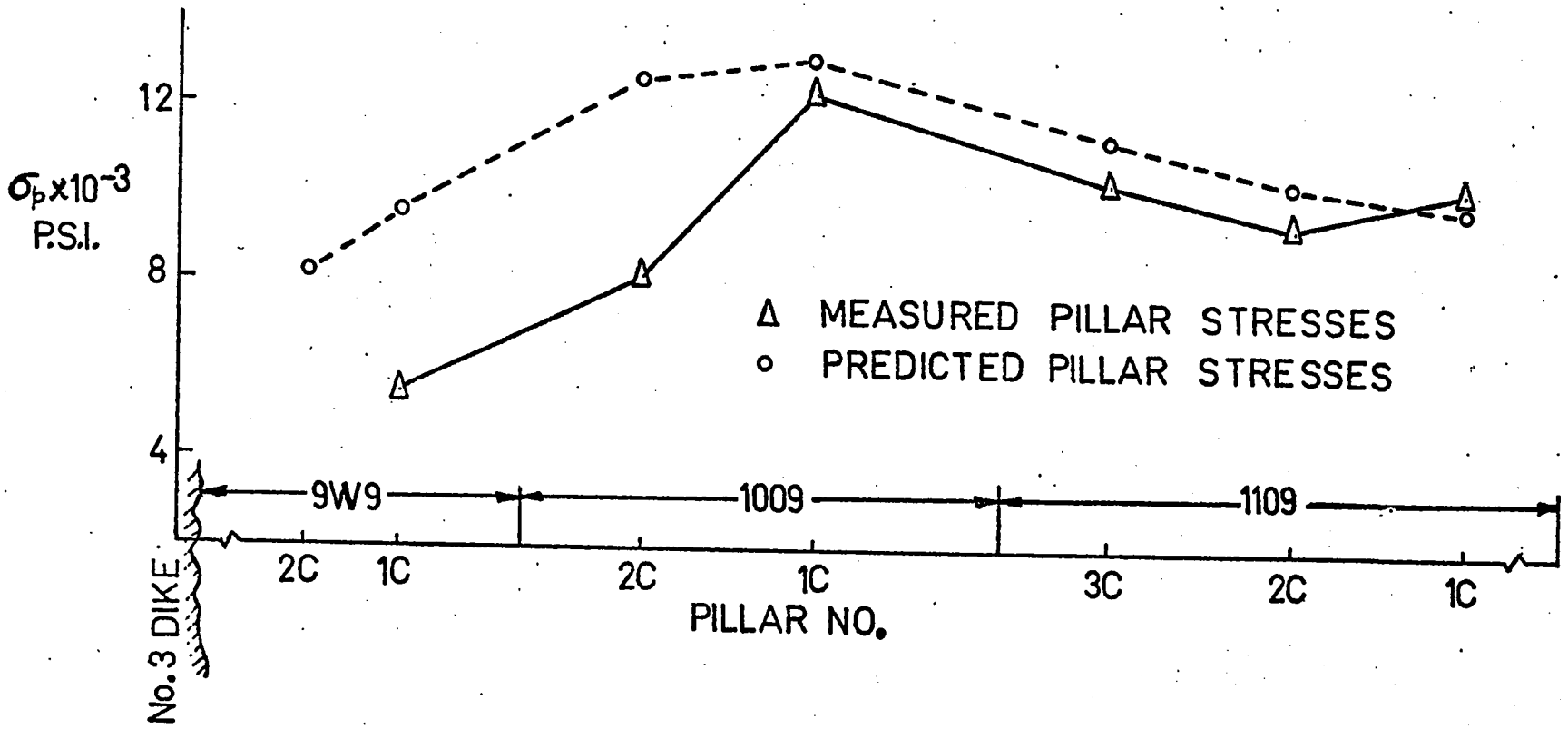

COMPARISION BETWEEN THE MEASURED AND THE PREDICTED PILLAR STRESSES THROUGH THE CENTRAL PILLARS

FIGURE 5-6

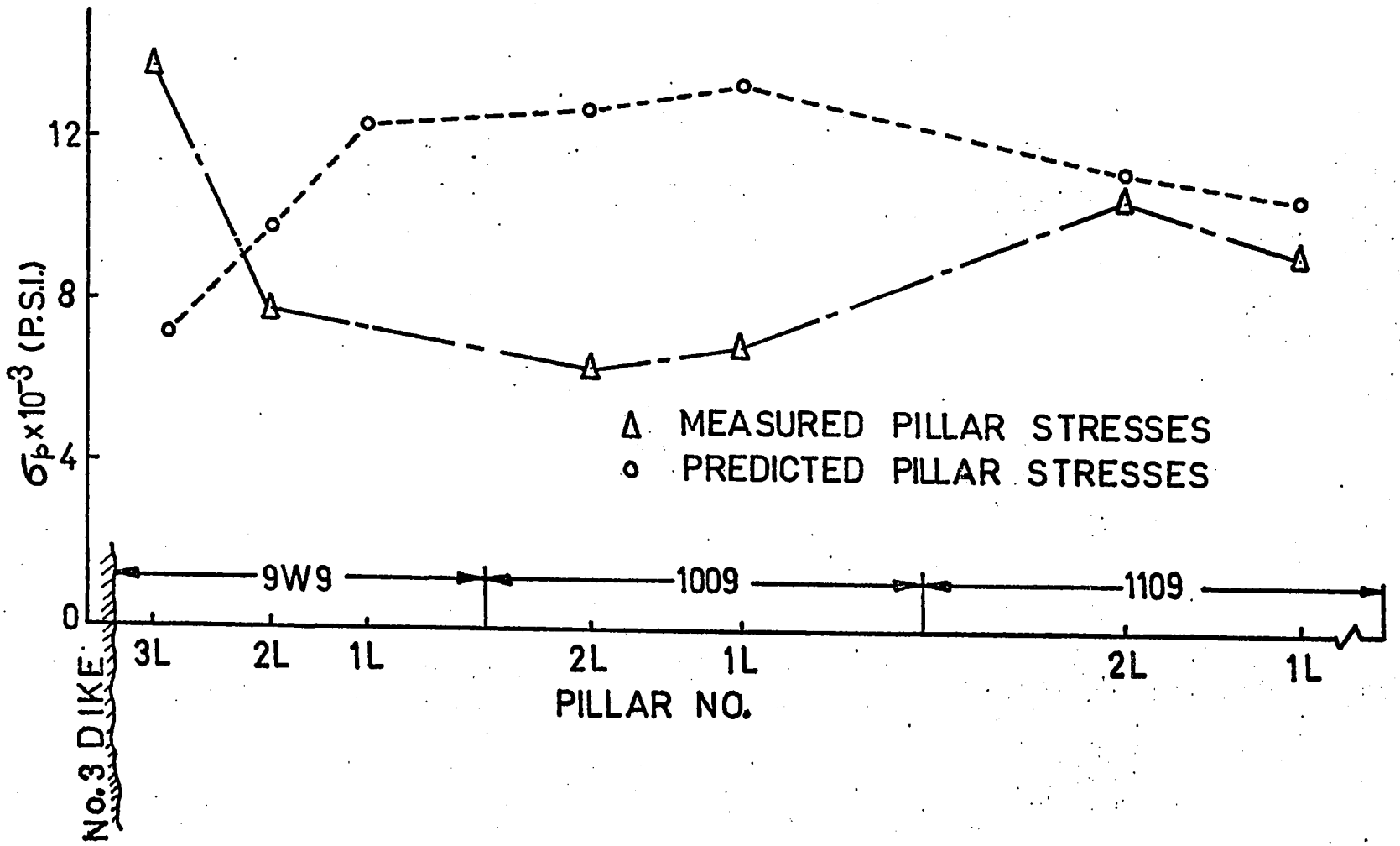

COMPARISION BETWEEN THE MEASURED AND THE PREDICTED PILLAR STRESSES THROUGH THE LEFT RIB PILLARS

FIGURE 5-7

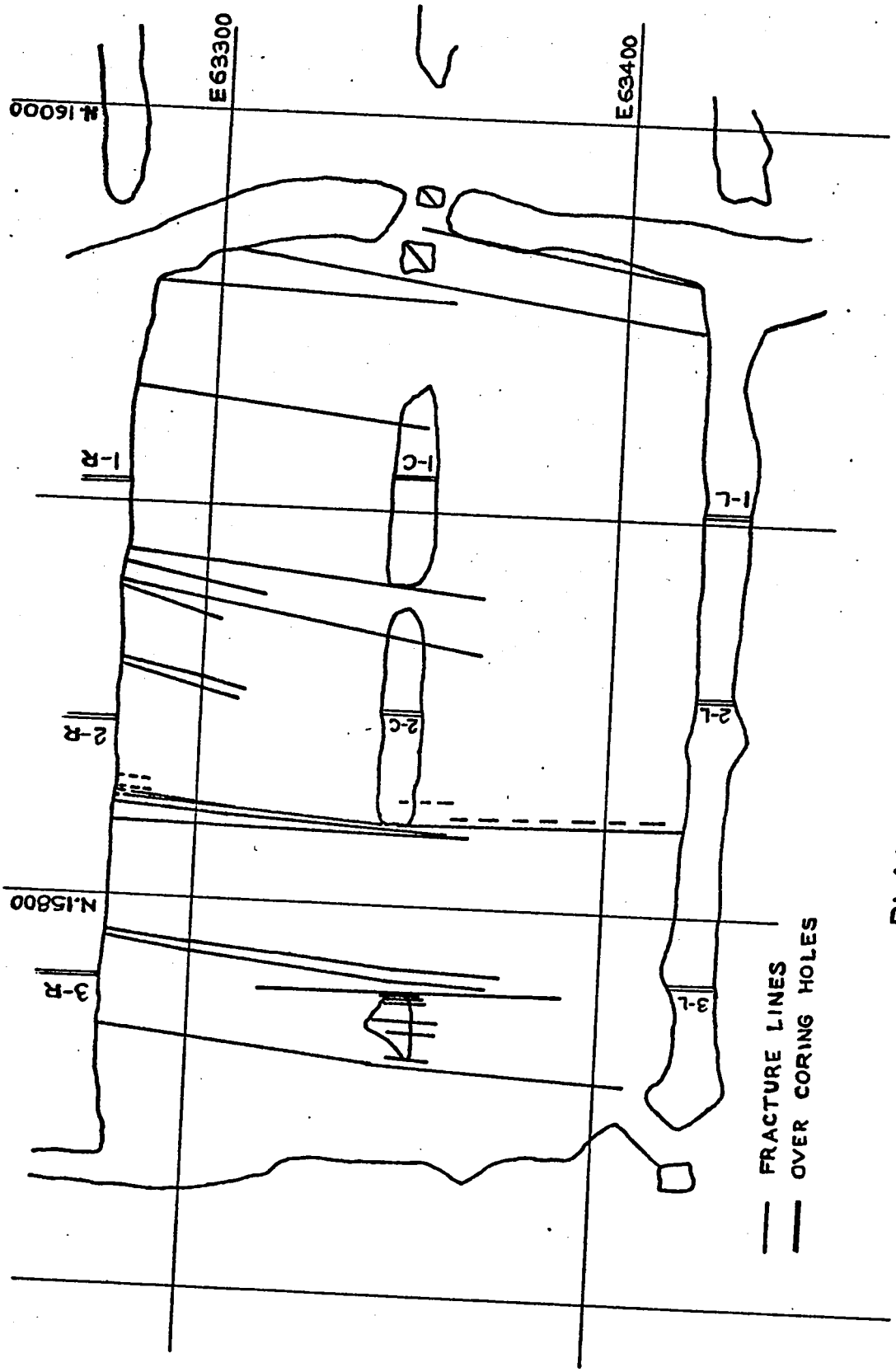

PLAN OF STOPE 9W9 (Ref. 42)

FIGURE 5-8

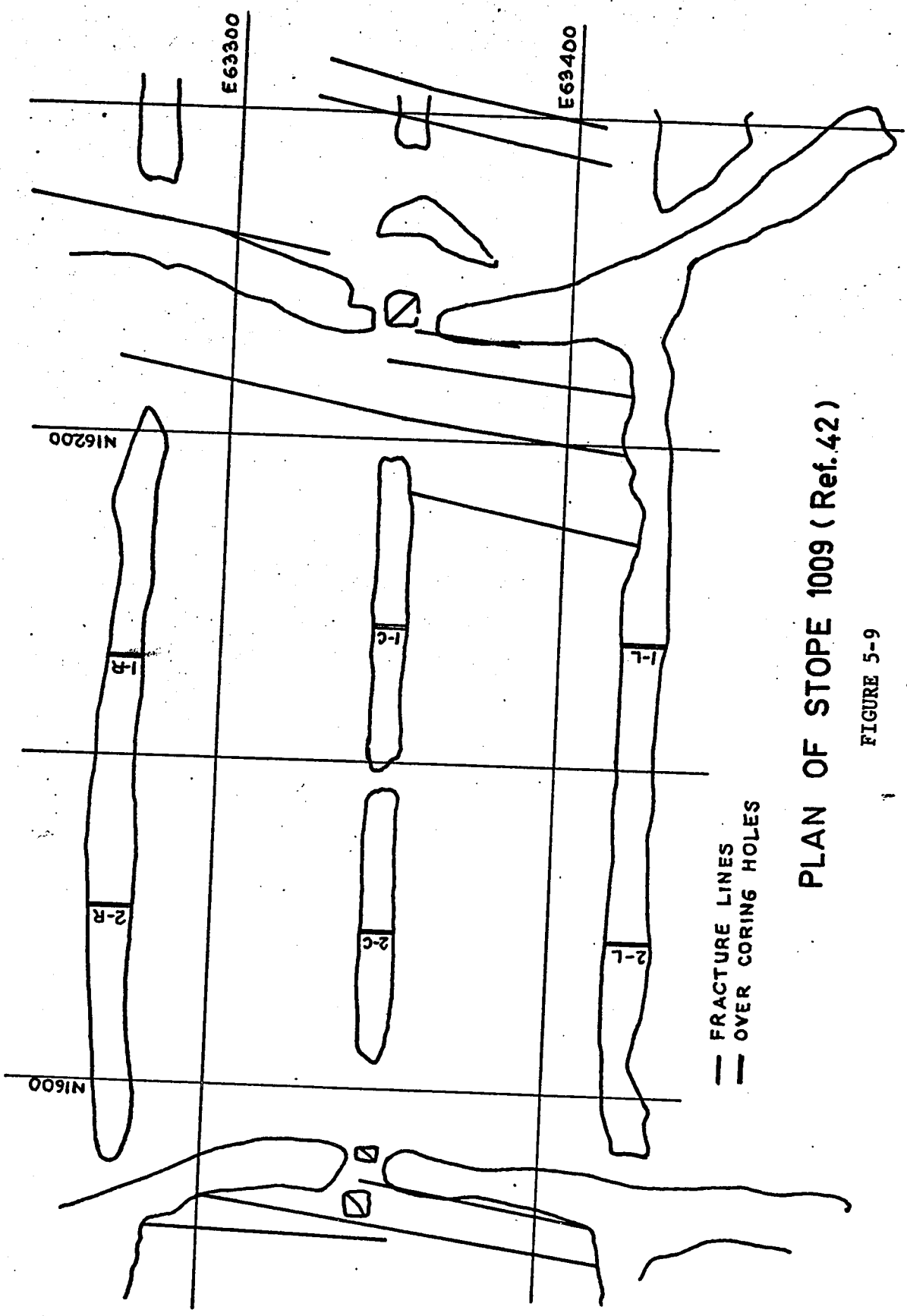

PLAN OF STOPE 1009 (Ref. 42)

FIGURE 5-9

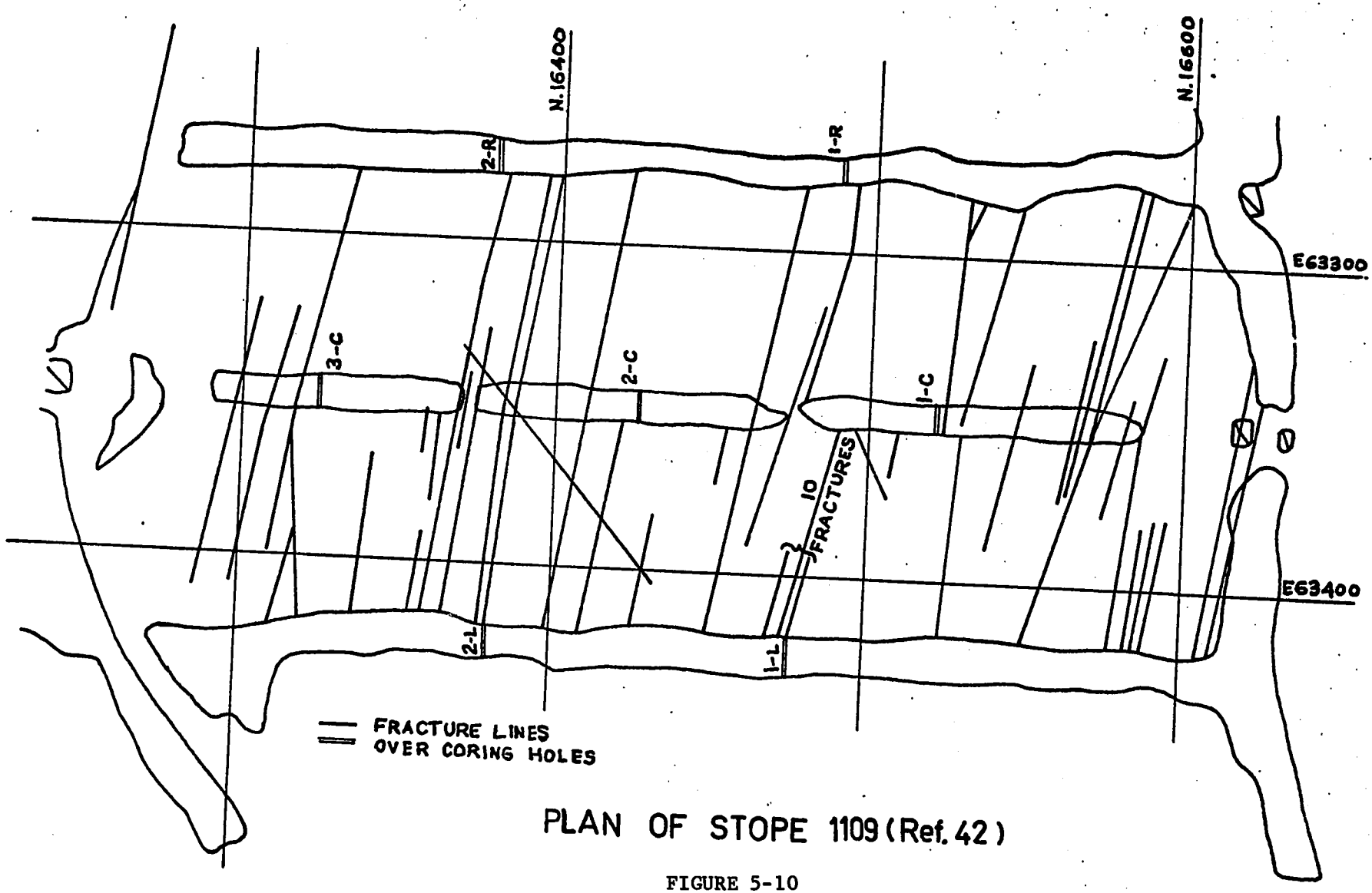

PLAN OF STOPE 1109 (Ref. 42)

FIGURE 5-10

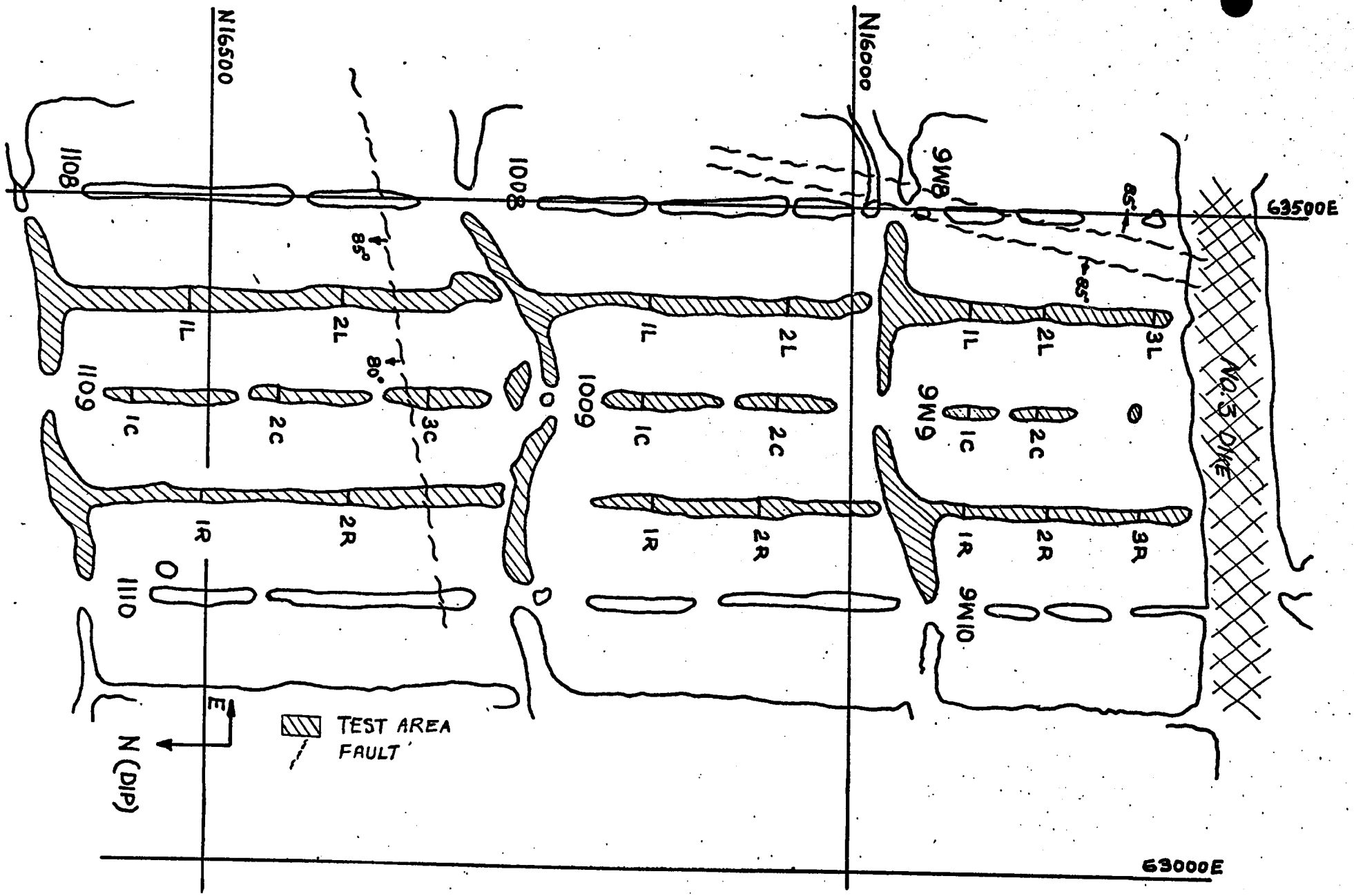

PLAN SHOWING THE FAULTS IN AND ADJACENT TO THE TEST AREA

FIGURE 5-11

2. 1009 stope on the other hand is free of dikes and faults, and the frequency of joints is relatively less than in 9W9 and 1109 stopes (Figure 5-9).

3. 1109 stope has a fault passing through it (see Figure 5-11), and the frequency of joints or fracture lines is relatively high (Figure 5-10).

4. A study of the area adjacent to the test locations shows the presence of two normal north-south striking faults which dip around 80-85^{o} but opposite to each other (Figure 5-11). These faults appear to have influenced the measured values particularly in the row of left rib pillars.

It is reasonable to conclude that the geological disturbances caused or contributed to the local variations in the measured pillar stresses in the three stopes. It has been shown (47,48) that the post-mining adjustments are influenced by the spatial distribution of the joints.

The measured and predicted stress values were further compared on contour maps shown in Figures 5-12 and 5-13. Close examination of these diagrams show that the measured values and the predicted values exhibit NE-SW trends. Furthermore, there is relatively close agreement between the two contour maps in 1109 stope and the western right rib section of 9W9 stope. The discrepancy is greatest in the eastern half (left rib and central section) of the 1009 stope. To clarify the extent of the discrepancies between the measured and predicted values,

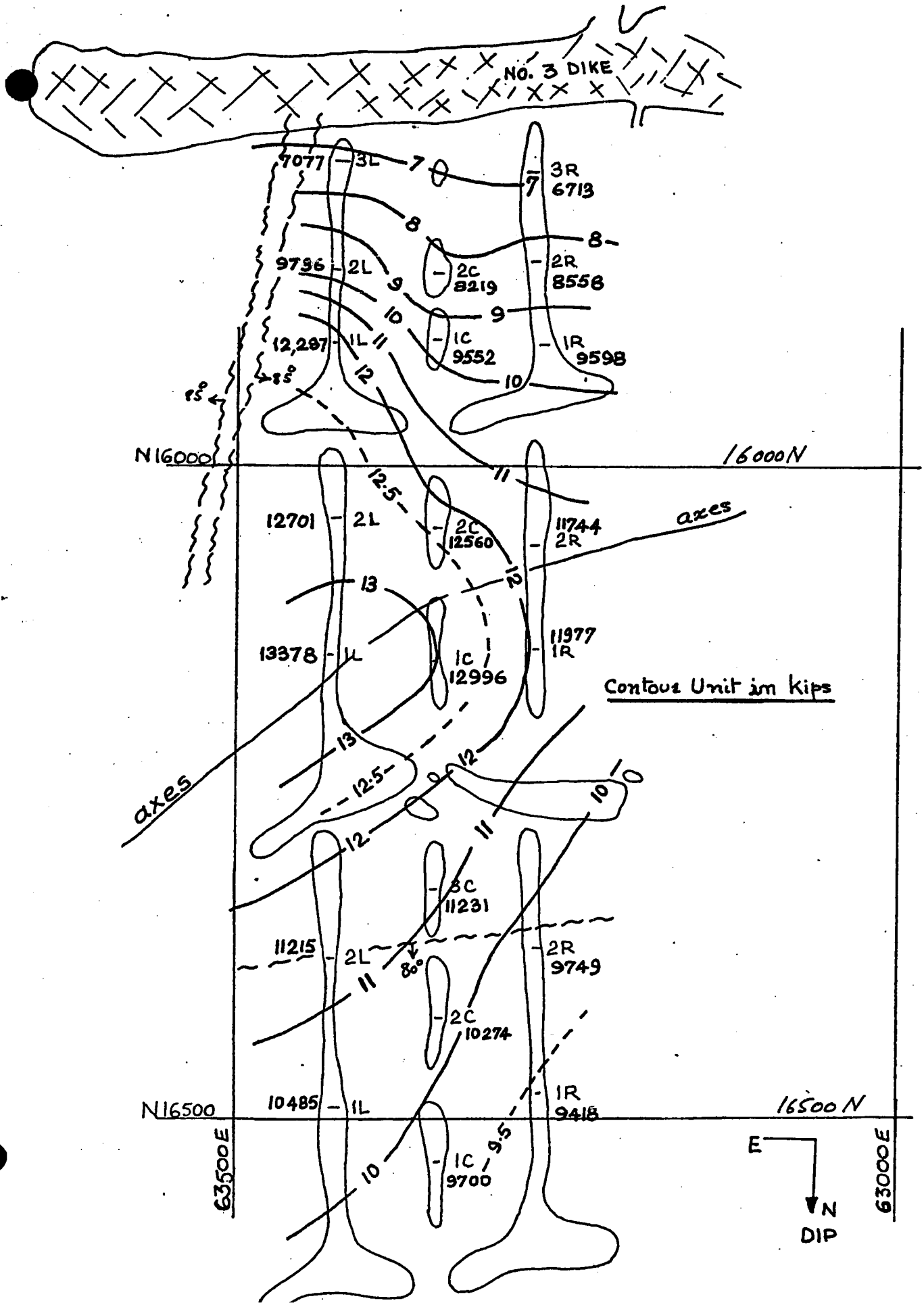

A CONTOURED DISTRIBUTION OF PREDICTED VALUES

FIGURE 5-12

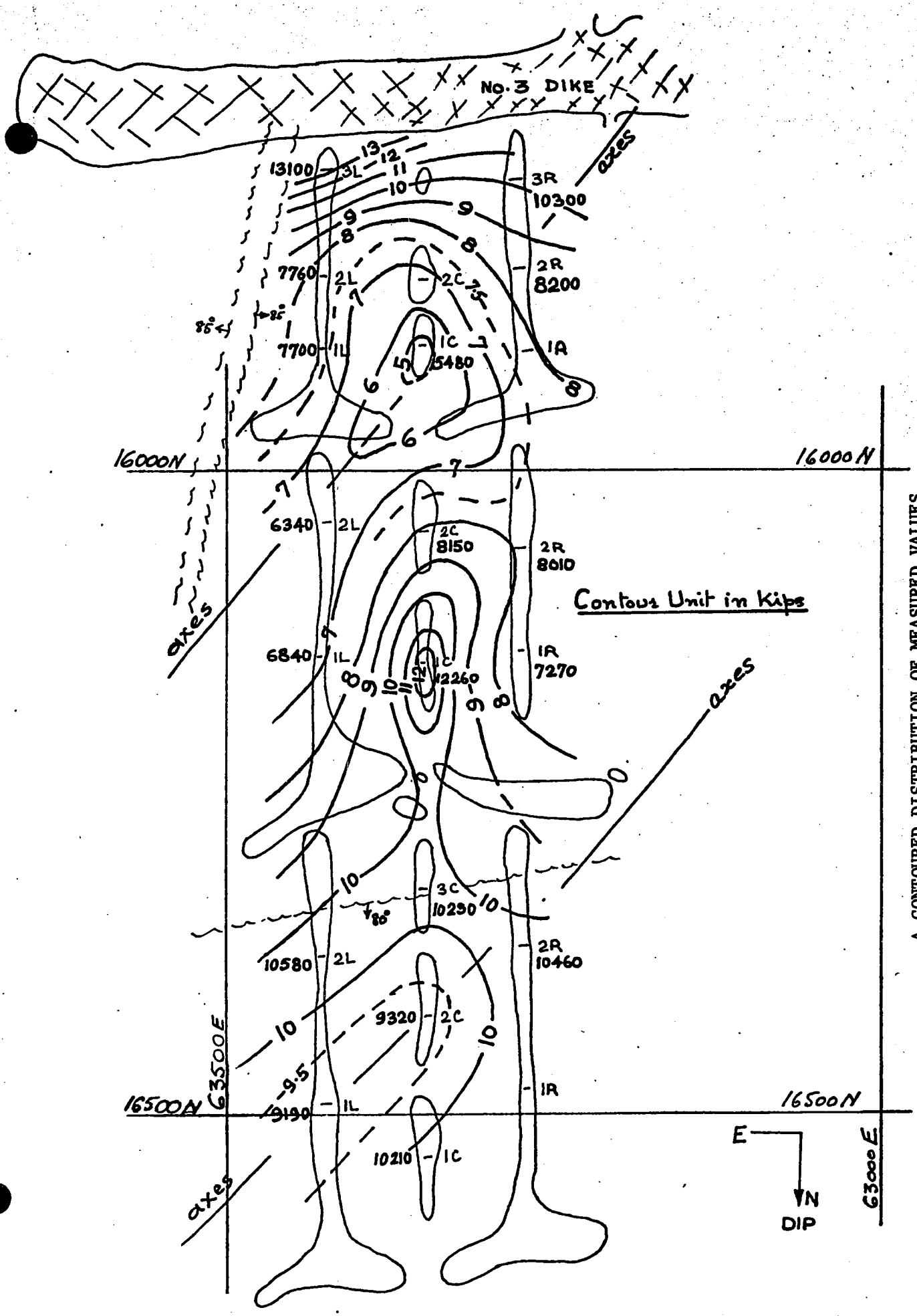

FIGURE 5-13

A CONTOURED DISTRIBUTION OF MEASURED VALUES

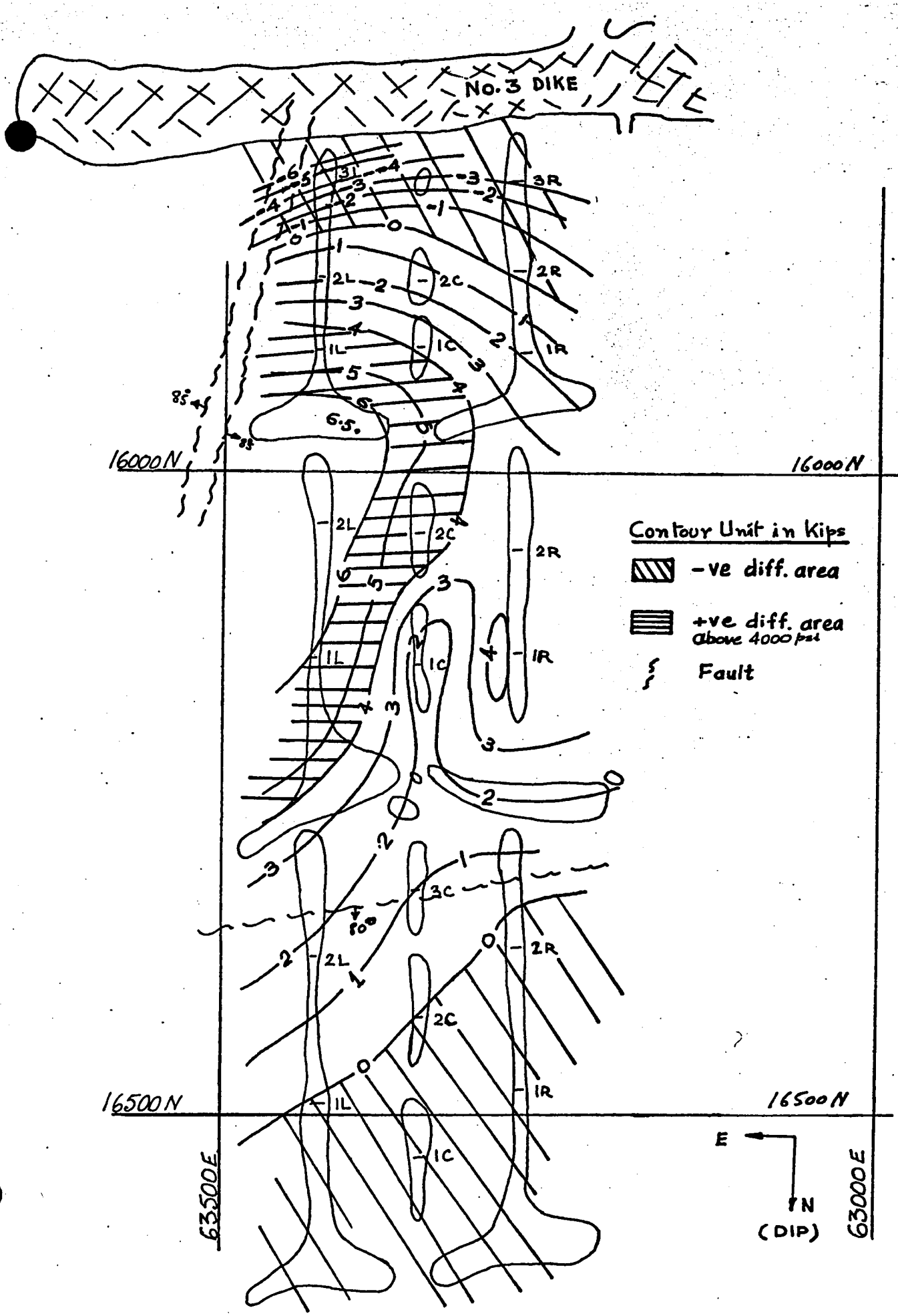

A CONTOURED DISTRIBUTION OF DISCREPANCES BETWEEN PREDICTED AND MEASURED VALUES

FIGURE 5-14

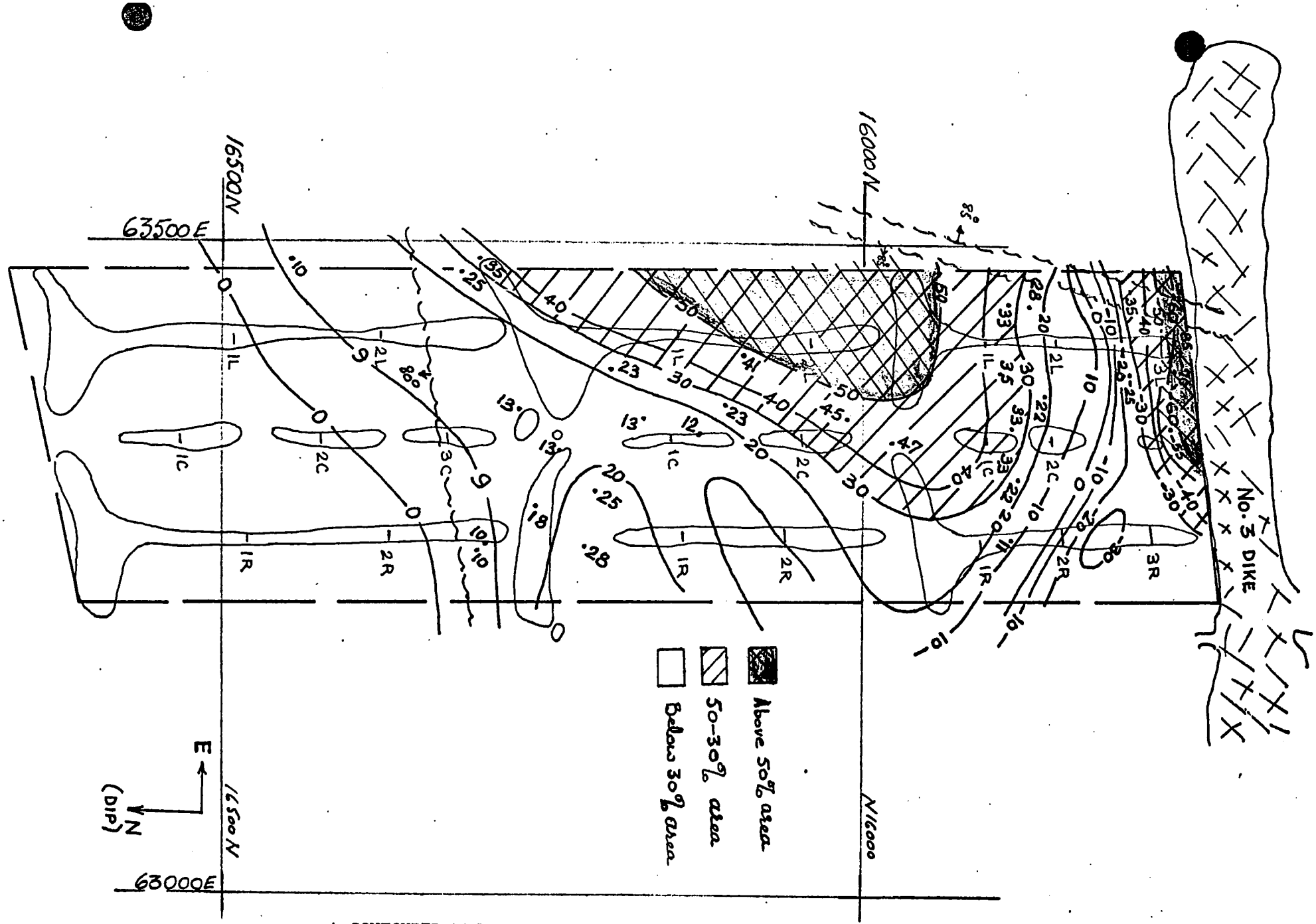

A CONTOURED DISTRIBUTION OF PERCENTAGE DISCREPANCES BETWEEN

PREDICTED AND MEASURED VALUES

FIGURE 5-15

a third contour map was drawn, Figure 5-14, in which the differences between the predicted and measured stresses are plotted. This map shows that in the majority of the area the discrepancy is less than 4000 psi or 30 percent (see Figure 5-15) of the predicted values.

The areas of disagreement are essentially on the eastern flank (left rib section) of the test area and appears to be directly due to the influence of N-S faults, mentioned earlier, and shown in these diagrams.

To compare measured and predicted values, it would, therefore, be necessary to remove structurally influenced measured stress readings. It is realized, that this may oversimplify the measured stress pattern but it should be acceptable in the comparison contemplated, because the tank analogue represents a simple model.

A similar model study was made without simulating the dikes. Figure 5-1 shows the photograph of this model. The pillar stresses thus predicted are given in Table 5-3. The most significant thing to observe in this study is that the predicted stresses in 9W9 stope are higher than in 1009 and 1109 stopes. This is due to the fact that 9W9 stope is practically in the mid span with respect to the geometry of the whole reef plane. Such a location will call for higher displacement values and thus higher pillar stresses. The absence of dikes has not only influenced the values of 9W9 stope but that of 1009 and 1109 stopes as well. These results are higher than the ones previously calculated.

TABLE 5-3

Predicted Pillar Stresses (Dikes removed)

S_o = 950 psi, k = 3.36, $E = E_p = 12.0 \times 10^6$ psi, $\mu = \mu_p = 0.18$

h = 4.0 ft., B = 10.0 ft., R = 0.86, $\delta_{w(centre)}$ = 65.00 m m

No.	δ_w(m m)	σ_p(psi)
9-1R	63.803	14,288
9-2R	64.011	14,332
9-3R	64.203	14,372
9-1C	63.745	14,276
9-2C	64.036	14,337
9-1L	62.988	14,117
9-2L	63.531	14,231
9-3L	63.963	14,322
10-1R	59.624	13,412
10-2R	60.673	13,632
10-1C	58.895	13,259
10-2C	60.466	13,589
10-1L	59.237	13,331
10-2L	60.715	13,641
11-1R	51.149	11,636
11-2R	51.873	11,788
11-1C	50.022	11,400
11-2C	51.292	11,666
11-3C	53.827	12,197
11-1L	50.180	11,433
11-2L	51.887	11,791

It may be argued that such a simulation is not logical because one cannot ignore the presence of dikes in the mine but at the same time it is a good academic exercise to prove the effect of dikes as a massive support.

A comparison has been made using three different approaches, tributary area method, two-dimensional deflection hypothesis and the three-dimensional method. These calculated values in terms of stress concentrations are given in Table 5-4.

The tributary area method predicts that the concentration of stresses is the same at all the locations, while the two-dimensional hypothesis based on improved theory (Equation 1-2(b)) predicts the minor variations. The three-dimensional appraoch is believed to be more valid to actual mining conditions, as the pillar loading within the whole mining zone is a function of the geometry of workings in both dip and strike directions. For example, the range of stress concentrations predicted by Equation (1-2(b)) is from 5.14 to 6.18, on the other hand the range of concentrations varies from 6.07 to 13.08 using Equation (2-12). These concentrations for the three sections of pillars (right, central and left) are plotted in Figures 5-16 through 5-18. The significant differences are quite evident.

TABLE 5-4

Comparison of the Predicted Pillar Stresses using three Different Approaches

(1) Tributary Area Method
(2) Two-Dimensional Deflection Hypothesis
(3) Three-Dimensional Method

No.	1	2	3
9-1R	6.14	-	9.104
9-2R	6.14	5.333	8.019
9-3R	6.14	5.165	6.066
9-1C	6.14	5.453	9.023
9-2C	6.14	-	7.651
9-1L	6.14	5.325	11.943
9-2L	6.14	5.141	9.248
9-3L	6.14	5.487	6.449
10-1R	6.14	6.177	11.607
10-2R	6.14	5.814	11.362
10-1C	6.14	6.129	12.679
10-2C	6.14	5.823	12.221
10-1L	6.14	6.187	13.081
10-2L	6.14	5.869	12.369
11-1R	6.14	-	8.913
11-2R	6.14	5.691	9.262
11-1C	6.14	5.398	9.210
11-2C	6.14	5.718	9.815
11-3C	6.14	5.372	10.822
11-1L	6.14	5.603	10.036
11-2L	6.14	5.946	10.805

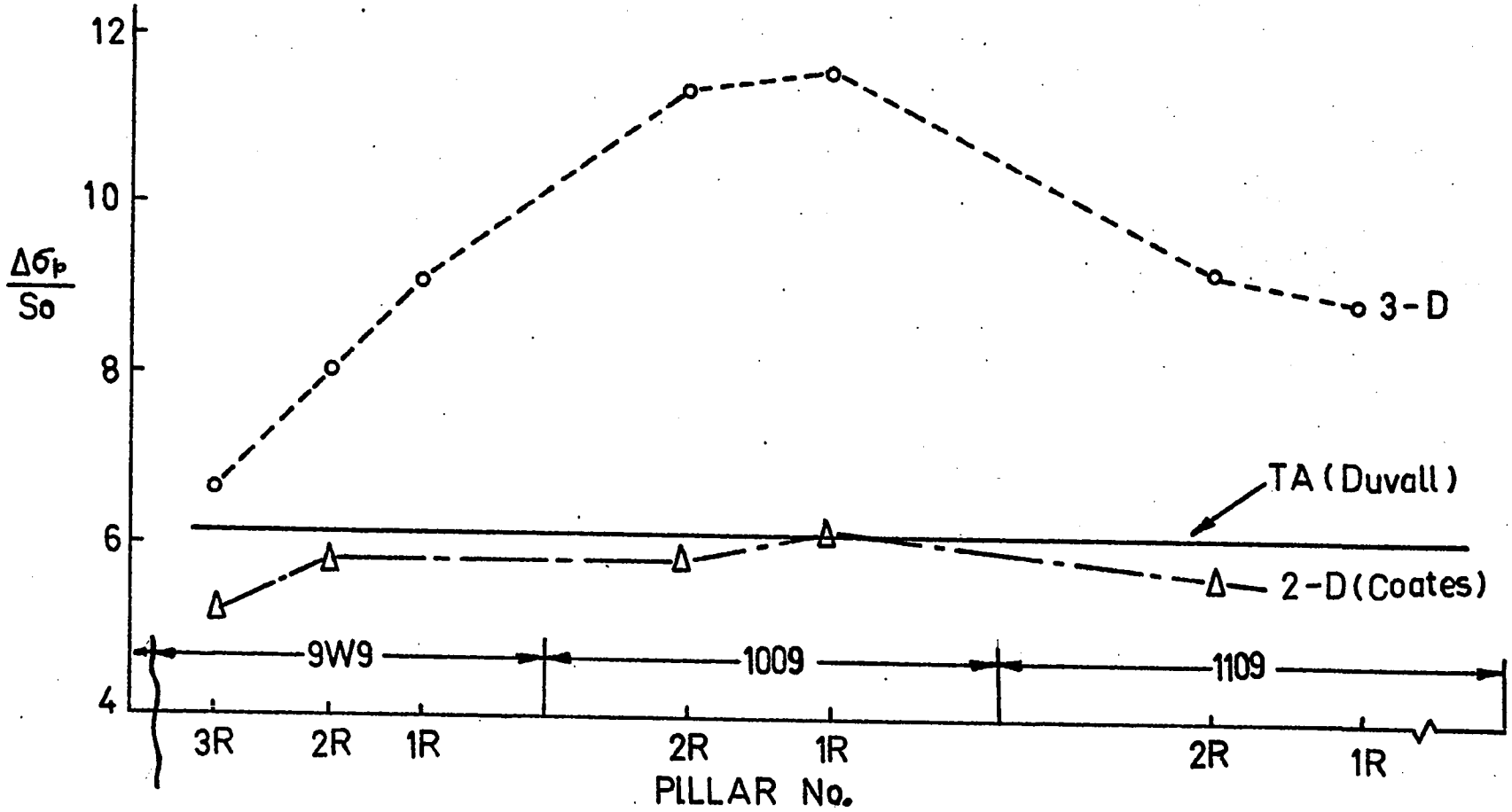

COMPARISION OF THE PILLAR STRESSES USING TA METHOD, 2-D DEF. HYPOTHESIS AND THE 3-D METHOD THROUGH THE RIGHT RIB PILLARS

FIGURE 5-16

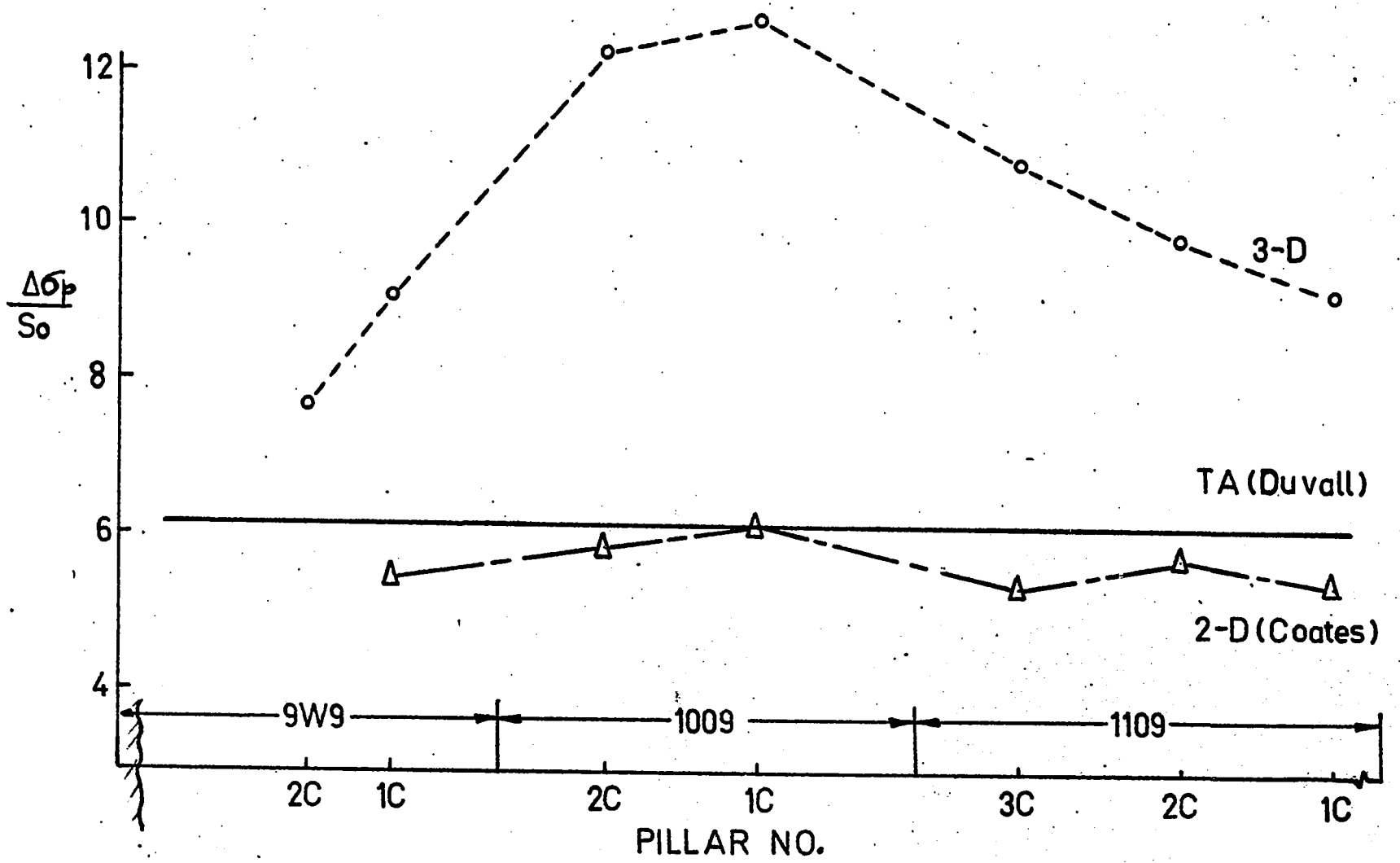

COMPARISION OF THE PILLAR STRESSES USING TA METHOD, 2-D DEF. HYPOTHESIS AND THE 3-D METHOD, THROUGH THE CENTRAL PILLARS

FIGURE 5-17

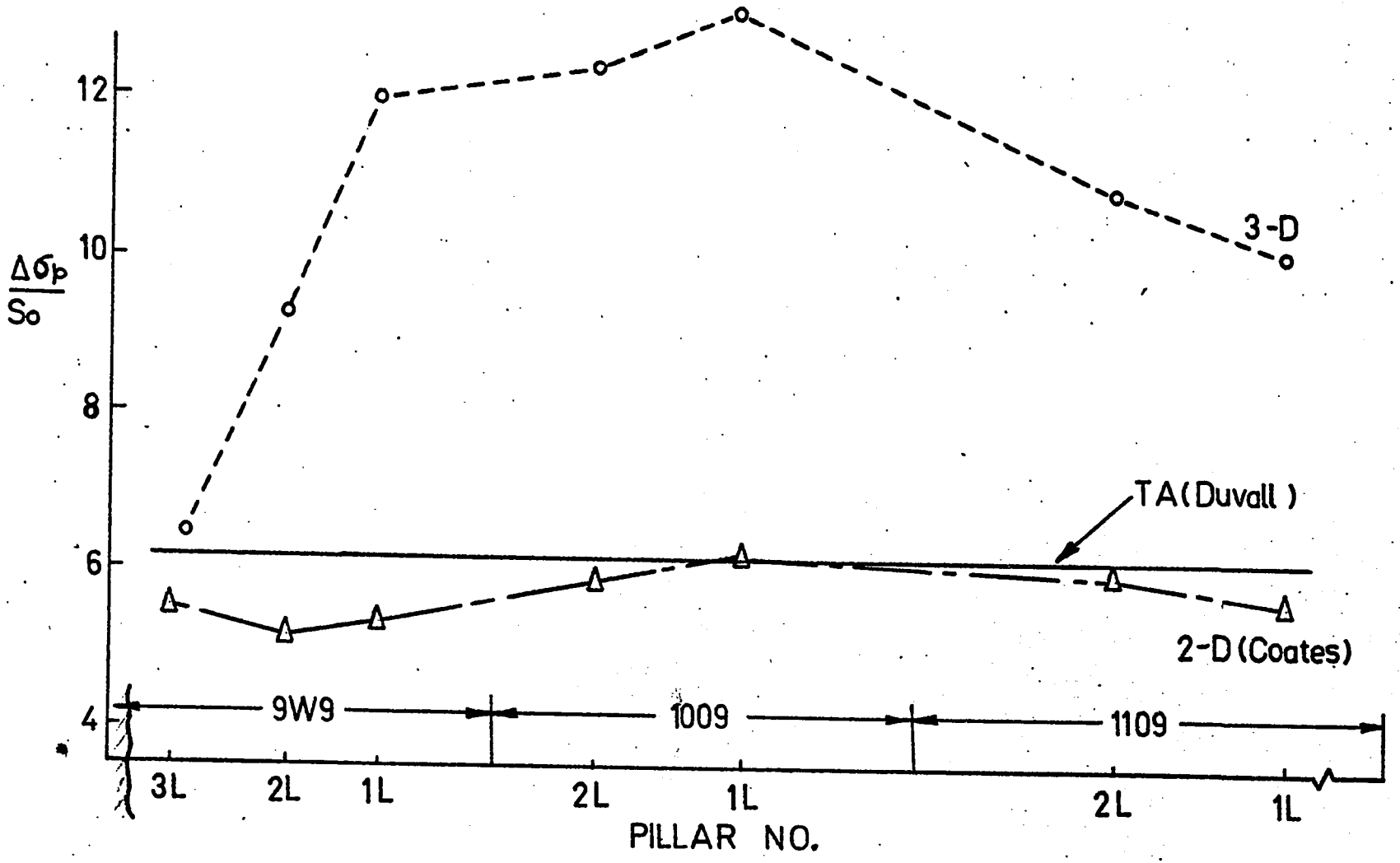

COMPARISION OF THE PILLAR STRESSES USING TA METHOD, 2-D DEFLECTION HYPOTHESIS AND THE 3-D METHOD, THROUGH THE LEFT RIB PILLARS

FIGURE 5-18

Possible causes for the Discrepances:

The discrepances between the measured and predicted pillar stresses could be due to any of the following.

1. The predicted results disregard the effects producted on the pillar stresses by the presence of geological disturbances such as, faults, minor folds and fractures, which could change the field stresses locally to an unpredictable extent. Also the pillar stresses are obtained for average dimensions of pillars, which may not be accurate for all pillars.

2. Recent studies (49,50) have shown that there exists a stress concentration at the end of the borehole due to field stress along the axis of the hole, which was not included in the calculations. Thus the field stress measurements with present techniques, can be accepted only with reservations.

3. The predicted values are actually the increase in the normal stress, S_o. This stress may not conform with field conditions. There is no doubt that such difficulties will always be present until more reliable techniques for measuring the pre-mining stresses are available.

4. The percentage extraction is one of the most important factors in predicting pillar stresses. By varying this factor, even by 2 percent, in the high extraction range a noticeable change takes place in the predicted values. Therefore an optimum extraction ratio must be maintained.

TABLE 5-5

Predicted Pillar Stresses for Different Extraction Ratios

S_o = 950 psi, k = 3.36, $E = E_p = 12.0 \times 10^6$ psi, $\mu = \mu_p = 0.18$

h = 4.0 ft, B = 10.0 ft. $\delta_{w(centre)} = 27.299$

No.	$\Delta\sigma_p/S_o$ for R = 0.80	R = 0.82	R = 0.84	R = 0.86	R = 0.88	R = 0.90
9-1R	6.08	6.87	7.86	9.10	10.72	12.91
9-2R	5.35	6.06	6.92	8.02	9.44	11.37
9-3R	4.05	4.58	5.24	6.06	7.14	8.60
9-1C	6.02	6.82	7.79	9.02	10.62	12.79
9-2C	5.11	5.78	6.61	7.65	9.01	10.85
9-1L	7.97	9.02	10.31	11.94	14.06	16.93
9-2L	6.17	6.98	7.98	9.25	10.89	13.11
9-3L	4.30	4.87	5.57	6.45	7.59	9.15
10-1R	7.75	8.77	10.02	11.60	13.66	16.46
10-2R	7.58	8.58	9.81	11.36	13.38	16.11
10-1C	8.46	9.58	10.95	12.68	14.93	17.98
10-2C	8.16	9.23	10.55	12.22	14.39	17.33
10-1L	8.73	9.88	11.29	13.08	15.40	18.55
10-2L	8.26	9.34	10.68	12.37	14.56	17.54
11-1R	5.95	6.73	7.70	8.91	10.50	12.64
11-2R	6.18	6.99	7.99	9.26	10.90	13.13
11-1C	6.15	6.96	7.95	9.21	10.84	13.06
11-2C	6.55	7.41	8.47	9.81	11.56	13.92
11-3C	7.22	8.17	9.34	10.82	12.74	15.34
11-1L	6.70	7.58	8.67	10.03	11.82	14.23
11-2L	7.21	8.16	9.33	10.80	12.72	15.32

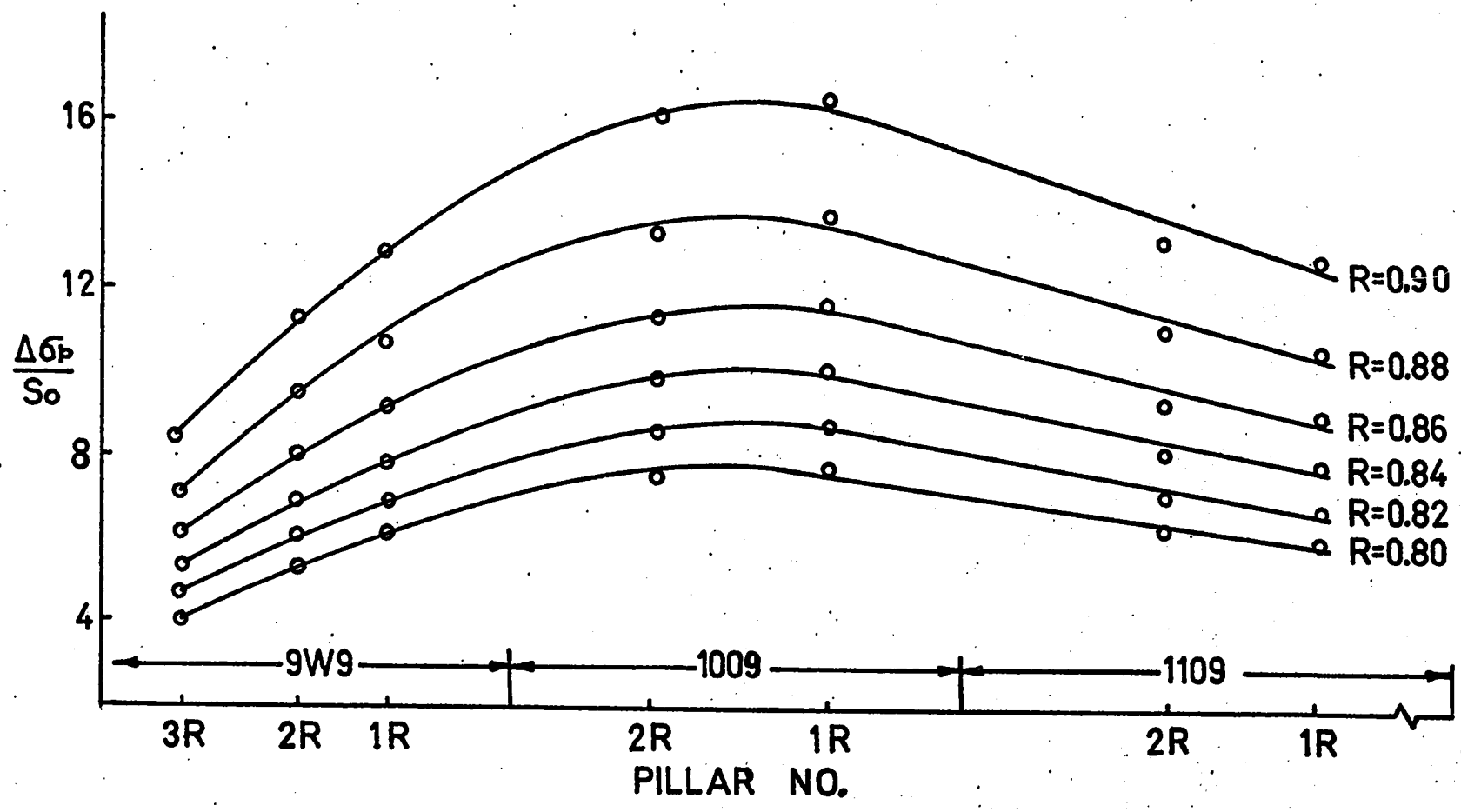

EFFECT OF PERCENTAGE EXTRACTION ON PREDICTED PILLAR STRESSES THROUGH THE RIGHT RIB PILLARS

FIGURE 5-19

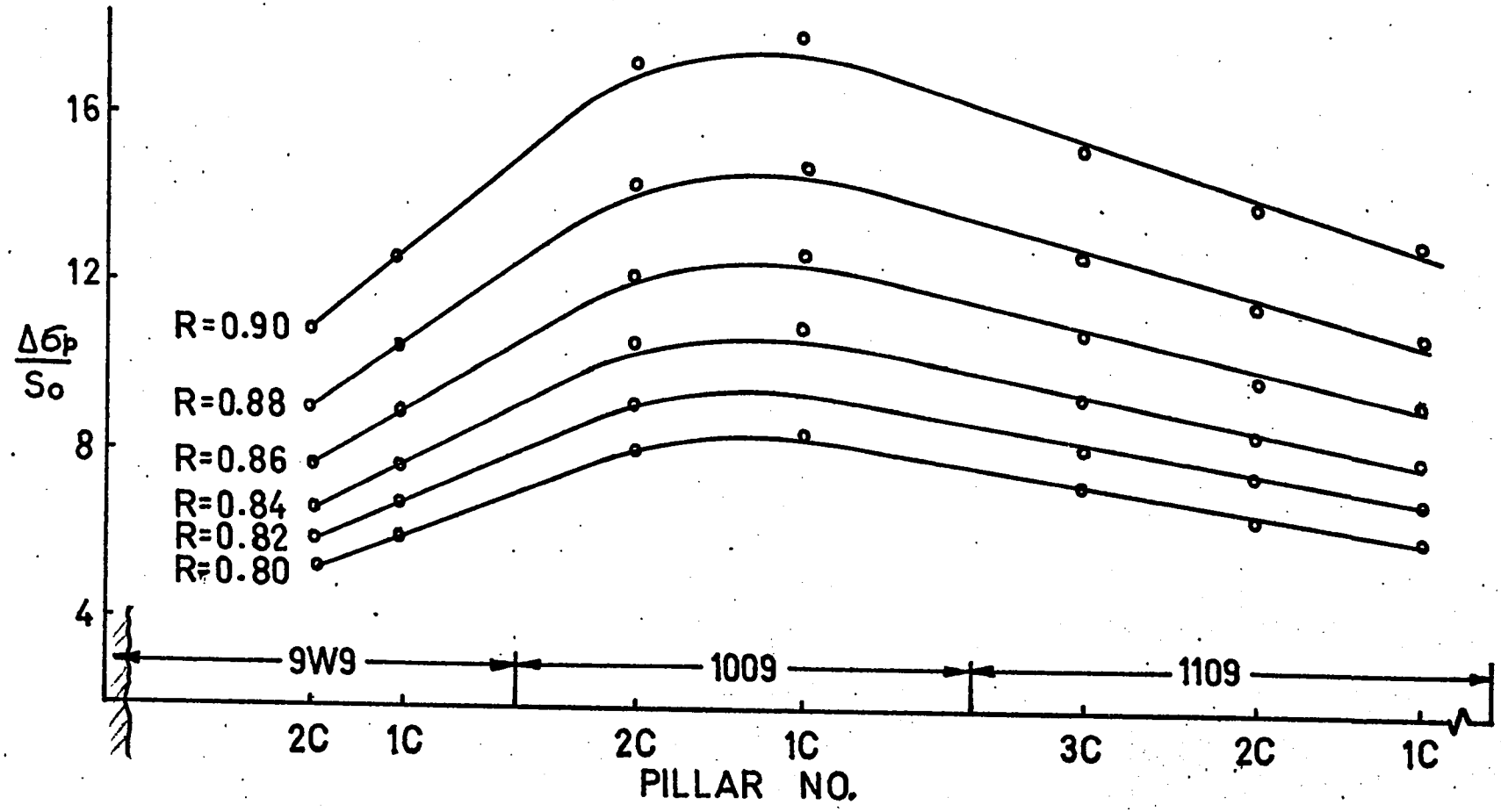

EFFECT OF PERCENTAGE EXTRACTION ON PREDICTED PILLAR STRESSES THROUGH THE CENTRAL PILLARS

FIGURE 5-20

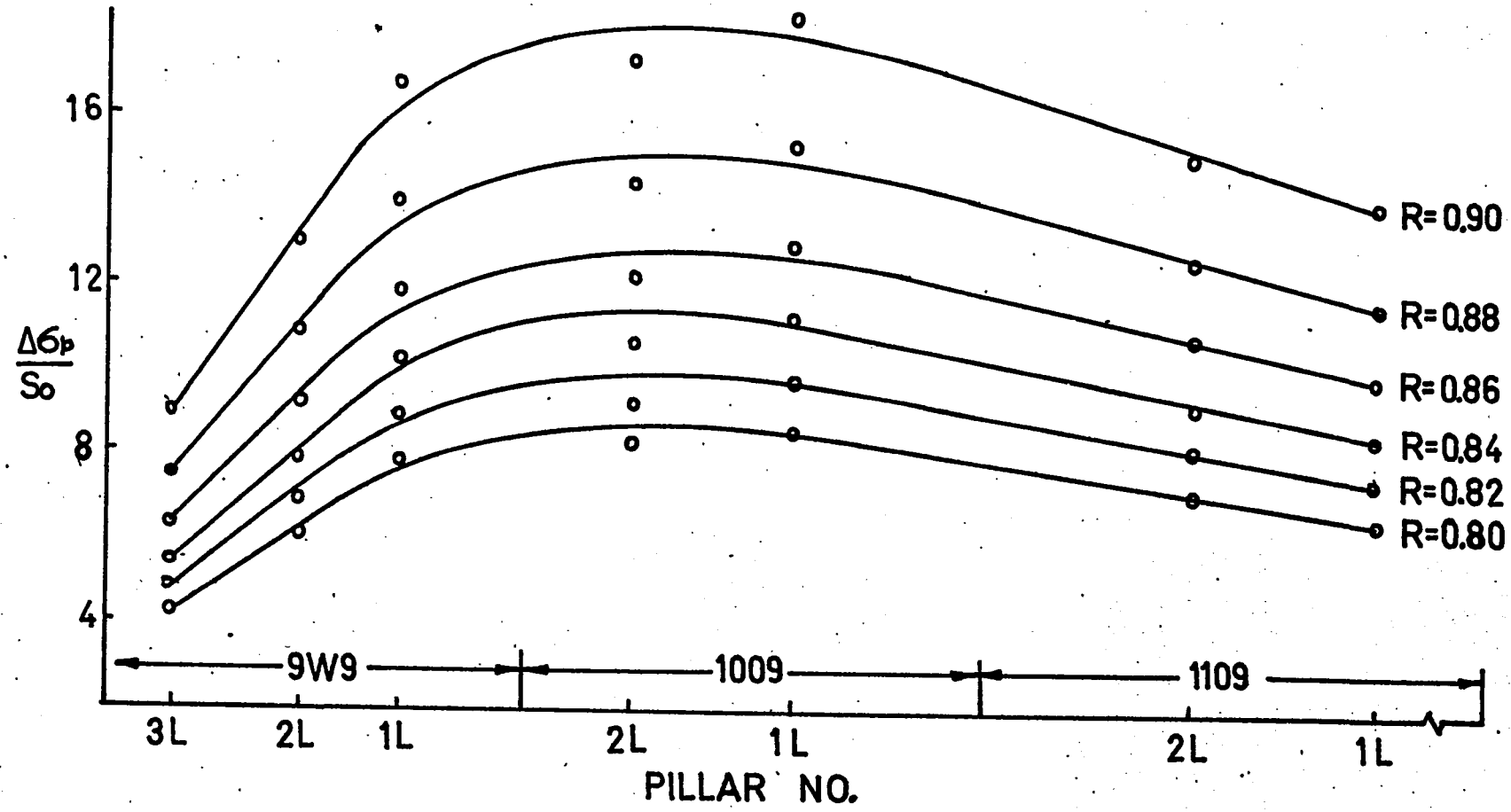

EFFECT OF PERCENTAGE EXTRACTION ON PREDICTED PILLAR STRESSES THROUGH THE LEFT RIB PILLARS

FIGURE 5-21

Figures 5-19 through 5-21 show the effect of percentage extraction on the predicted stresses graphically. The extraction ratio in this study has been varied between 0.80 to 0.90 in increments of 0.02. This seems to be the range within which the Nordic mine has been worked. The predicted values are the data in Table 5-5. Examining Figures 5-19, 5-20 and 5-21 the trend of the stress concentrations in all the three sections of the pillars is increasing with the increasing recovery.

CHAPTER VI

MODEL STUDIES FOR ABUTMENT STRESSES

General: The data obtained from the analogue in the form of spot voltage for a mine model not only permit the calculation of displacements but can also be used to calculate the induced stresses in the solid rock surrounding the mine excavations in a tabular orebody (26, 27, 28). The necessary equations to calculate such stresses in an isotropic homogeneous elastic medium are given in Appendices B-II and B-III.

For the prediction of abutment stresses, the two mining outlines simulated are:

1. the Nordic Mine and
2. the Kerr-Addison Mine.

These mine outlines are used because some stress measurements have been made and the elastic constants of the rock substance are available for each mine.

NORDIC MINE MODEL:

The abutment stress measurements in the Noridc mine were made between December 1965 and the end of 1967. The simulation study is based on mining outlines for 1965 (42) and 1967 (74). These outlines are shown in Figure 6-1. The model study is based on leaving about 14 percent of the ore as pillars. Figure 6-2 shows a photograph of such a model with a 1965 outline.

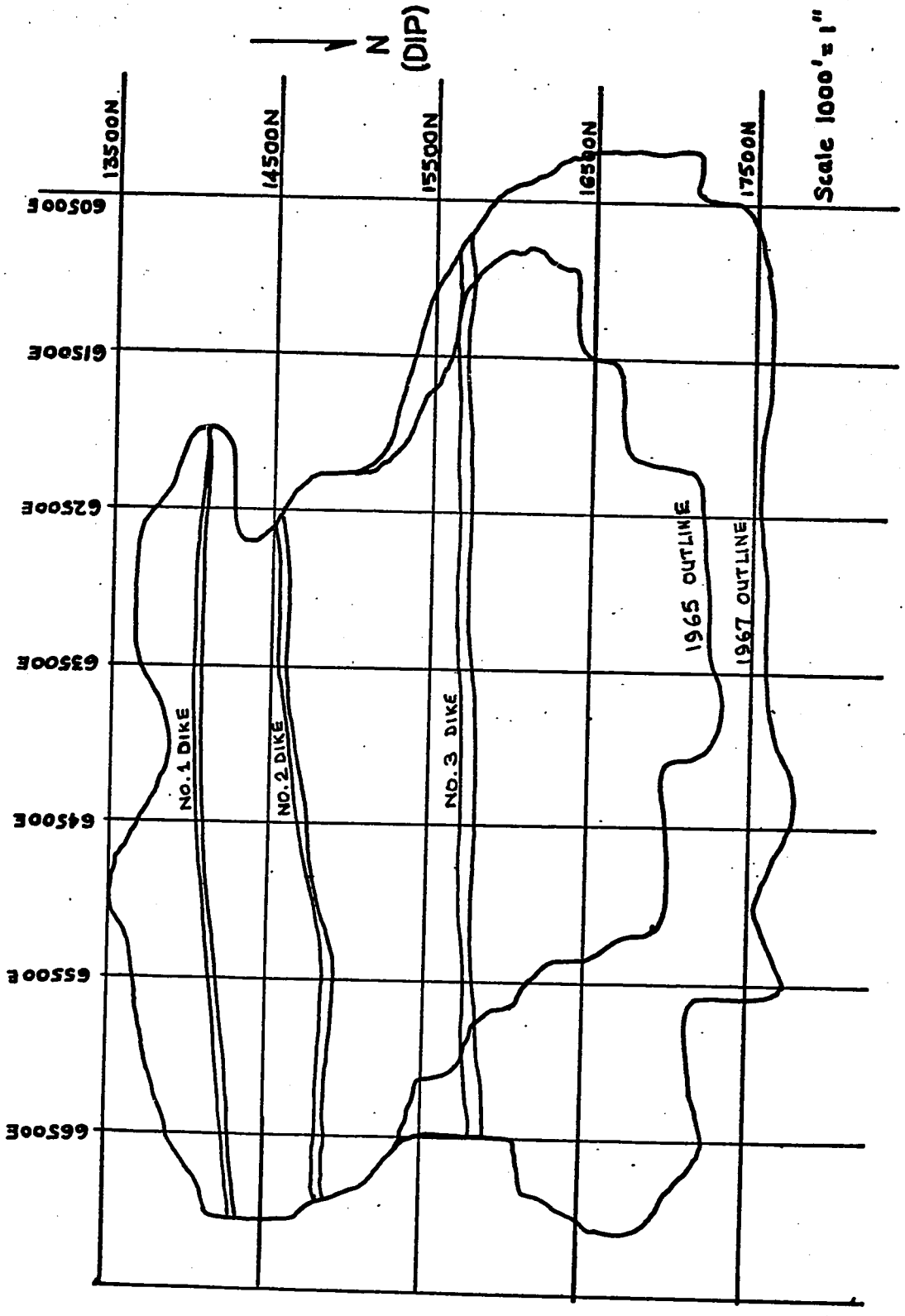

PLAN OF NORDIC MINE SHOWING 1965 AND 1967 BOUNDARIES

FIGURE 6-1

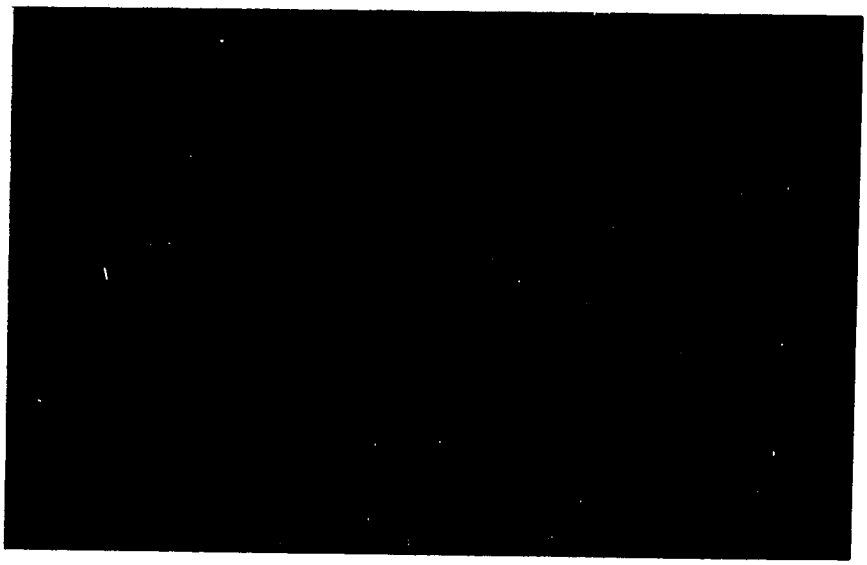

A SIMULATED MINE MODEL OF NORDIC MINE SHOWING 1965 OUTLINE

FIGURE 6 - 2

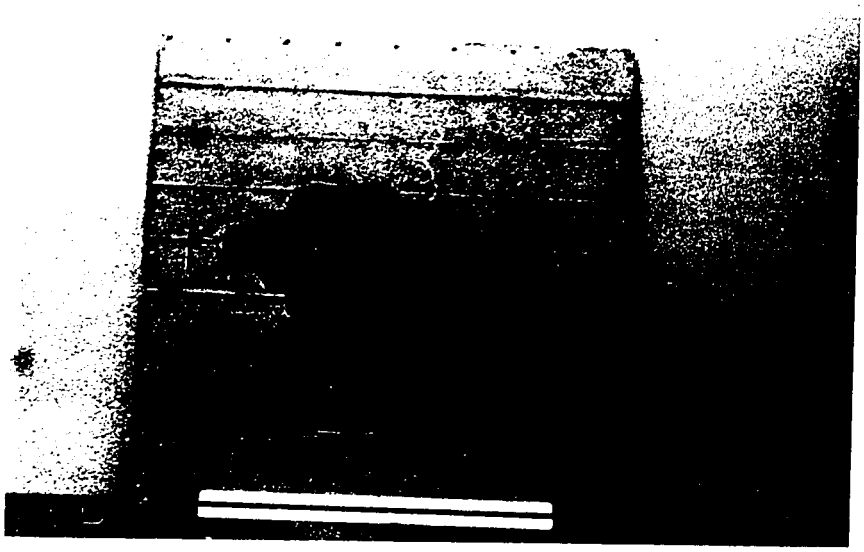

A SIMULATED MINE MODEL OF NORDIC MINE SHOWING 1965 OUTLINE

FIGURE 6 - 2

The coordinates of the locations at which the induced stresses have been calculated are given in Table 6-1.

The assumptions regarding the elastic constants are the same as used for the model study of pillar loading.

In Situ Stress Measurements:

Method of Measurement: The abutment stresses in this mine were measured (54,55) by using the strain cell developed at the South African Council of Scientific and Industrial Research (63) and modified at the Mining Research Centre at Elliot Lake (69). This strain cell containing electrical resistance strain gauges is glued on the flattened end of a BX(2-3/8 inch diameter) borehole drilled in the rock, after the end of the borehole is ground flat and smooth with a square-faced diamond bit and a flat-faced diamond impregnated bit.

The strain cell measures the change in strain of the rock on which it is glued when the stress is relieved by extending the borehole beyond the gauges by means of the coring drill. The measuring element is a rectangular strain gauge rosette, the individual gauges of which are oriented to measure changes in strain in the vertical, 45°, and horizontal directions. The measuring leads from the gauges are connected to 4 pins in an insulated connector plug. The plug and the gauge both are encapsulated in a silicone rubber compound which provides physical protection as well as waterproofing for the strain gauges.

TABLE 6-1

Locations of the Holes Simulated on the Mine Model of Nordic Mine for Abutment Stresses

No.	Level	N	E	Approximate Drilling Dates
A	700 East Haulage	15,890	66,862	Jan. 1967
B	900 East Haulage	16,460	66,995	Dec. 1966
C	1000 East Sill	16,870	67,240	Jan. 1967
D	1100 West Sill	16,652	60,157	Sept. 1966
E	1300 West Sill	17,032	59,300	Sept. 1966(x)
F	1400 West Haulage	17,300	60.255	May 1967
G	1400 West Ore	17,380	60.498	June 1967
H	1400 East Sill	17,390	63,970	Sept/Oct. 1966
I	1400 East Ore	17,535	64,295	Nov. 1966
J	1400 West Extension	17,620	61,950	Dec. 1965

(x) This hole could not be simulated on the model

Analysis of Data:

The field results obtained by using this technique, have been adjusted for stress concentrations due to the field stress along the axis of the borehole (55). Table 6-2 gives the maximum, minimum and the average (arithmetic) for both major and minor measured principal stresses.

The range of the values provided by the data is so wide as to reflect on the accuracy of measurements and/or technique. Nevertheless, for study purposes an arithmetic mean was calculated.

The induced stresses in the abutment zones, based on the model study, are data given in Table 6-3 together with the locations at which measurements were made.

While the geometries of the underground openings make it difficult to establish the exact relationships between the locations at which stresses were measured and the mining boundaries at the time that the measurements were made, it is thought that reasonable accuracy has been maintained in plotting the locations for the model study.

On comparing the model values with measured values (Tables 6-2 and 6-3), the model values fall within the spread of the measured values. This agreement is quite remarkable when one considers that the model is an idealized version of the field conditions.

TABLE 6-2

Measured Stresses in the abutments

at Nordic Mine(*)

Location No.	Major Principal Stresses (psi)			Minor Principal Stresses (psi)		
	Average of all the Measurements	Max. Recorded	Min. Recorded	Average of all the Measurements	Max. Recorded	Min. Recorded
A 700 East Haulage	1783(14) (13 ft.)(x)	4023	548	375(14)	1224	-1321
B 900 East Haulage	3876(10) (28 ft.)(x)	8490	1244	280(10)	1505	-2304
C 1000 East Sill	4153(6) (14 ft.)(x)	6572	1854	1176(6)	3422	-189
D 1100 West Sill	4928(25) (18 ft.)(x)	9604	2681	2211(25)	3438	324
F 1400 West Sill	4192(17) (39 ft.)(x)	6556	1799	1231(17)	2099	381
G 1400 West Ore	4149(16) (17 ft.)(x)	5422	3376	2686(16)	4502	818
H 1400 East Sill	5445(16) (32 ft.)(x)	8403	2528	1403(16)	4333	-394
I 1400 East Ore	2256(7) (43 ft.)(x)	3829	1152	-128(7)	1058	-908
J 1400 West Ext.	5151(30) (18 ft.)(x)	10,499	3131	1743(30)	4764	152

(*) These values are calculated from Table 3, Ref. (55).

( ) The number in the paranthesis indicates the number of observations at each location.

(x) Average distance from the abutment.

TABLE 6-3

Calculated Principal Stresses from the Nordic Mine Model

No.	Location	Principal Stresses (psi) σ_1	σ_2	σ_3
A	700 East Haulage	2670	-1847	-10,651
B	900 East Haulage	9363	5135	2627
C	1000 East Sill	1413	730	40
D	1100 West Sill	4667	3410	-553
F	1400 West Sill	1967	1032	-141
G	1400 West Ore	2240	1106	-55
H	1400 West Sill	2138	881	249
I	1400 East Ore	1696	668	94
J	1400 West Extension	8188	3789	-371

The complex nature of the field stress measurements is depicted by the values given in Table 6-2, particularly at locations B,J and D. In the case of minor principal stresses the most erratic model value (Table 6-3) is at location A, which has a maximum deviation from the field measurements.

On examining the geometry of location A closely, it is evident that the location is closest to both,the number 3 dike and the most complex mining boundary. The high tensile stress at this location is probably due to one or both of these features. It has been suggested earlier (56) that the presence of dike could influence the stress distribution locally.

The model value also suggest that the number three dike exerts an influence on the abutment stresses in the down dip direction. At locations A,B and D nearest the dike, the deviation in the values is maximum while the effect is less pronounced further away (namely at locations C,F,G,H and I). The values at J, both from field measurements and the model are in essential agreement, but are anamalously high and at present defy interpretation. However, it is suggested that the proximity to complex mining boundary is the cause of the high model value at location J,

A comparison of the model values and field measurements at each location is possible on the basis of the distance from the mining boundary. But since the values are directly dependent on the geometry of the outline, such a comparison may not be logical.

The effect of complex geometry can be visualized by a reference to the stress profile, Figures 6-3 and 6-4 representing comparatively simple sections along 6900E coordinate (see Figure 6-1). The principal stresses calculated refer to the models, one with 1965 stoping outline and the other with 1967 stoping outline. These two Figures suggest the following conclusions.

1. The stress gradient, as expected, gradually decreases with increasing distance from the mining boundary and eventually reaches field stress conditions. It also confirms that stress concentration takes place only in the immediate vicinity of the openings (65,66). However, such a relationship is not always apparent with more complicated geometry, refer also to Figure 6-10.

2. The two graphs show a significant difference in the magnitude of abutment stresses, although the distance of the locations from the mining boundary is the same in both cases. This is the result of extending the mining boundaries between 1965 and 1967 (Figure 6-1). The same section if studied on the basis of two-dimensional approach would show little difference in the concentrations, because the only parameter that could be taken into consideration would be the axis ratio.

Such a study indicates, beyond doubt, that the stress concentrations at mining boundaries are affected by the geometry of the entire mined out area. It therefore emphasises the importance of examining abutment stresses by the three-dimensional method.

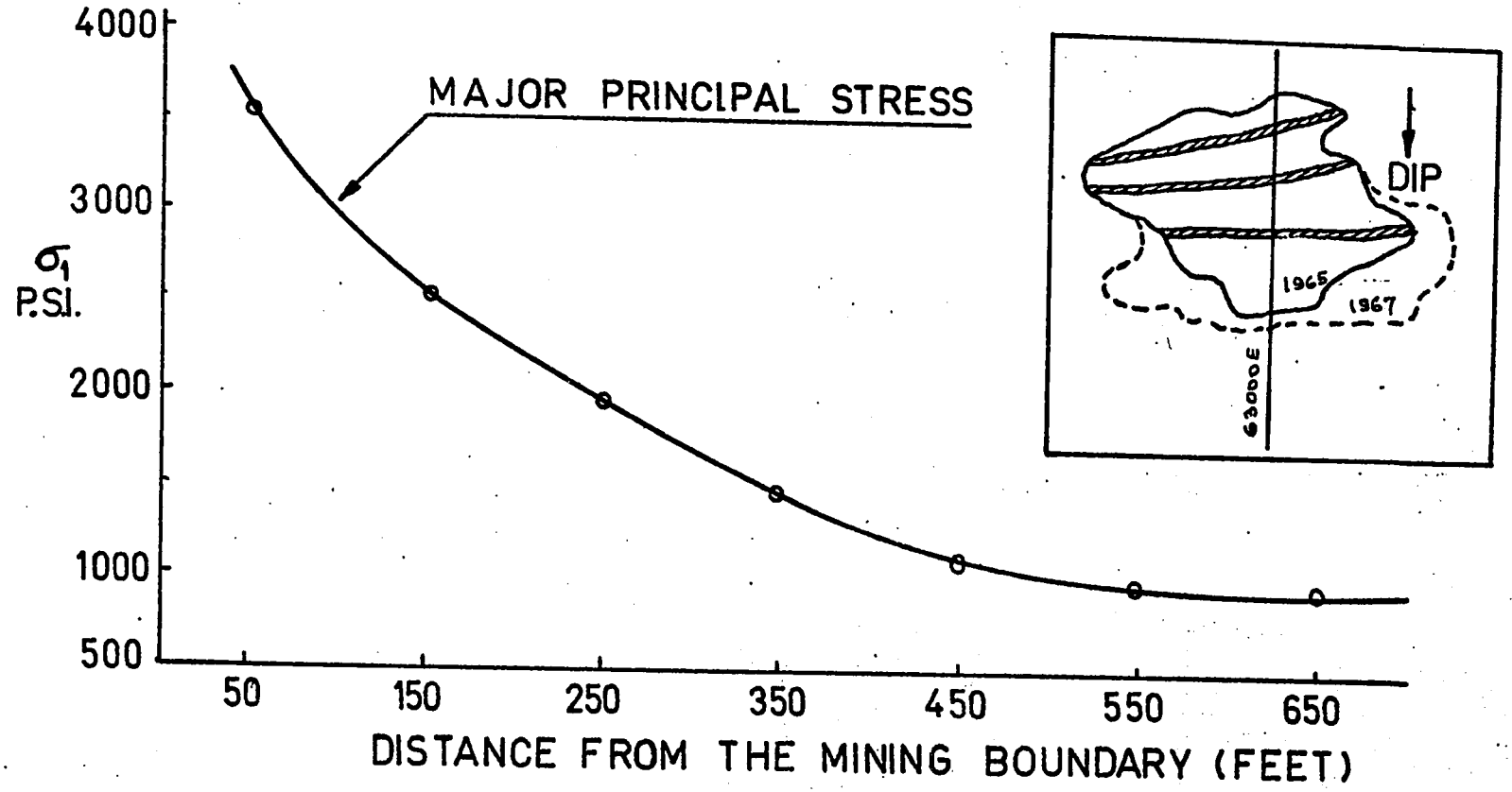

A STRESS PROFILE IN AN ABUTMENT ZONE ALONG 63000E DOWN DIP, BASED ON 1965 MINING OUTLINE MODEL

FIGURE 6-3

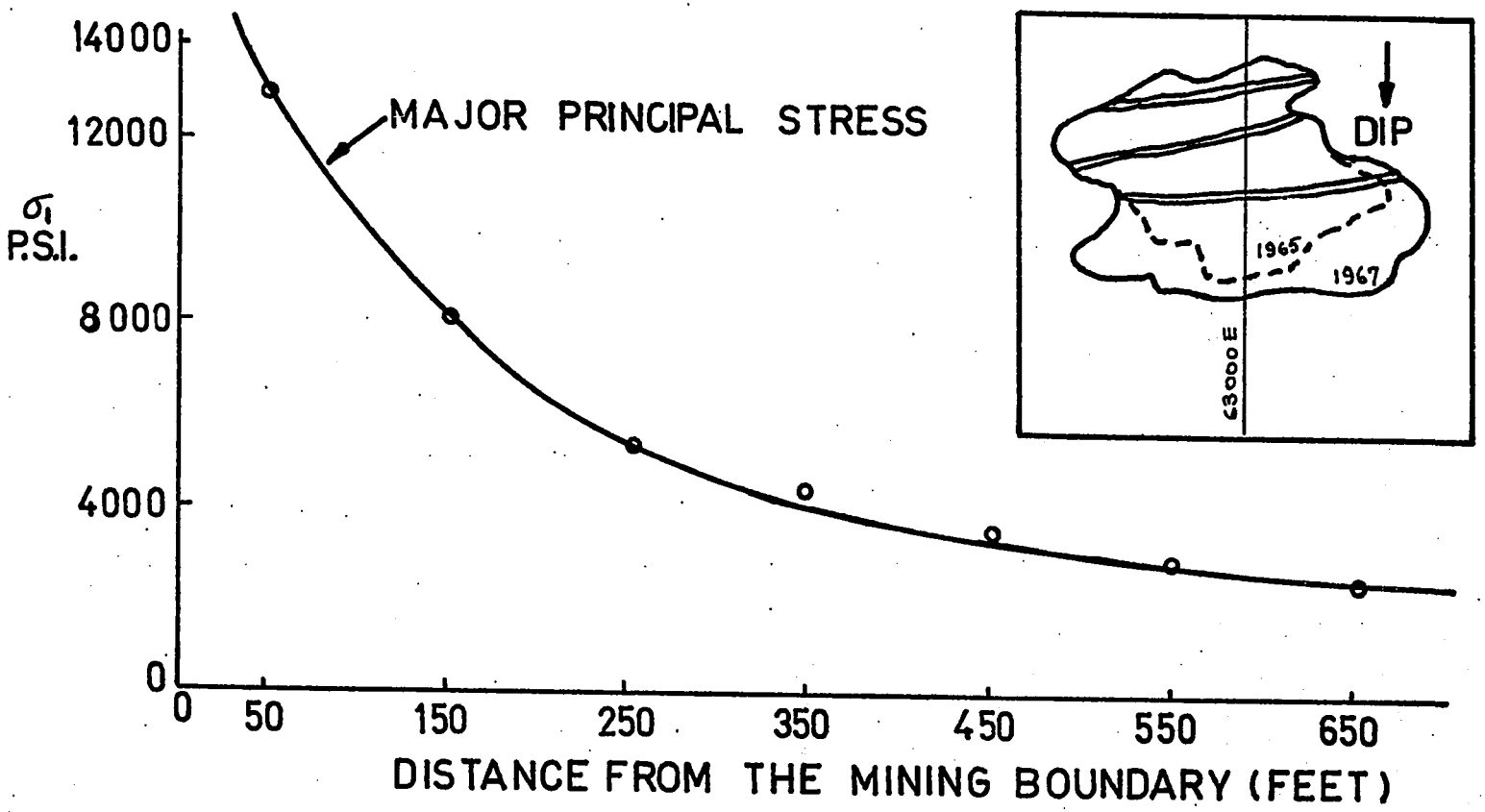

A STRESS PROFILE IN AN ABUTMENT ZONE ALONG 63000E DOWN DIP BASED ON 1967 MINING OUTLINE MODEL

FIGURE 6-4

Interpretation of Model values using Stereographic Projection:

The computed principal stresses from the model study for each location have been plotted on a stereonet, Figure 6-5. The orientations of these stress vectors are given in Table 6-4.

Figure 6-5 shows that most of the computed stress orientations fall in a series of restricted fields or areas in the net.

The azimuth and the plunge of each stress component was derived from the computed vectors plotted on the stereonet. These are given in Table 6-5. The stereonet shows a variance of approximately 45 degrees in the overall distribution of stresses which may be entirely due to the model geometry. However, most of the calculated principal stress vector orientations show an acceptable spread in the net, the densest distribution of stress orientations being that of the intermediate principal stress, σ_2. In those cases where there is a pronounced deviation from the mean, it is evident that the locations representing these points indicate that the changes are probably due to their proximity to the dike.

From the above analysis it can be inferred that the influence of the dike is most prominent at points A,B,C and D (see Table 6-5), all of which are relatively close to the dike abutment zone.

The correlation between the field values and computed values shows that the field conditions in this mine can be approximated by the data obtained from an ideal model.

TABLE 6-4

Orientations of the model principal stresses with respect to the strike, dip and perpendicular directions of the excavation

Location	Stress Vector	Orientation in Degrees along Strike	Dip	Perpendicular
A	σ_1	61.61	127.03	129.92
	σ_2	135.48	133.74	83.10
	σ_3	58.97	113.60	40.75
B	σ_1	26.59	116.58	91.18
	σ_2	120.90	31.04	87.85
	σ_3	25.05	64.99	88.94
C	σ_1	62.66	132.24	54.50
	σ_2	125.72	74.82	39.77
	σ_3	48.14	46.10	74.26
D	σ_1	19.89	73.95	101.44
	σ_2	105.07	77.76	160.43
	σ_3	77.41	159.65	105.77
F	σ_1	53.76	50.30	119.50
	σ_2	121.35	99.53	146.97
	σ_3	51.97	138.76	103.61
G	σ_1	60.99	46.53	122.68
	σ_2	121.83	105.24	143.94
	σ_3	45.73	132.57	103.63
H	σ_1	78.85	41.20	129.03
	σ_2	113.00	122.03	138.86
	σ_3	25.87	113.07	101.11
I	σ_1	80.02	38.24	126.47
	σ_2	106.60	122.54	142.53
	σ_3	19.56	107.93	97.62
J	σ_1	70.97	40.86	124.56
	σ_2	117.03	113.66	142.74
	σ_3	28.31	116.68	98.82

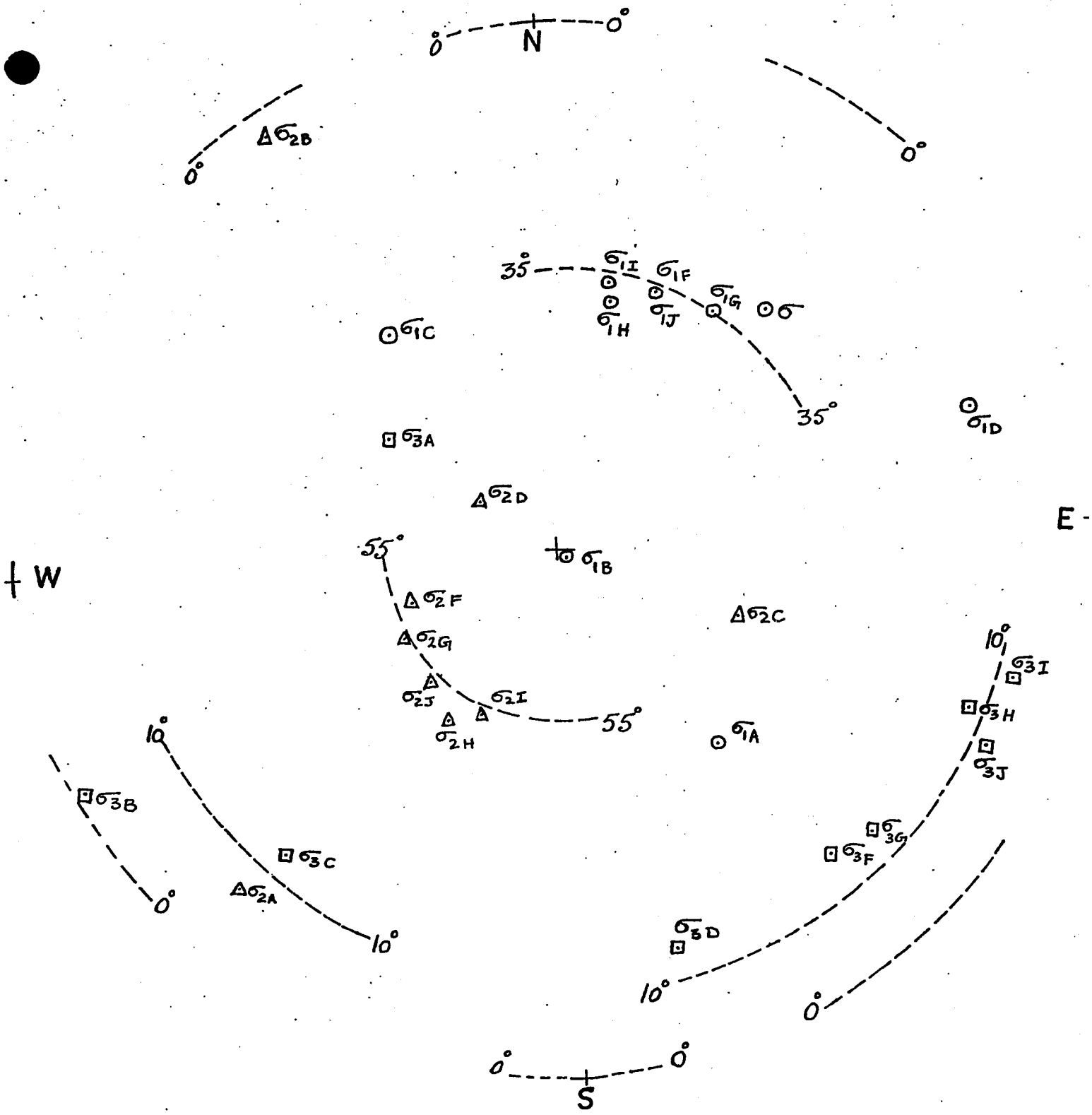

STEREOGRAPHIC PROJECTION OF THE MODEL PRINCIPAL STRESS VECTORS

FIGURE 6-5

TABLE 6-5

Plunge and Strike of the Model Principal Stresses Vectors

σ_1, σ_2 and σ_3

No.	Location	Stress Vector	Plunge	Strike
A	700 East Haulage	σ_1	40°	N38° E
		σ_2	09°	S45°W
		σ_3	50°	N54°W
B	900 East Haulage	σ_1	89	S67°E
		σ_2	09	N31°W
		σ_3	89	S65°W
C	1000 East Sill	σ_1	36	N31W
		σ_2	50	S68E
		σ_3	16	S46W
D	1100 West Sill	σ_1	13	N74°E
		σ_2	71	N32°W
		σ_3	14	S14°E
F	1400 West Haulage	σ_1	30°	N42E
		σ_2	57°	S74W
		σ_3	15°	S40E
G	1400 West Ore	σ_1	35	N35°E
		σ_2	53	S64W
		σ_3	13	S45E
H	1400 East Sill	σ_1	40°	N13°E
		σ_2	48°	S46°W
		σ_3	10°	S66°E
I	1400 East Ore	σ_1	36°	N13°E
		σ_2	52°	S38°W
		σ_3	06°	S71°E
J	1400 West Ext.	σ_1	36	N23E
		σ_2	52	S48W
		σ_3	70	S62E

KERR-ADDISON MINE MODEL:

Kerr-Addison Mine:

Geology: The geology of the mining area is discussed in detail elsewhere (52,53). The Kerr-Addison Gold mine is located in the Larder Lake district of Ontario. The regional structure is marked by strong, wide carbonatized shear zones and talc-chlorite schists. Locally this structure is called the Larder Lake "break" and has a width of 600 feet striking N 60°E and dipping 78° to North. It occurs between sediments to the north and volcanics (tuff and basic lava) on the south. The orebodies are disconnected and distributed throughout the area.

One of the main structural features is the Kerr fault, which occurs towards the southern edge (footwall) of the main ore zone. It is believed that the movements along the fault are responsible for the fracturing of the orebody and it also seems to have worked as a channel for the hydrothermal activity which has resulted in gold deposition (53).

The ore deposits are located within a strong competent rock (51), close to the fault. The surrounding ground seems to have been subjected to intense metamorphism.

Mining History: The mine has been worked from the surface downwards and where there are parallel orebodies, from hanging wall to footwall. The mine above 2200 level was worked by shrinkage and sub-level stoping,

but as ground conditions became more difficult, the above methods were replaced by cut-and-fill. The workings have been extended to the 4400 level (51).

Rockbursts have been frequent below 3100 level. Of 104 bursts, 52 have occurred between the 3100 and 3700 levels, 31 below 3700 level and 21 above 3100 levels, Figure 6-6 shows a longitudinal section of the main ore zone mapped in the year 1967 (51).

Stress measurements: The stress measurements in this mine have been made using the CSIR technique (63) mentioned earlier. All the calculations are based on using a stress concentration factor of 1.53 (51).

The locations where the in-situ stress measurements were made are shown in Figure 6-6. These locations in the mine are about 60 feet below 4000 level (see Figure 6-7) Hole 4 was drilled in the stope wall, holes 5 and 6 were drilled in the ore and hole 7 was drilled parallel to hole 6 to obtain the stress measurements near the collar where discing had occurred (51). High stress concentrations were recorded in the locations close to the mine openings. This was particularly noted in 4221-54 raise (see Figure 6-7), where the magnitude of major principal stress was of the order of 13,900 psi.

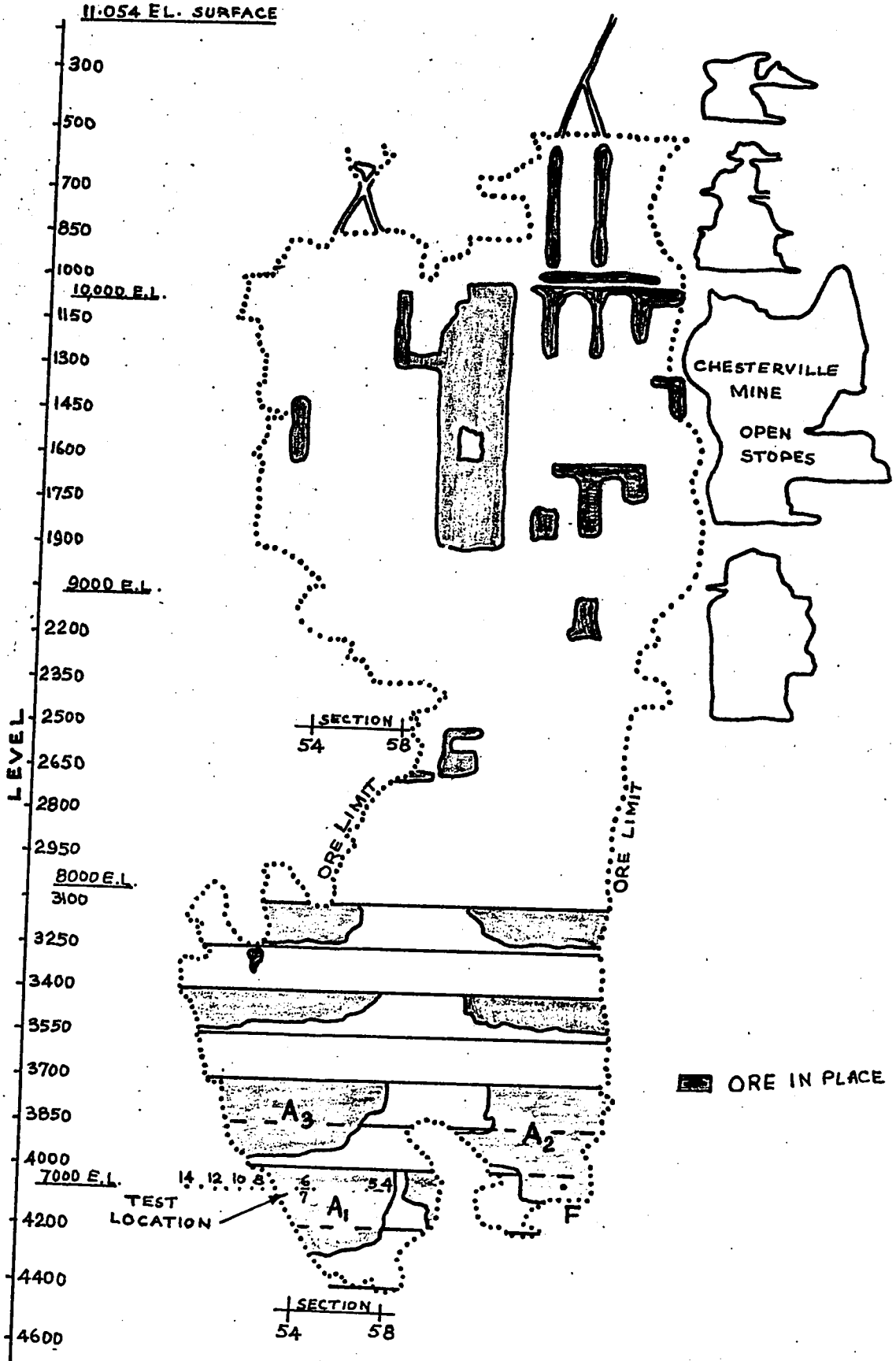

LONGITUDINAL SECTION OF KERR-ADDISON MINES (REF.51)

FIGURE 6-6

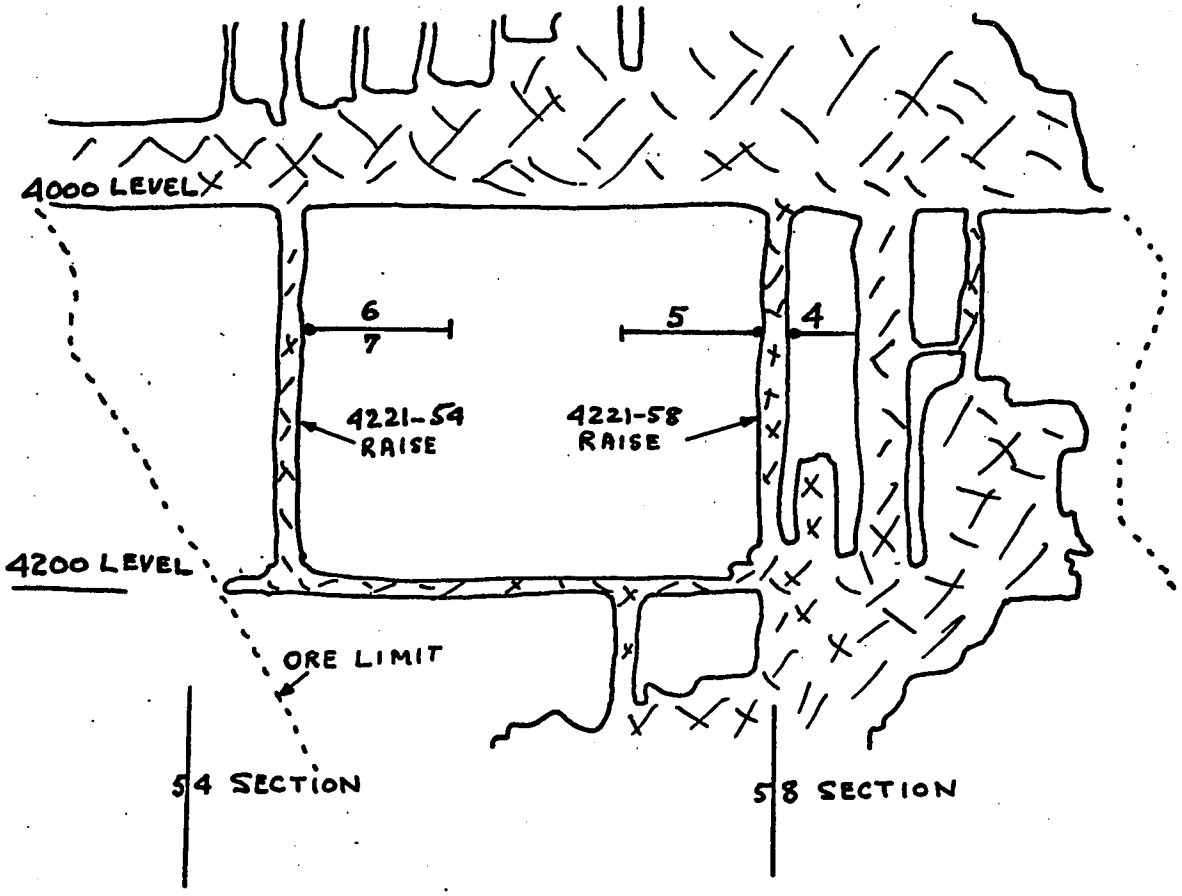

SECTIONAL VIEW OF THE TEST AREA
SHOWING THE LOCATION OF TEST HOLES
(REF. 51)

FIGURE 6-7

The Model Studies:

The basic requirement in the model study is that the orebody should be tabular in shape, bearing this in mind the following assumptions were necessary for this study.

1. The orebody is assumed to be tabular in shape and the longitudinal section shown in Figure 6-6 is considered a mine plan for all practical purposes. Figure 6-8 shows the photograph of the mine model.

2. Bearing in mind that the major stress is perpendicular to the plane of the orebody, the orebody is assumed to be either gently dipping around 9 degrees or flat at zero degrees dip. This simulation is shown in Figure 6-9.

3. The orebody is assumed to be dipping south with EW strike. In the first case the 9 degree dip is the result of assuming the shallow side of the mine approximately 2000 feet below surface and the dip side about 4600 feet. This places the centre of the mine equivalent to 3200 feet below surface.

In the second case the orebody is assumed to be flat and at an average depth of 4600 feet.

With such an approach for a model study, it is assumed that the orebody is subjected to an average gravity load of 3200 psi or 4600 psi, depending whether dipping or flat. The elastic constants used are average values calculated from tests conducted(51). These are 14×10^6 psi for Young's modulus and 0.27 for Poisson's ratio.

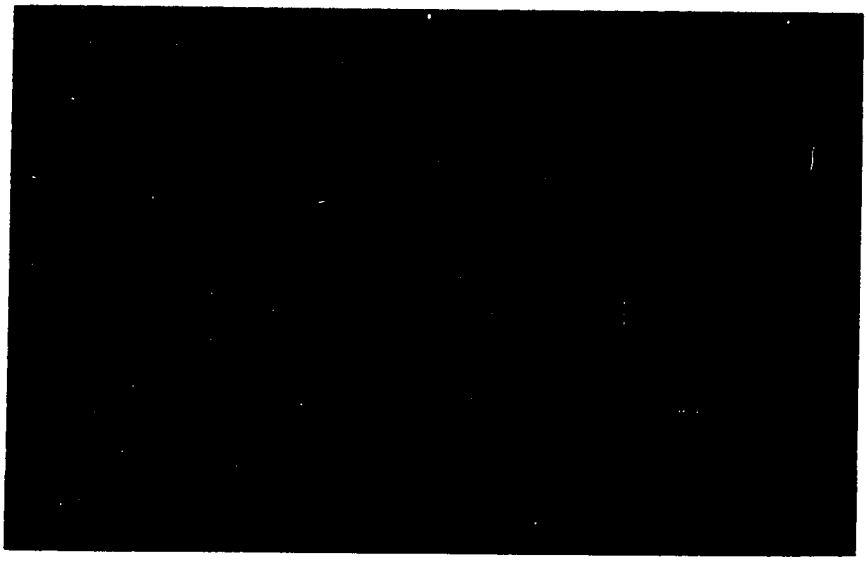

A SIMULATED MINE MODEL SHOWING KERR-ADDISON MINE OUTLINE

FIGURE 6 - 8

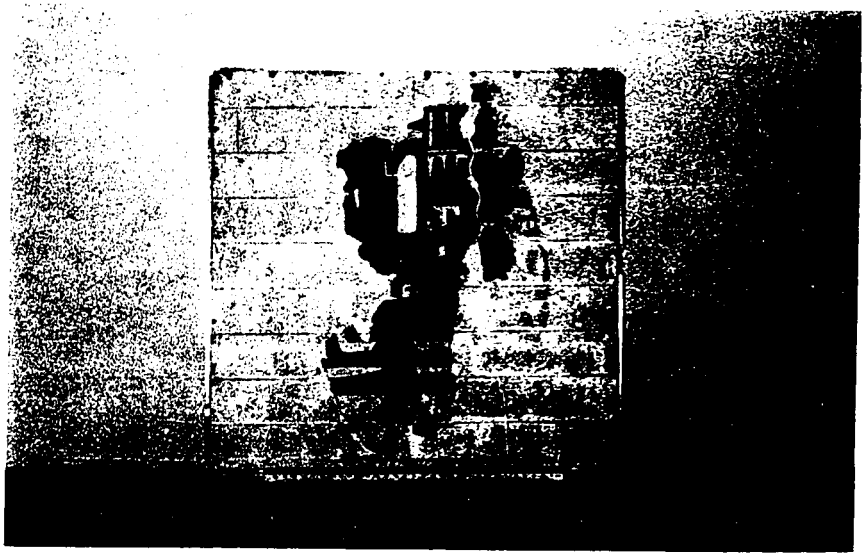

A SIMULATED MINE MODEL SHOWING KERR-ADDISON MINE OUTLINE

FIGURE 6 - 8

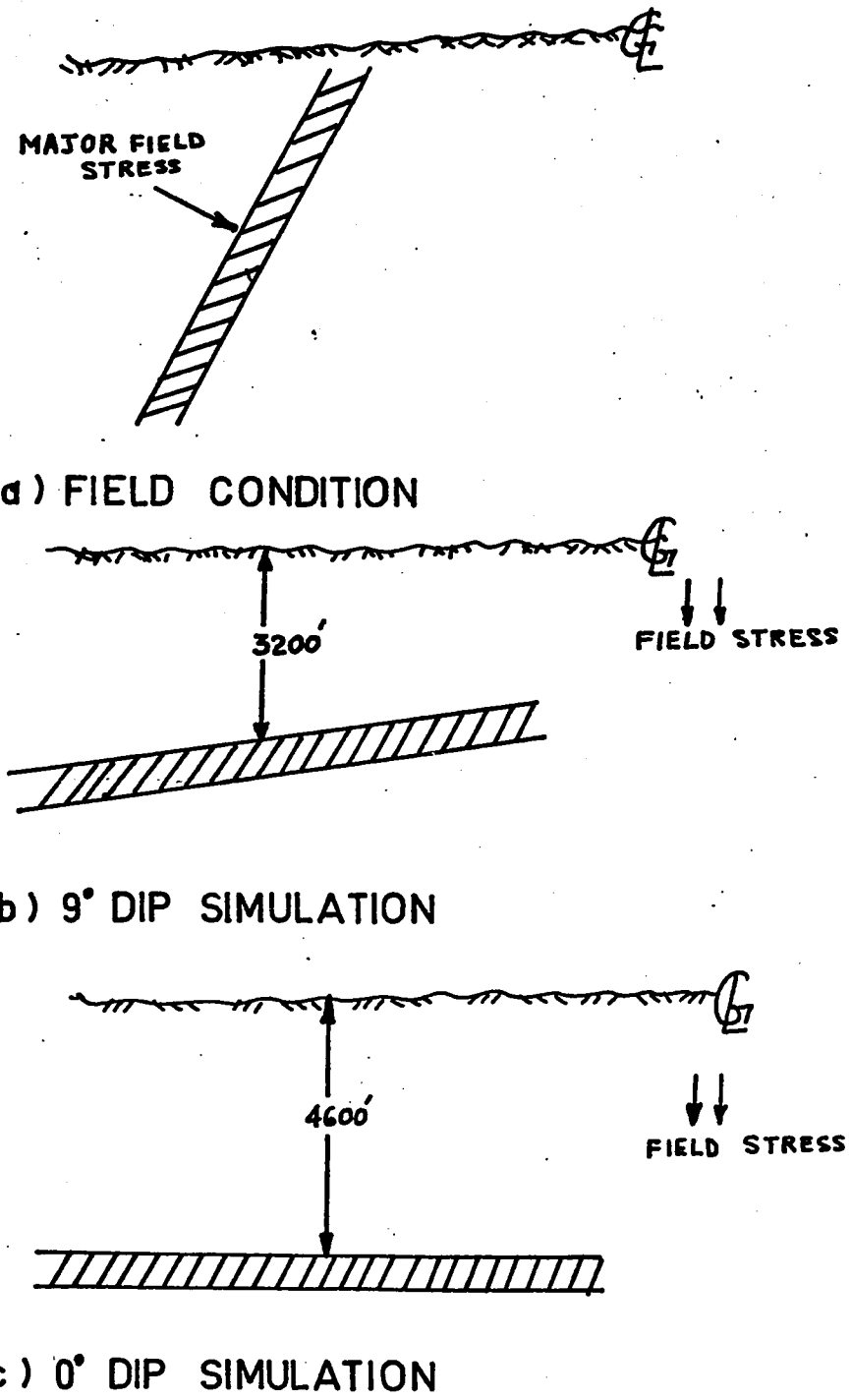

SIMULATION OF THE FIELD CONDITIONS

FIGURE 6-9

In the model study a k-factor of 0.37 has been used to calculate the horizontal component of the pre-mining stress.

The location where the induced principal stresses have been calculated are the same as those used for the field measurements. However, a location F well removed from the active mining zone has been included in this study, which might prove of comparative value.

Analysis of Data:

Table 6-6 and 6-7 give the model values for 9 degrees dip and zero degree dip respectively. The field measurements for the locations 4,5,6 and 7, as shown in Figure 6-6, are summarised in Table 6-8.

On comparing the model values with the field measurements the agreement does not seem to be good. The model study is based on the assumption that the orebody is tabular which is not true. Also, the variations in the magnitude of the field measurements are very wide.

However, it must be emphasized that the main purposes of this model study is to analyse the abutment stresses induced by the complex geometry of the mining openings.

The present study concerns itself with the analysis of the stresses in the peninsula abutment, A_1 (see Figure 6-6). The 9 degree dip model show that the magnitude of the major principal stress gradually increases and the minor principal stress, which is tensile in nature, decreases in magnitude towards the tip of peninsula. This suggests that the magnitude of the major principal stress is a function of the

TABLE 6-6

Calculated Principal Stresses for 9 degrees dip Model

S_o = 3149 psi μ = 0.27 , E = 14 x 10^6 psi , k = 0.37

Location No.	Principal Stresses		
	Major σ_1 psi	Intermediate σ_2 psi	Minor σ_3 psi
4	1866	745	-6992
5	2271	529	-6646
6	3790	129	-4060
7	3817	630	-3893
F	3141	955	-3911

TABLE 6-7

Calculated Principal Stresses for 0 Degree Dip Model

S_o = 4600 psi μ = 0.27 , E = 14 x 10^6 psi, k = 0.37

Location No.	Principal Stresses		
	Major σ_1 psi	Intermediate σ_2 psi	Minor σ_3 psi
4	2895	829	-3482
5	2866	859	-3879
6	2587	871	-5394
7	2545	812	-5606
F	2199	522	-471

TABLE 6-8

Field Stress Measurements

at Kerr-Addison Mines (x)

Location No.	Major Principal Stress (Psi)			Minor Principal Stress (psi)		
	Average of all the Measurements	Max. Recorded	Min. Recorded	Average of all the Measurements	Max. Recorded	Min. Recorded
4	8172(4)	10447	6814	2432(4)	3154	1212
5	6230(4)	8236	4788	2386(4)	3563	1712
6	4846(3)	5208	4668	1091(3)	2195	242
7	13924(1)	-	-	2475(1)	-	-

(x) These values have been summarised from Table 4. Ref. 51

( ) The number in the paranthesis indicates the number of observations at each location.

degree of confinement within the peninsula. This effect is further demonstrated by Figure 6-10. It is noted that the curve gradually falls in the solid ground.

The same conclusion holds good for zero degree dip model. However, in both the models the minor principal stress is tensile and of high magnitude. A similar observation was noticed in peninsula abutments A_2 and A_3. It is believed that the tensile stresses are mainly due to the peninsula type geometry.

The high tensile stresses induced by the mining in these zones are likely to initiate fracture in the rock mass. Even in the absence of discontinuities, fracture can occur if tensile stresses develop even in moderate values. This does not necessarily constitute a mining problem because the fractured material retains the ability to resist the load to some extent. In other words, the strength of the rock mass is not reduced to zero with the onset of fracture. Deist (70) has shown that fractured rock possess appreciable and definite strength.

This brings up the problem whether the mining zones with high tensile stresses as predicted by the model study could stay stable. It is most likely that such concentrations will not occur in actual practice as a redistribution of stresses would result, should the stresses exceed the strength. Also the model does not take into account the gradual process of mining, rather a sudden creation of a large excavated area. The stress relief that normally occurs in the various mining areas, cannot be accounted for in the model study

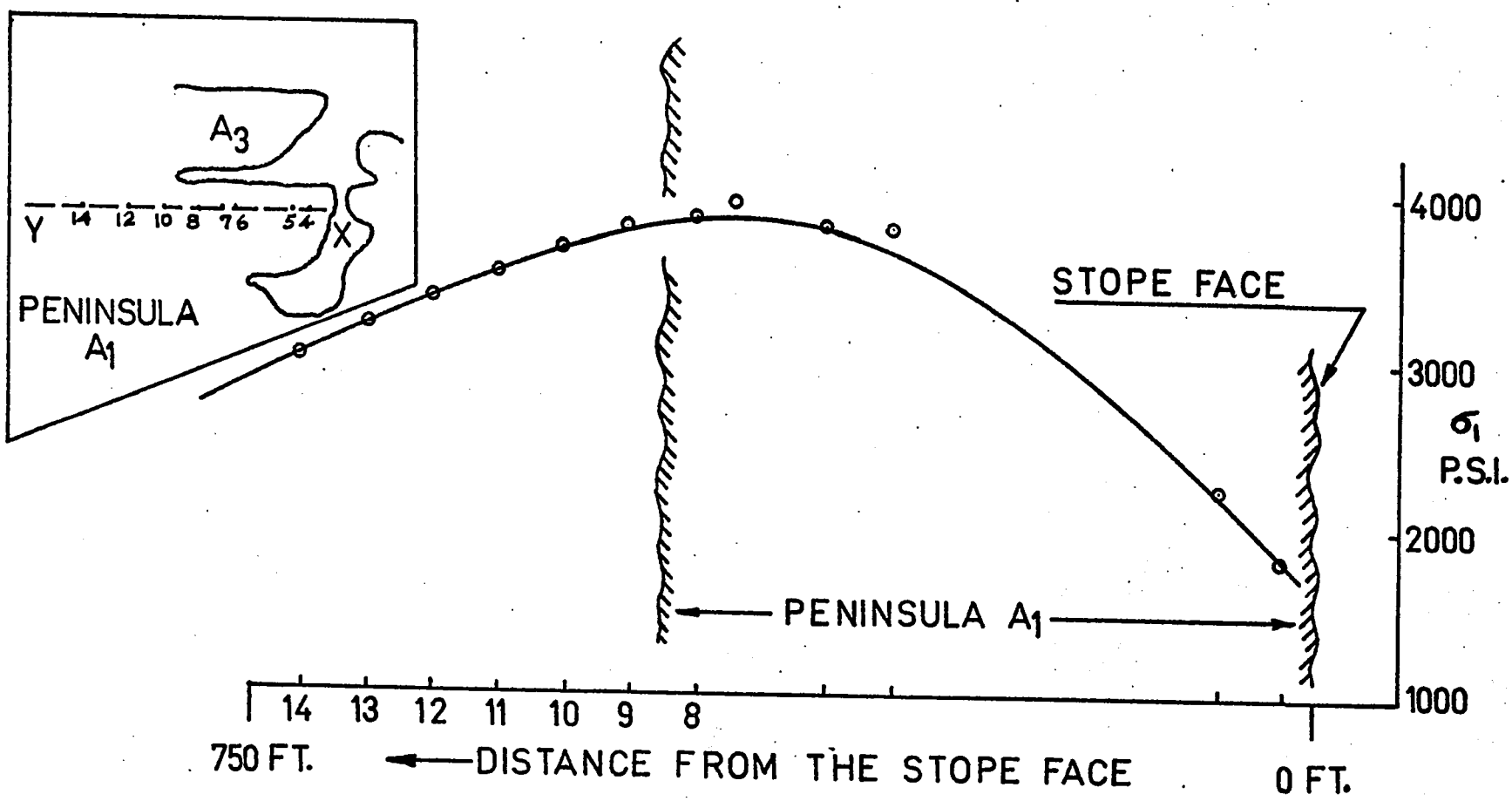

A STRESS PROFILE ALONG A SECTION X-Y PASSING THROUGH THE TEST LOCATIONS IN PENINSULAR ABUTMENT A_1

FIGURE 6-10

but could be assumed in reducing the peak stresses in the actual mining operation.

Moreover, a knowledge of the original state of stress in the rock mass also could assist in predicting stresses from model studies. Some of these difficulties would possibly be solved by the development of techniques for the measurement of pre-mining stresses in a three-dimensional stress field.

As a result of this study, it is thought that the stresses predicted should provide guidance towards the knowledge of stresses in the abutments of a mine within an elastic rock mass. Bearing in mind the effect of complex geometry on the abutment stresses, an acceptable design criteria can be worked out for the safe operation of the mine.

CHAPTER VII

CONCLUSIONS

As a result of studies in stress distribution using the electrical tank analogue it is possible to predict pillar stresses within irregular mining outlines in deep tabular orebodies. This analytical approach in three-dimensions is a distinct advance in the analytical methods in two-dimensions presently available.

1. Figure 7-1 shows the relationship between the stress concentration and the height of the pillar, which indicates that with the increase in pillar height there is a significant decrease in the pillar loading. This suggests that the stored energy densities are highest in thin orebodies, which, as a result are more susceptible to sudden failure and rockbursts.

2. With other parameters constant the change in the pillar loading by changing the breadth of the pillar is relatively insignificant (Figure 7-2). However, where the breadths of pillar vary, the pillar loadings could also vary, giving rise to higher densities in narrower pillars.

3. The effect of varying the extraction ratio, R, on pillar loading is by far the most significant (see Figure 7-3).

4. The influence of varying the elastic constants E_p and μ_p, of the pillar rock with respect to wall rock was studied and results plotted in Figures 7-4 and 7-5 respectively. As indicated by Figure 7-4

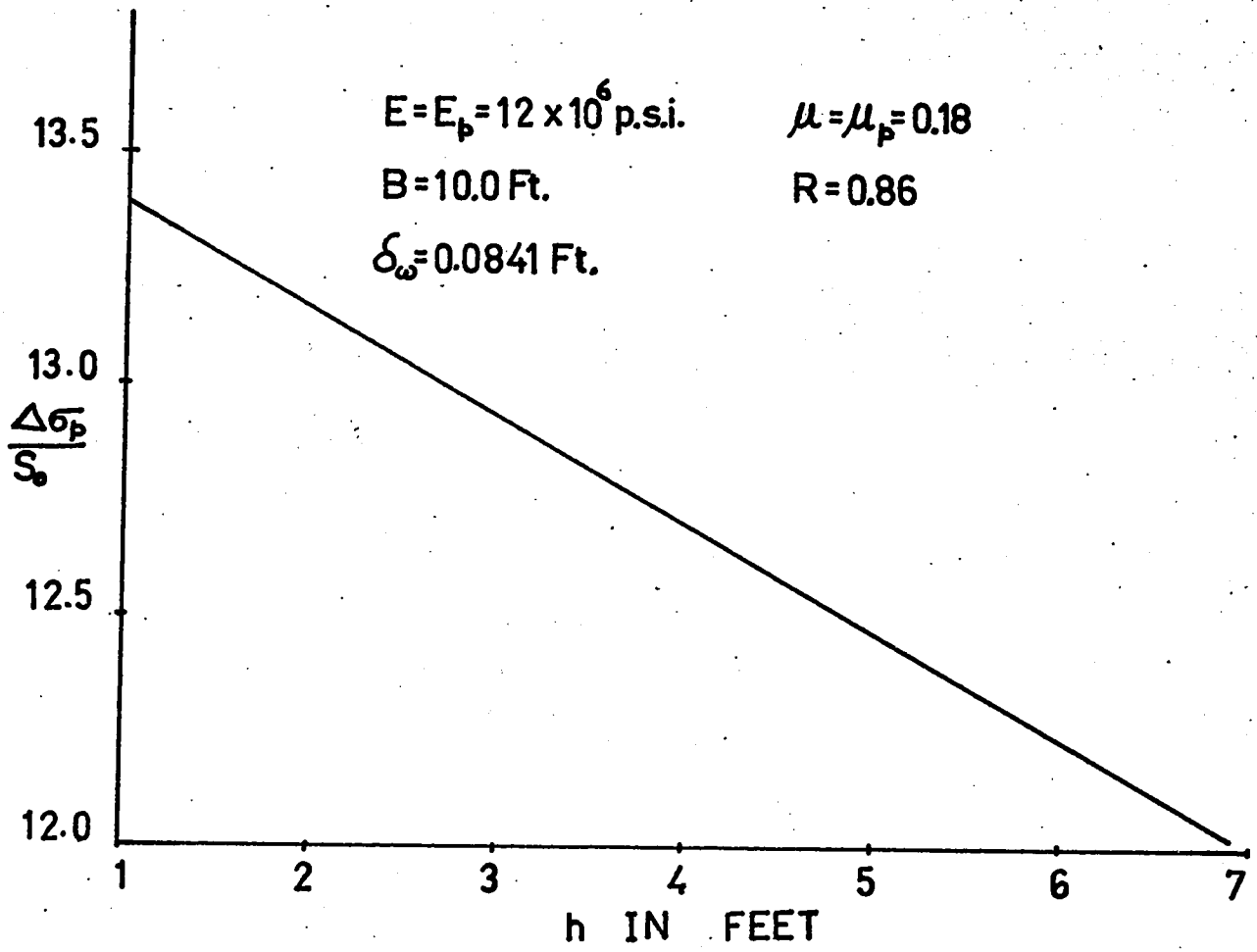

EFFECT OF h ON PILLAR STRESSES

FIGURE 7-1

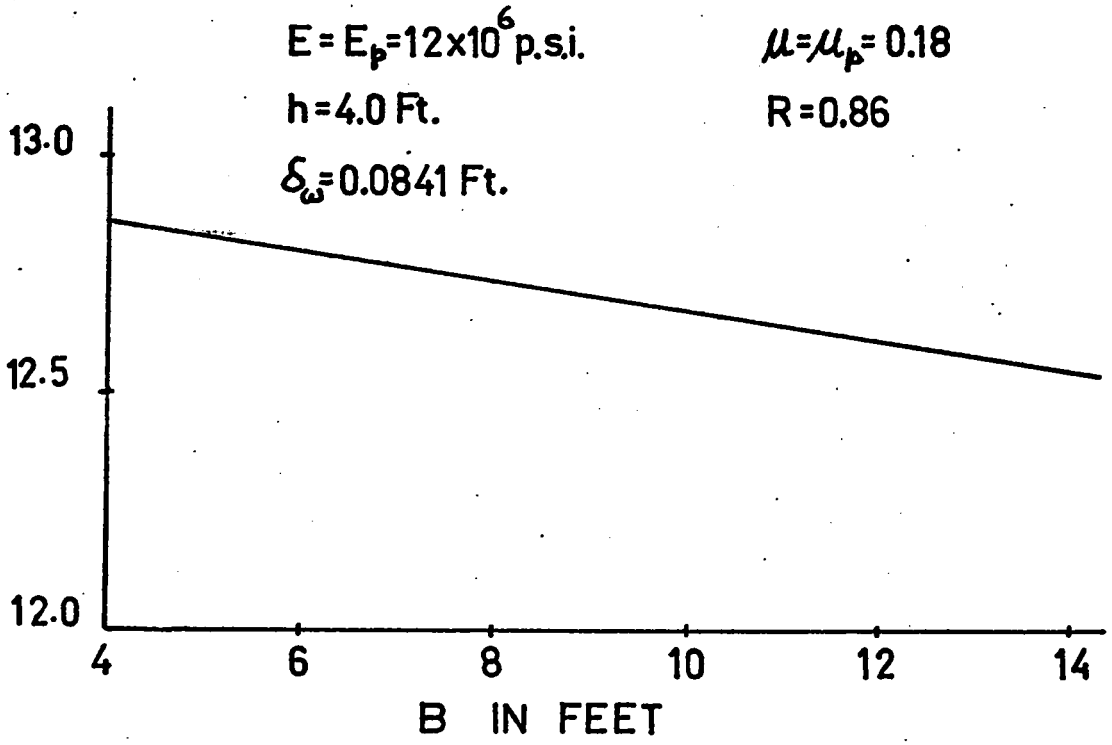

EFFECT OF B ON PILLAR STRESSES

FIGURE 7-2

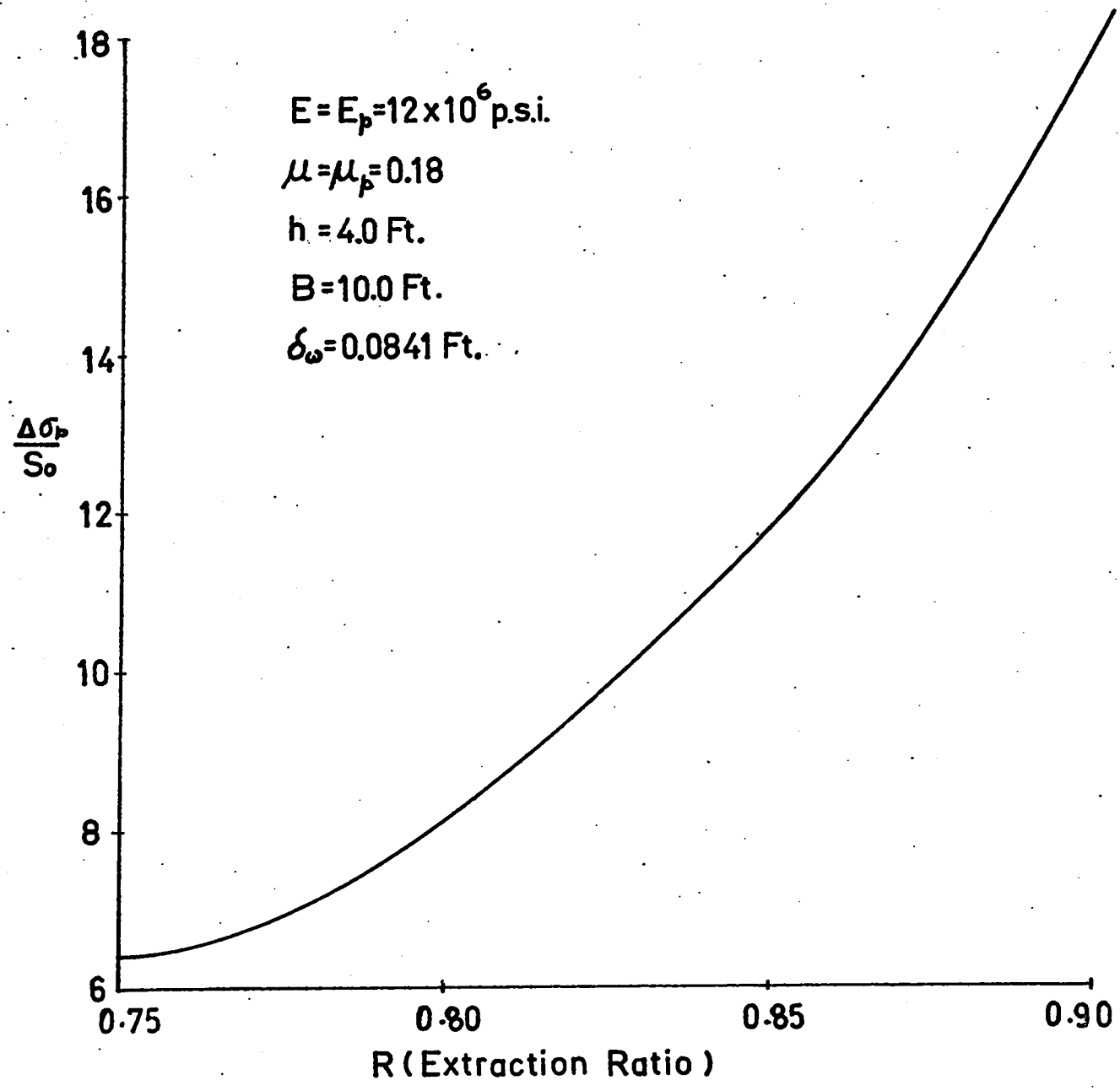

EFFECT OF R ON PILLAR STRESSES

FIGURE 7-3

pillar loadings will vary with differences in E. It could be that relatively incompresible pillars contain stored energy of a higher order of magnitude than pillars with lower compressibility. Such conditions contribute towards rockburst potentials.

The variation of the Poisson's ratio, μ_p, of the pillar rock shows a decrease in the pillar loading with the increase in μ_p.

5. The effects of varying stress ratio, k, on the pillar loading is insignificant (see Figure 7-6) A similar effect also has been observed earlier (23) by Coates while studying pillar loading on two-dimensional basis.

The range in values included in this study for the parameter k was from 1.0 to 4.36.

6. The stresses induced in abutment zones are a function of the geometry of the excavations. The model studies can help in the design of support and in planning the sequence of operation. The study has shown the value of the electric tank analogue when complicated geometry is involved.

7. From the field studies it would seem that the field stresses around a mine cannot be assumed to be homogeneous. However, the predicted values should provide an order of magnitude for both pillar and abutment stresses.

8. Furthermore, it is concluded that the geological features have influenced the in situ stress measurements to a considerable extent.

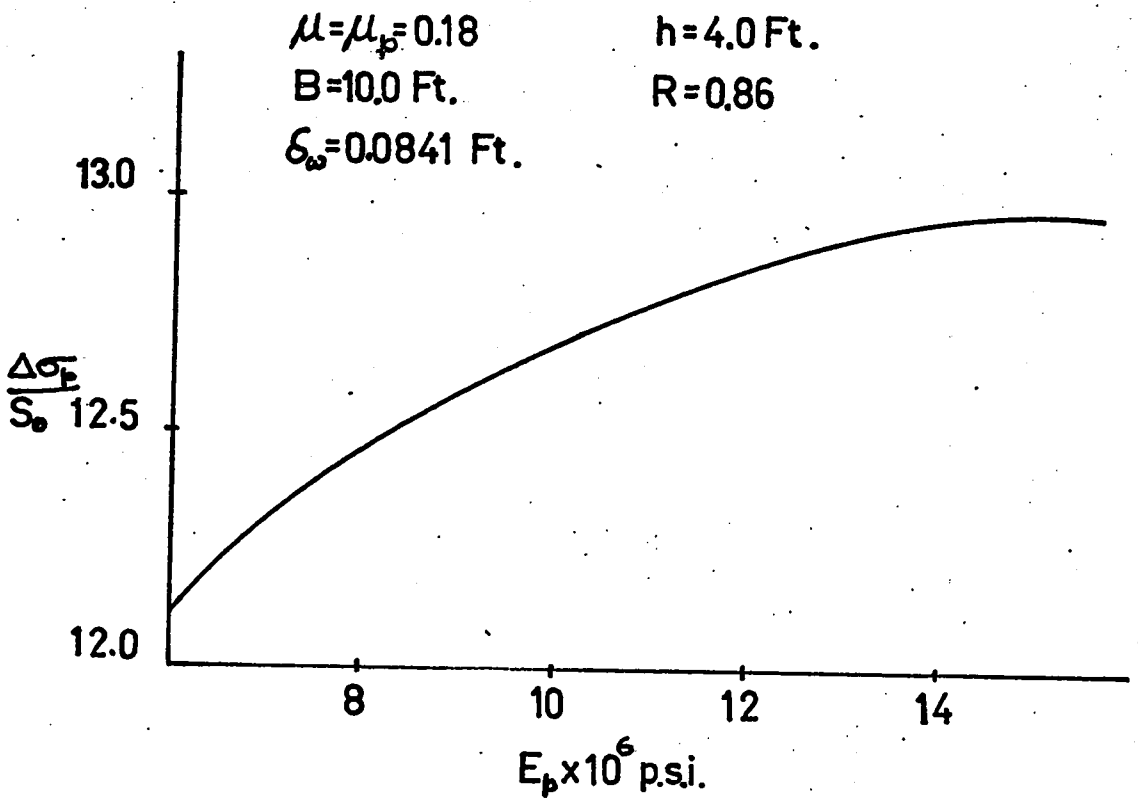

EFFECT OF E_p ON PILLAR STRESSES

FIGURE 7-4

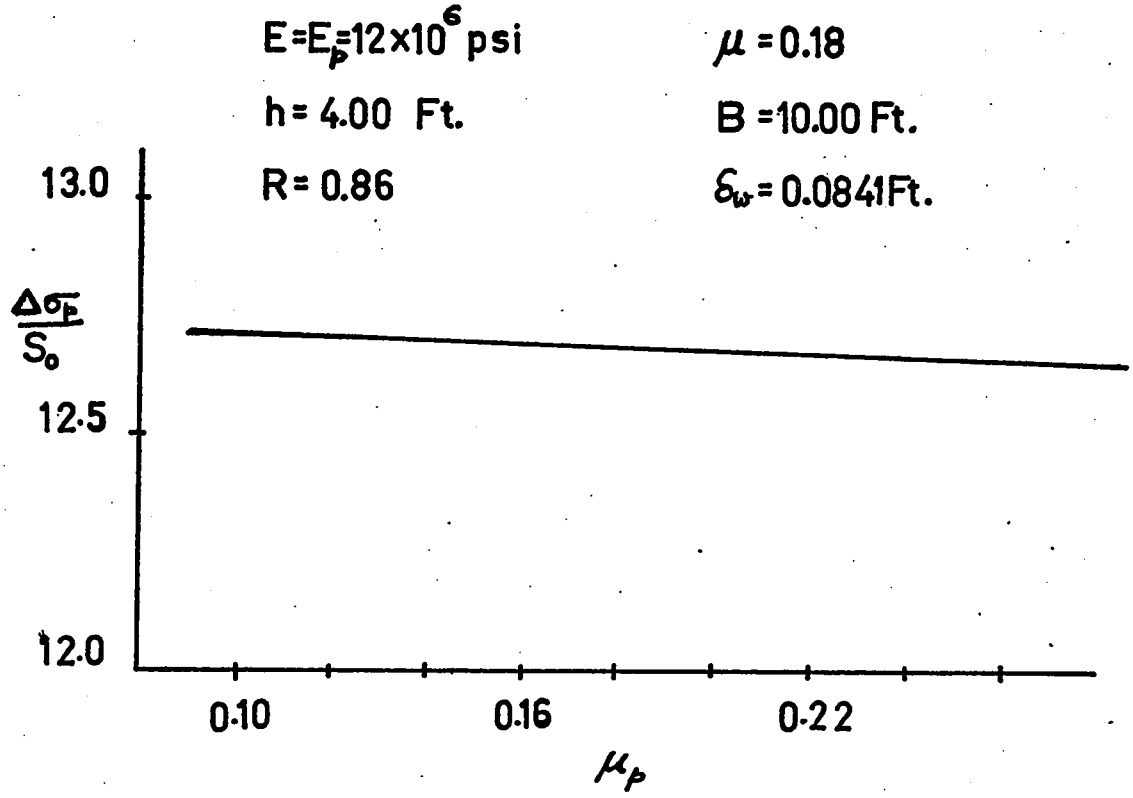

EFFECT OF μ_p ON PILLAR STRESSES

FIGURE 7-5

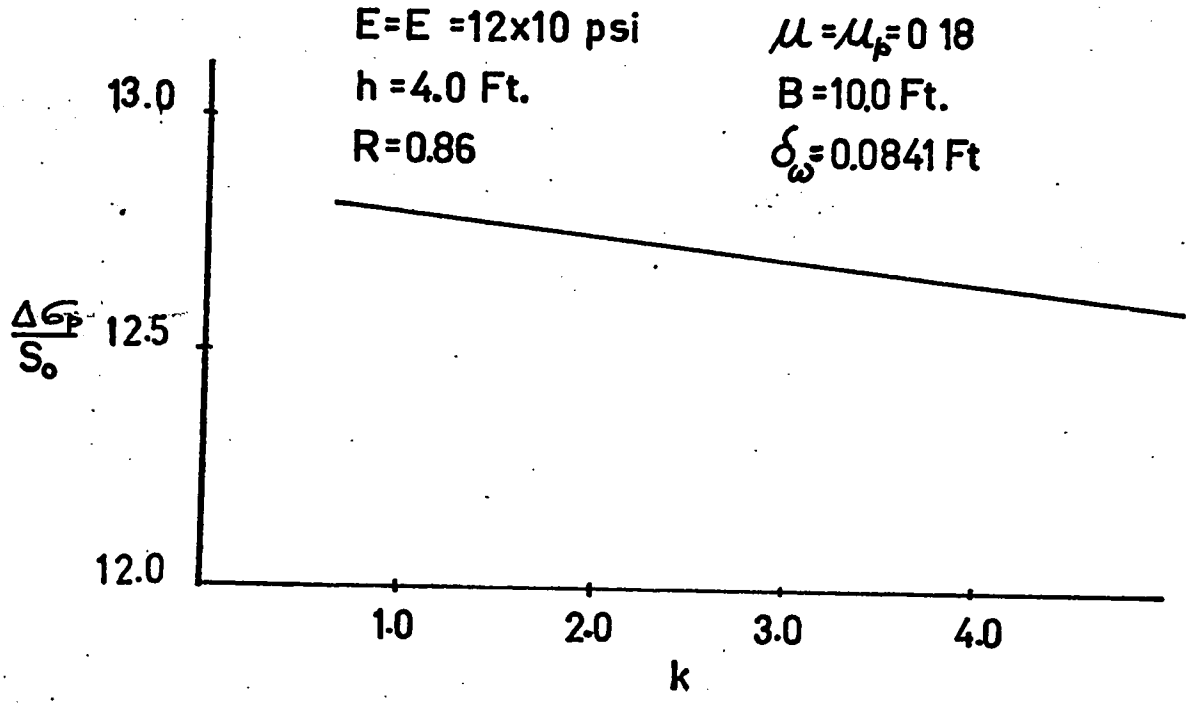

EFFECT OF k ON PILLAR STRESSES

FIGURE 7-6

It is therefore, suggested that future analysis of the in situ stress measurements must be closely related to the geological features, such as, joints, faults, minor folds and dikes.

9. In the present study, the influence of the dike has been demonstrated on the predicted values.

By using the three-dimensional method for pillar loading, it would be possible to predict the effect of any change in the pillar loads due to varying the outlines of mining area, the pillar height, ratio of extraction and related parametes. Moreover, further comparison of the predicted values with actual field measurements should eventually yield acceptable design criteria.

Thus for a standard room and pillar geometry the three-dimensional approach should be adequate for predicting pillar loads so long as the orebody is tabular in shape and assumed to be in an infinite elastic medium. The same conclusion holds good for abutment stresses.

BIBLIOGRAPHY

1. Serata, S., "Theory and Model of Underground Opening and Support System", Proc. of the 6th. Symposium on Rock Mechanics, University of Missouri, Rolla, pp. 260-292, (Oct.1964).

2. Zahary, G., "Rock Mechanics at International Minerals and Chemical Corporation (Canada) Ltd.," Proc. of the 3rd. Canadian Rock Mechanics Symposium, University of Toronto, Toronto, pp. 1-17, Jan. 1965).

3. "The Coal Miners Pocketbook", 12th. Edition, McGraw-Hill Book Co. Inc., New York, pp. 642, (1928).

4. Greenwald, H.P., Howarth, H.C., and Hartmann, I., "Experiments on Strength of Small Pillars of Coal in the Pittsburgh Bed", USBM, Technical Paper 605, (1939).

5. Greenwald, H.P., Howarth, H.C., and Hartmann, I., "Experiments on Strength of Small Pillars of Coal in the Pittsburgh Bed", USBM, RI 3575, (June 1941).

6. Steart, F.A., "Strength and Stability of Pillars in Coal Mines", J. of Chem., Met. and Mining Society of South Africa, Vol. 54, pp. 309-325, (1953-54).

7. Holland, C.F.and Gaddy, F.L. "Some Aspects of Permanent Support of Overburden on Coal Beds", West Virginia Coal Mining Institute, Proceedings, pp. 55,(1956).

8. Holland, C.F., "Causes and Occurance of Coal Mine Bumps", AIME, Trans. Vol. 211, pp. 994-1004B, (1958).

9. Duvall, W.I., "Stress Analysis Applied to Underground Mining Problems, Part II: Stress Analysis Applied to Multiple Openings and Pillars", USBM, RI 4387, (Nov. 1948).

10. Coates, D.F., "Pillar Loading, Part I: Literature Survey and New Hypothesis", Mines Branch Research Report R 168, Canada, Department of Mines and Technical Surveys, Ottawa, (Oct. 1965).

11. Tincelin, E. and Simou, P., "Collapse of Areas Worked by Small Pillar Method - Practical Conclusions and an Attempt to Formulate Laws for Phenomena Observed", International Conf. on Strata Control, Paris (1960).

12. Coates, D.F., "Theoretical Considerations of the Effect of the Ratio of the Width of Mine Area to Depth of Operations in Pillar Loading - Elastic and Plastic Analysis", Appendix D in Report by the Special Committee on Mining Practices at Elliot Lake, Part II, Ontario Department of Mines, Bull. 155, Toronto (1961).

13. Hover, K., and Menzel, W., "Comparative Study of Pillar Loads in Potash Mines Established by Calculation and by Measurements Below Ground", International Journal of Rock Mechanics and Mining Science, Vol. 1 (1964).

14. Denkhaus, H., " A Critical Review of the Present State of Scientific Knowledge Related to the Strength of the Mine Pillars", Journal of South African Inst. of Min. and Met., Vol. 63, No. 2, (Sept. 1962).

15. Panek, L., " Stresses about Mining Openings in a Homogeneous Rock Body", Edwards Bros. Inc., Ann Arbor, Michigan (1951).

16. Hiramatsu, Y. and Oka, Y., "Photoelastic Investigations into the Earth Pressure Acting on Pillars", Journal of Min. and Met., Japan, Vol. 79, No. 905 (1963).

17. Trumbachev, V. and Melnikov, E., "Distribution of Stresses in the Intervening Pillars at Medium and Steep Dips", Proc. International Conf. on Strata Control and Rock Mechanics, Columbia University, New York (1964).

18. Obert, L., "Measurement of Pressures on Rock Pillars in Underground Mines, Part I", USBM RI 3444 (1939).

19. Obert, L., "Measurement of Pressure on Rock Pillars in Underground Mines, Part II", USBM RI 3421 (1940).

20. Mohr, F., "Measurement of Rock Pressure", Mine and Quarry Engineering, pp. 178-189, (May 1956).

21. Leeman, E., and Heerden, W., "Stress Measurements in Coal Pillars", Colliery Engineering (Jan. 1964).

22. Dare, W., "Measuring Changes in Pillar Strain during Pillar Recovery", USBM RI 6056 (1962).

23. Coates, D.F., "Pillar Loading, Part II: Model Studies", Mines Branch Research Report R 170, Canada, Department of Mines and Technical Surveys, Ottawa (Nov. 1965).

24. Roark, R., "Formulas for Stress and Strain", McGraw-Hill, Book Co. Inc. New York, (1954).

25. Sneddon, I., "Stress in the Neighbourhood of a Crack", Proc. Roy. Soc. of London, Series A, Vol. 187, pp. 229 (1946).

26. Salamon, M.G.D. "Elastic Analysis of Displacements and Stresses Induced by Mining of Seam or Reef Deposits, Part I: Fundamental Principles and Basic Solutions as Derived from Idealized Models", Journal of South African Inst. of Min. and Met., Vol. 64, No. 4, (Nov. 1963).

27. Salamon, M.D.G., "Elastic Analysis of Displacements and Stresses Induced by Mining and Seam or Reef Deposits, Part II: Practical Methods of Determining Displacement,Strain and Stress Components from a given Mining Geometry", Journal of South African Inst. of Min.and Met., Vol. 64,No.6, (Jan. 1964).

28. Salamon, M.D.G., "Elastic Analysis of Displacements and Stresses Induced by Mining of Seam or Reef Deposits, Part IV: Inclined Reef", Journal of South African Inst. of Min. and Met. Vol. 65, No. 5, (Dec. 1964).

29. Salamon, M.D.G., Ryder, J.A. and Ortlepp, W.D., "An Analogue Solution for Determining the Elastic Response of Strata Surrounding Tabular Mining Excavations", Journal of South African Inst. of Min. and Met., Vol.65, No.2,(Sept. 1964).

30. Hetenyi, M., "Hand Book of Experimental Stress Analysis", John Wiley and Sons Inc., New York, (1950).

31. Ortlepp, W.D., 'Personal Communication.

32. Adams, W.C., On the Forms of Equipotential Curves and Surfaces and Lines of Electrical Force", Roy. Soc. (London). Vol. 23, pp. 280-84, (1875).

33. Hepp, G. "Measurements of Potential by means of the Electrolytic Tank", Philips Technical Review, Vol. 4, pp.223-230,(1939).

34. Karplus, W.J., "Analog Simulation ", McGraw-Hill Book Co. Inc., New York, (1958).

35. Sander, K.F., and Yates, J. G., "The Accurate Mapping of Electrical Fields in an Electrolytic Tank" Proc. Inst. Electrical Engrs., Vol. 100, Part II, pp. 167-183, (1953).

36. Dowex: "Ion Exchange", The Dow Chemical Co. Midland, Michigan, (1964).

37. Einstein, P.A., "Factors Limiting the Accuracy of Electrolytic Plotting Tanks", British Journal of Applied Physics, Vol. 2, pp.49-55, (1951).

38. Burfoot, J.C., "Probe Independence in the Electrolytic Tank", British Journal of Applied Physics, Vol. 6, pp.67-68, (1955).

39. Coates, D.F., "Pillar Loading, Part III: Field Measurements" Mines Branch Research Report R 180, Canada, Department of Mines and Technical Surveys", Ottawa (Feb. 1966).

40. Coates, D.F., and Grant, F., "Stress Measurements at Elliot Lake", Canadian Min. and Met. Bull., Trans., Vol. LXIX, pp. 182-192, (1966).

41. Roscoe, S.M., "Geology and Uranium Deposits, Quirka Lake-Elliott Lake, Blind River Area, Ontario ", Geological Survey of Canada Preliminary Report, Paper 56-57, (1957).

42. Bain, I., "The Geological Structure and Probable Rock Stress Environment in the Quirke Syncline and Particularly in the Algom Nordic Mine Test Area, Elliot Lake, Ontario", Mines Branch Divisonal Report FMP 65/106-MRL, Canada , Department of Mines and Technical Surveys, Ottawa (July 1965).

43. Morrison, R.G.K., Corlett, A.V., and Rice, H.R., "Report of the Special Committee on Mining Practices at Elliott Lake", Ontario Department of Mines Bull. 155 (1961).

44. Parsons, R.C., and Sullivan, J.D., "Moduli Determinations for the Elliot Lake Stress-Relief Overcoring Work", Mines Branch Divisional Report FMP 65/137 MRL, Canada, Department of Mines and Technical Surveys, Ottawa (Oct. 1965).

45. Yu, Y.S., "Sonic Measurements at Nordic Mine, Rio Algom Mines Ltd., Elliot Lake, Ontario", Mines Branch Divisonal Report FMP 66/189-MRL, Canada, Department of Mines and Technical Surveys, Ottawa (Dec. 1966).

46. Yu, Y.S., "Diametrical Compression Tests for Elliot Lake Strain-Relief Overcoring Work", Mines Branch Divisional Report MR 67/13, Canada, Department of Mines and Technical Surveys, Ottawa (May 1967).

47. Schwellnuss, J.E., "Methods of Analyzing the Geometry in Joints", Proc. of the Fourth Canadian, Rock Mechanics Symposium, Ottawa (March 1967).

48. Schwellnus, J.E., Personal Communication.

49. Bonnechere, F. and Fairhurst, C., "Determination of Regional Stress Field from 'Doorstoper' Measurements", Journal of South African Inst. of Min. and Met. (July 1968).

50. Talapatra, D.C., and Udd, J.E., "A photoelastic Study of Stress Relief of Overcoring", Preprint, Int. Symposium on the Determination of Stresses in Rock Masses, Lisbon, (May 1969).

51. Zahary, G., Stress Measurements, Kerr-Addison Gold Mines", Mines Branch Divisional Report MR 67/51. Canada, Department of Energy, Mines and Resources, Ottawa, (August 1967).

52. Thomson, J.A., "Geology of McGassay and McVittic Townships, Larder Lake Area, Ontario, Department of Mines, Vol. L, Part VII, (1964).

53. Mine Staff, "Technological Description of Kerr-Addison Gold Mines,Ltd.,", Canadian Mining Journal, (April 1951).

54. Udd, J.E. and Grant, F., "Measurement of stresses in the Abutment Zones, Nordic Mine, Rio Algom Mines Ltd., Elliot Lake, Ontario", Mines Branch Divisional Report MR 67/52-ID, Canada Department of Energy, Mines and Resources, Ottawa , (August 1967).

55. Udd, J.E., "Preliminary Calculations of Stresses in the Abutment Zones, Nordic Mine, Elliot Lake, Ontario, Mines Branch Internal Report MR 68/35-ID, Canada Department of Energy Mines and Resources, Ottawa, (March 1968).

56. Ortlepp, W.D., "The Effect of Stoping on the Stability of a Remote Pre-Existing Tunnel", Proc. of the 4th Canadian Rock Mechanics Symposium, pp. 205-223, Ottawa (March 1967).

57. Potts, E.L.J., "Underground Instrumentation", Quart. Colorado School of Mines, Vol. 52, pp. 135-182, (July 1957).

58. May, A.N., "Instruments to Measure the Stress Conditions in the Rocks Surrounding Underground Openings", Int. Strata Control Conference, Paris, Paper D.3, (May 1960).

59. Hast, N., "The Measurement of Rock Pressure in Mines", Saveriges Geologiska Undersokning, Scr. C. Arsbok 52, No. 3, Stockholm, (1958).

60. Panek, L.A., "Methods for Determining Rock Pressure" Fourth Symposium on Rock Mechanics, Pennsylvania State University, (1961).

61. Obert, L., Merrill, R.H., and Morgan, T.A., "Borehole Deformation Gauge for Determining the Stress in the Mine Rocks", USBM, RI 5978 (1962).

62. Jaeger, J.C., and Cook, N.G.W., "Theory and Application of Curved Jacks for Measurement of Stresses", Proc. Int. Conference on the State of Stress in the Earths Crust. Santa Monica, California, (1963).

63. Leeman, E.R. "The Measurement of Stress in Rock, Part I, II and III", Symposium on Rock Mechanics and Strate Control in Mines, April, 1963-June 1965, pp.248-373. The South African Int. of Min. and Met., Johannesburg (1965).

64. Van Heerden, W.L. and Grant, F.," A Comparison of Two Methods for Measuring Stress in Rock", The Int. Journal of Rock Mechanics and Sciences, Vol. 4, pp.376-382, Pergamon Press, Oxford, England, (1967).

65. Mahtab, M.A., "A Study of Field Stress Distribution Around an Elliptical Hole under Different Loading Conditions", M. Eng.Thesis, McGill University, Montreal, (1965).

66. Dhar, B.B., "Stresses in Depth Around an Oval Opening in an Elastic Medium", M.Eng. Thesis, McGill University, Montreal, (1966).

67. Dhar, B.B., Geldart, L.P. and Udd, J.E., "Stresses in Depth Around Elliptical and Ovaloidal Openings in an Infinite Elastic Medium", (To be published in CIMM, Bull. April 1970).

68. Kirsch, C., "Die Theorie der Elastizitat und die Bedurfnisse der Festigkeitslehre", V.1.D. (Verein Deutscher Ingenieure) Journal, Vol. 42, No. 29, pp. 797-807, Sonnabend, (July 1898).

69. Van Heerden, W.L., Szombatty, C. and St. Louis, A.V., "A New Strain Cell Installing Tool", Divisonal Report FM 66/37-MRL, Mines Branch, Ottawa, (March 1966).

70. Deist, F.H., "A Non-linear continuum approach to the Problem of Fracture Zones and Rockbursts", J.S. Afr. Inst. Mining and Metallurgy, (May 1965).

71. Salamon, M.D.G. "A Method of Designing Bord and Pillar Workings", J.S. Afr. Inst. of Min. and Met., Vol. 68, No.2, pp.68-78, (Spet. 1967).

72. Obert, L. and Duvall, W.I., "Rock Mechanics and the Design of Structures in Rock", John Wiley and Sons,Inc., New York, (1967).

73. Ramsay, J.G., "Folding and Fracturing of Rocks", McGraw-Hill Book Company, New York, (1967).

74. Udd. J.E., "A Study of Fracture Pattern at the Nordic Mine. Elliot Lake, Ontario, Mines Branch Internal Report MR 68/36-ID, Canada, Department of Energy, Mines and Resources, Ottawa (March 1968).

75. Morrison, R.G.K., "Personal Notes .(1969).

76. Terzaghi, K., "Theoretical Soil Mechanics", pp. 382-83, John Wiley and Sons, Inc., New York, (1961).

77. Denkhaus, H., "Critical Review of Strata Movement Theories and their Application to Practical Problems", Journal of South African Inst. of Min. and Met. (March 1964).

APPENDIX A-I

Determination of the Displacement Components based on the Face Element Principle:

Salamon (26) has developed a solution to calculate the displacement components in the solid rock surrounding mine excavations (in the plane of the deposit). The basic principle of this solution is to divide the excavated area into small elementary areas and then to perform the integration over the whole area. Such small areas have lateral dimensions much smaller (infintesimal), and are normally referred to as face elements.

The fundamental assumptions necessary to describe the state of the stress and displacements in elastic stress analysis are the boundary conditions, the equilibrium and the compatibility of the elastic body.

The boundary conditions in general are:

1. That the ground surface must be stress free. Thus the stress and displacements at the surface induced by the creation of mine openings must be zero. This applies also at any point remote from the excavations.

2. As the lateral dimensions of a horizontal excavation in the reef are usually much larger than the vertical it is sufficient to specify the conditions on the back and floor (hanging and footwalls)

The mine is normally composed of several production areas of varying shapes and sizes. For the time being,we assume that the lateral dimensions of the excavated areas are such, that complete closure has not taken place or, in other words, the hanging wall and footwall are not in contact with each other.

To establish the continuity of displacements, it is necessary to define the boundary candidions both for the unmined regions and the excavated areas of the reef plane. Broadly speaking, there will be two areas in the mine at the horizontal reef level, one the excavated areas and the other unmined regions. Let all the excavated areas be referred to collectively as EA. These will induce displacements in the surrounding rock mass. In terms of a rectangular coordinate system x,y and z, the displacement components at a point (x,y) are defined as:

1. the vertical closure, δ_w, in the direction of z-axis, normal to the reef plane, and

2. the ride components δ_u and δ_v are the displacements, in the x and y directions, of a reference point on the floor of the reef.

In case of horizontal strata the most important displacement component is the vertical closure δ_w, the magnitude of the ride components are usually small in comparison with vertical closure and may be neglected for the time being (26).

The boundary conditions for a horizontal strata in terms of elementary areas thus can be written as follows:

at the reef level $(z = Z)$

$$\left.\begin{aligned} &\delta_u = \delta_v = 0 \\ &\delta_{w(roof)} - \delta_{w(floor)} = \delta_z \quad \text{within the area } \Delta EA \\ &\delta_{w(roof)} - \delta_{w(floor)} = 0 \quad \text{outside } \Delta EA \end{aligned}\right\} \qquad (A\text{-}1)$$

where ΔEA is the area of the face element, δ_z is the convergence and Z is the depth of the reef (or seam) below the surface.

Since the face element, ΔEA, is very small (infinitesimal), it can be regarded as a point. It can therefore be concluded that the elementary distribution of displacements and stresses are independent of the shape of the face element and thus axially symmetrical.

The qualitative expressions for the elemantary displacement components based on dimensional analysis have been derived (26). The variables that define the displacements have been divided into two groups. Group one includes the boundary values and the geometrical variables, group two includes the parameters involving the properties of the strata. Since the distributions of displacements are axially symmetrical only the vertical $(\Delta\delta_w)$ and the radial horizontal $(\Delta\delta_r)$ elementary displacement components with vertical 'z' and horizontal 'r' coordinates need to be considered. (Remembering that these

displacements are the result of vertical closure, δ_z). Figure A-1 explains this principle. The expressions as derived (26) for these displacement components are given below:

$$\left.\begin{aligned} \Delta\delta_w &= \frac{\delta_z}{\pi}\,\frac{\Delta EA}{z^2}\,\phi_1\left(\frac{r^2}{z^2},\ \frac{z}{Z},\ M_1,M_2,M_3\ \ldots\right) \\ \Delta\delta_r &= -\frac{\delta_z}{\pi}\,\frac{\Delta EA}{z^2}\,\frac{r}{z}\,\phi_2\left(\frac{r^2}{z^2},\ \frac{z}{Z},\ M_1,M_2,M_3\ \ldots\right) \end{aligned}\right\} \qquad (A\text{-}2)$$

where M_1,M_2,M_3 --- are the dimensionless products formed from the second group of variables and ϕ_1,ϕ_2 are two undetermined functions.

The elementary displacement component in the radial plane given by Equation (A-2) can be resolved into two horizontal components $\Delta\delta_u$ and $\Delta\delta_v$ in x and y directions respectively. The only change necessary in Equation (A-2) is to replace r once by (x_o-x_1) and then by (y_o-y_1). The simple transformation is explained in Figure A-1.

The total displacement at a point say $P(x_o,y_o,z_o)$ in the solid rock can be obtained by integrating the elementary displacements of the whole mining area, provided the convergence distribution given by $\delta_z(x_1,y_1)$ is known (Figure A-1). Then the vertical displacement will be given by the following double integral .

Therefore

$$\delta_w = \frac{1}{\pi}\iint_{EA}\delta_z\,(x_1,y_1)\ \phi_1\left(\frac{r^2}{z^2},\frac{z}{Z},\ M_1,M_2,M_3,\ ..\right)\frac{dx_1dy_1}{z^2} \qquad (A\text{-}3)$$

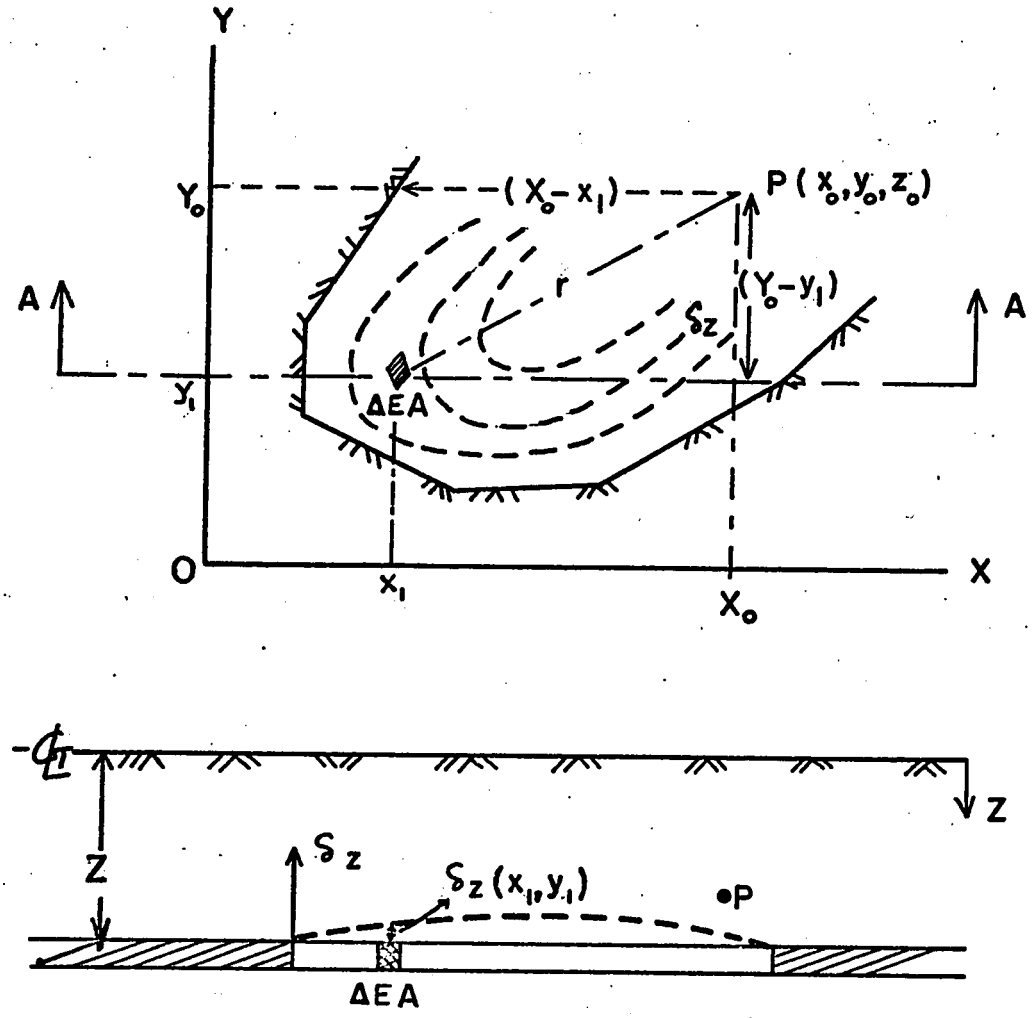

SECTION AT A-A

TRANSFORMATION OF THE RADIAL TO HORIZONTAL COMPONENTS

FIGURE A-1

where $r^2 = (x_o - x_1)^2 + (y_o - y_1)^2$ and the double integral is taken over the regions of mining collectively referred to as EA.

The horizontal components δ_u and δ_v can be obtained in a similar manner.

With the knowledge of two functions ϕ_1 and ϕ_2 the displacement components can be obtained with a known closure. These functions as derived for isotropic homogeneous elastic models (26) are given below.

$$\left.\begin{aligned} \phi_1 &= \frac{z^3}{8(1-\mu)} \left[\frac{2(2-\mu)z^2 + (1-2\mu)r^2}{(r^2 + z^2)^{5/2}} \right] \\ \text{and} \\ \phi_2 &= \frac{z^3}{8(1-\mu)} \left[\frac{2(1+\mu)z^2 - (1-2\mu)r^2}{(r^2 + z^2)^{5/2}} \right] \end{aligned}\right\} \qquad \text{(A-4)}$$

Substituting ϕ_1 in Equation (A-3) we have,

$$\delta_w = \frac{1}{8(1-\mu)\pi} \iint_{EA} \delta_z(x_1, y_1) \; z \left[\frac{2(2-\mu)z^2 + (1-2\mu)r^2}{(r^2 + z^2)^{5/2}} \right] dx_1 dy_1 \qquad \text{(A-3a)}$$

The evaluation of the integral in Equation (A-3a) is possible only with simple geometries, therefore a numerical method of evaluating the integral for complex geometries is necessary. Such an approach has been explained in detail by Salamon (27).

Thus with the known closure δ_z, the three normal displacement components δ_w, δ_u and δ_v can be calculated in the solid rock surrounding the mine excavations.

The Determination of Closure, δ_z, in horizontal Deposits: The determination of closure distribution of irregular mining excavations is beyond mathematical solution. However, the problem has been solved by using analogue methods to determine the closure distribution (27). The basic assumption is that the excavations are considered to be in an infinite medium.

Again, assuming an infinite medium and also that the plane of the reef is a plane of symmetry and free of shear stresses, the general boundary conditions can be defined as follows.

Let the coordinate system be such that the origin is at the reef plane with z-axis pointing towards footwall. Since the reef is assumed to be in a plane of symmetry, the general boundary conditions may be limited to the floor (footwall) of the reef only,

at the reef level, $(z = 0)$

$$\left.\begin{aligned} &\delta_{w(floor)} = 0 && \text{outside the excavated area EA} \\ &\delta_{w(floor)} = -\frac{1}{2}\delta_m && \text{within the excavated area EA, where the closure is complete,} \\ &\sigma_z = \gamma z = S_v && \text{within the excavated area where the closure is not complete,} \end{aligned}\right\} \quad \text{(A-5)}$$

and at infinity $(z = \infty)$

$$\delta_{w(floor)} = \delta_{u(floor)} = \delta_{v(floor)} = 0$$

where δ_m is the maximum closure (i.e. width of the reef from wall to wall) and S_v is the vertical component of the pre-mining stress field at the reef level.

In case of a homogeneous isotropic elastic model, the closure distribution has been solved in terms of the function F, a solution of Laplace's equation (Ref. 26, Appendix 1) . The general boundary conditions defined by Equation (A-5), thus, take the following form in terms of function F:

at the reef level, $(z = 0)$

$$F = 0 \qquad \text{outside the excavated area EA}$$

$$F = -\frac{\delta_m}{4(1-\mu)} \qquad \text{within the excavated area EA where the closure is complete}$$

$$\frac{\partial F}{\partial z} = \frac{(1+\mu)}{E} S_v \qquad \text{within the excavated area where closure is not complete}$$

(A-6)

and at infinity $(z = \infty)$

$$F = 0$$

The closure distribution δ_z in terms of the function F at the reef level $(z = 0)$ can be written as:

$$\delta_z = -\ 4(1-\mu)F \qquad \text{(A-7)}$$

In other words it may be said that the closure is proportional to the magnitude of the function F.

This section may be concluded with the remark that the components of normal closure can be calculated in terms of the function F for a horizontal strata. The only problem remaining is the determination of the function F itself, which will be discussed later. The next step is the determination of the closure in inclined deposits.

Determination of closure in Inclined Deposits: The displacements induced in the solid rock surrounding an inclined excavation have been discussed in detail by Salamon (28), a brief description of which follows.

As in the previous case, let the origin of the coordinate system be at the reef plane with the positive z-axis pointing towards the footwall, and let the boundary conditions be limited to the reef plane and at infinity.

In inclined deposits, the components of the pre-mining stress field at the reef plane will be S_o, the normal component, S'_x and S'_y the shear components. Similarly the closure will have three components δ_z the normal closure δ_x and δ_y the ride components in x and y directions respectively.

The general boundary conditions (Equation A-5) can be extended to the inclined deposits with the following modifications,

at the reef level ($z = 0$)

$$\left.\begin{aligned}
&\delta_z = \delta_x = \delta_y = 0 && \text{outside the excavated area EA}\\
&\delta_z = \delta_m,\ \delta_x = \Delta_1\delta_m,\ \delta_y = \Delta_2\delta_m && \text{within the excavated area where closure is complete}\\
&\sigma_{z(\text{floor})} = S_o,\ \tau_{xz(\text{floor})} = S'_x,\ \tau_{yz(\text{floor})} = S'_y && \text{within the excavated area where the closure is not complete}
\end{aligned}\right\} \quad (A\text{-}8)$$

and at infinity ($z = \infty$)

$$\delta_{w(\text{floor})} = \delta_{x(\text{floor})} = \delta_{y(\text{floor})} = 0$$

where Δ_1 and Δ_2 are the constants, δ_m is the maximum normal closure and τ_{xz}, τ_{yz} are the shear components.

In case of horizontal deposits for the determination of closure distribution the solution is based on the assumption that the reef plane is free of shear stresses, a similar solution exists in which the reef plane (i.e. at $z = 0$) is assumed to be free of normal stress (Ref. 28 , Appendix I). Such a solution makes it possible to separate the normal stress components and the related closure from those of shear stress and ride. The net displacement components δ_w, δ_u and δ_y in the z,x and y directions respectively, will be composed of three parts each, one part due to normal closure and the other two due to ride in x and y directions respectively. Mathematically these components can be expressed as:

$$\left.\begin{aligned} \delta_W &= \delta_w + \delta_{wx} + \delta_{wy} \\ \delta_U &= \delta_u + \delta_{ux} + \delta_{uy} \\ \delta_V &= \delta_v + \delta_{vx} + \delta_{vy} \end{aligned}\right\} \qquad \text{(A-9)}$$

where δ_w, δ_u and δ_v are the components of displacement due to closure, $\delta_{wx}, \delta_{ux}, \delta_{vx}$ due to ride in x direction and $\delta_{wy}, \delta_{uy}, \delta_{vy}$ due to ride in y direction. Similar relations hold good for the strain and stress components.

For the determination of the components due to closure, the assumptions necessary to establish the boundary conditions are the same as used in Equation (A-6) and (A-7), hence need not be discussed again. The determination of the ride components in inclined deposits will not be discussed here, as the requirement for the present study is only the determination of the vertical closure δ_w, due to the normal component of the field stress.

APPENDIX A-II

The Principle of the Analogue Method:

The solution of the function F (Equation (A-6) is possible, if an analogy can be found between the function F and any other function which could be determined experimentally, provided both the functions are a solution of Laplace's equation and satisfy the same boundary conditions. Such an analogy has been established (27) is explained here briefly.

Introducing a function say Ω , which satisfies the Laplace's equation

$$\nabla^2 \Omega = 0 \qquad \text{(A-10)}$$

and is subjected to the following boundary conditions:

at the reef level ($z = 0$)

$\Omega = 0$	outside the excavated area EA,	(A-11)
$\Omega = -\Omega_o$	within the excavated area where closure is complete,	
$\frac{\partial \Omega}{\partial z} = 1$	within the excavated area where the closure is not complete,	

and at infinity ($z = \infty$)

$\Omega = 0$.

Because of the similarity of the boundary conditions defined by Equation (A-6) and (A-11), it can be seen that the convergence at any point on the reef plane ($z = 0$) is proportional to the function Ω.

Therefore, a relationship exists between δ_z and Ω in the following form:

$$\delta_z = - C \Omega \qquad \text{(A-12)}$$

provided, the condition in the zone of complete closure defined by Ω_o is calculated from the following formula

$$\Omega_o = \frac{\delta_m}{C} \qquad \text{(A-13)}$$

The constant C for homogeneous isotropic elastic model has been determined (27) in terms of elastic constants E and μ and the normal component S_o of the pre-mining stress field, and is equal to $-4(1-\mu^2)S_o/E$.

Now substituting for C in Equation (A-12) we have:

$$\delta_z = 4(1-\mu^2)S_o/E\ \Omega \qquad \text{(A-14)}$$

The Equation (A-3a) can now be written in terms of the function Ω after substituting for δ_z.

Therefore,

$$\delta_w = \frac{4(1-\mu^2)S_o}{8\pi(1-\mu)E} \iint_{EA} \Omega\,(x_1,y_1)z\left[\frac{2(2-\mu)z^2 + (1-2\mu)r^2}{(r^2+z^2)^{5/2}}\right]x_1 dy_1 \qquad \text{(A-15)}$$

or

$$= \frac{(1+\mu)S_o}{4\pi E} \iint_{EA} \Omega\,(x_1,y_1)z\left[\frac{2(2-\mu)z^2 + (1-2\mu)r^2}{(r^2+z^2)^{5/2}}\right]dx_1 dy_1$$

In the same manner the formula for other displacement components can be constructed.

Thus with the knowledge of the function Ω , which satisfies the Laplace's equation (Equation (A-10)) and the boundary conditions defined by the Equation (A-11), it is possible to determine the elastic closure, δ_z. It is known (30) that the potential V, associated with steady state current flowing in a homogeneous continuous medium satisfies the Laplaces equation. This means that the functions Ω and V are the solutions of the same basic equation. Based on this analogy, it is shown that an electrolytic tank can be constructed to determine the function , Ω experimentally(29).

However, it must be mentioned that since these analogies place the reef plane in an infinite medium, therefore, the closure distribution obtained can be regarded as an approximation. And for calculation purposes the finite depth elementary components should be used in the course of integration or summation (27).

The Coordinate System and the boundary conditions of the Electrolytic tank: Consider an electrolytic tank with the rectangular coordinate system X_1, Y_1, Z_1 and the linear dimensions of the tank be of the ratio of L_1/L_2, where L_1 is the linear distance in terms of the tank coordinates and L_2 in terms of the mine coordinates. Now if the voltages as shown in Figure A-3 are imposed on the electrodes, the boundary conditions of the electrolytic tank will be:

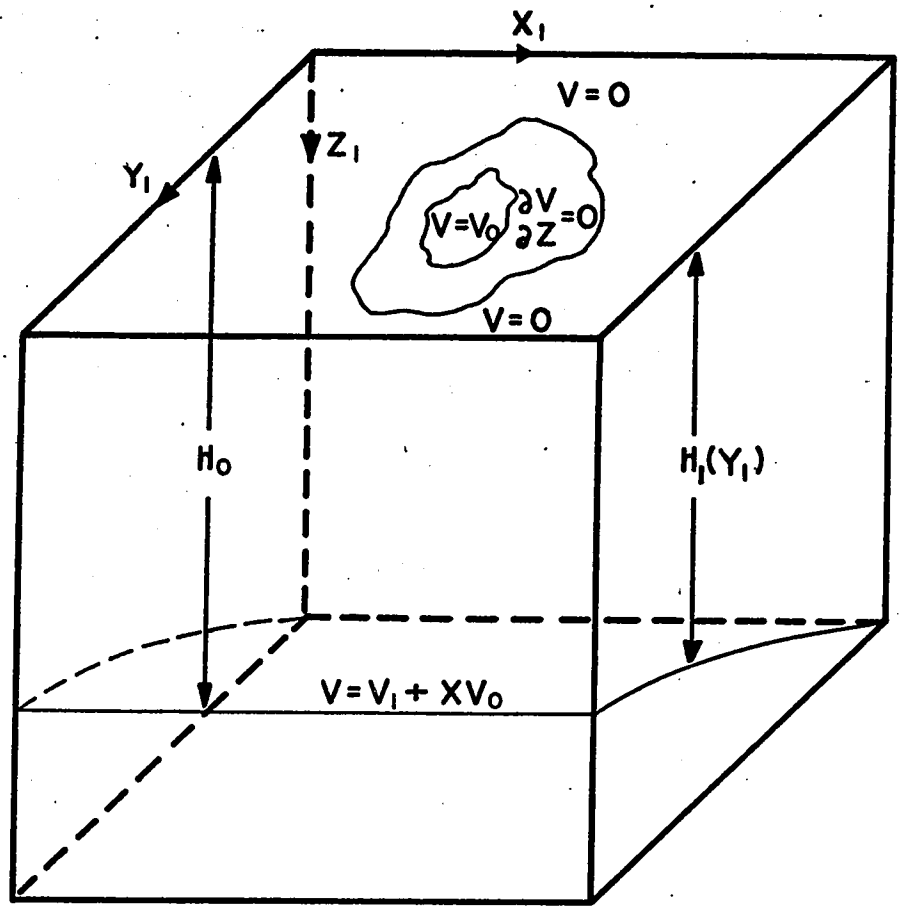

ELECTRICAL ANALOGY OF MINING SITUATION (Ref. 29)

FIGURE A-2

at the level of the top electrode $(Z_1 = 0)$

$$\left.\begin{array}{ll} V = 0 & \text{outside the area of excavations} \\ V = V_o & \text{within the area of excavations where closure is complete} \\ \dfrac{\partial V}{\partial Z_1} = 0 & \text{within the area of excavations where closure is not complete} \end{array}\right\} \quad \text{(A-16)}$$

and at the bottom electrode $(Z_1 = H_1(Y_1)$

$$V = V_1 + x\, V_o \quad .$$

In the Equation (A-16), V is the potential in the tank, $H_1(Y_1)$ is the position of the bottom electrode with respect to top electrode. The condition defined by the voltage gradient $\partial V/\partial Z_1$ in the area where the closure is not complete is the result of electrolyte being in contact with the non-conductor which does not permit any current flow through the surface. It may be noted that in these conditions, the tank voltage gradient $\partial V/\partial Z_1$ is proportional to current density in the Z_1 direction.

The analogy is complete, provided the potential, V is analogous to the function, Ω, at the reef plane ($z = 0$). To achieve this condition let the potential, V in the tank be divided into two components, V' representing the disturbance imposed by the modelled opening on the linear voltage distribution represented by the component $V_1(Z_1/H_1(Y_1))$. Therefore ,

$$V = V' + C \qquad \text{(A-17)}$$

where $C = V_1 Z_1 / H_1(Y_1)$.

In Equation (A-17) the function V' will satisfy the Laplace's equation $\nabla^2 V' = 0$, provided

$$\nabla^2 (Z_1 / H_1(Y_1)) = 0 \qquad \text{(A-18)}$$

However, at $Z = 0$, plane this condition is satisfied therefore,

$$V = V' \qquad \text{(A-19)}$$

The problem now reduces to the form where it is necessary to show the analogy between Ω and V' (because at $Z_1 = 0$ the second term in the Equation (A-17) is equal to zero).

Introducing the relationship given by Equation (A-17), the boundary conditions of Equation (A-16) will take the following form:

at the level of top electrode $(Z_1 = 0)$

$$\left.\begin{array}{ll} V' = 0 & \text{outside the area of excavations} \\ V' = V_o & \text{within the area of excavations where the closure is complete} \\ \dfrac{\partial V'}{\partial Z_1} = -\dfrac{V_1}{H_1(Y_1)} & \text{within the excavated area where the closure is not complete} \end{array}\right\} \qquad \text{(A-20)}$$

and at the bottom electrode $(Z_1 = H_1(Y_1))$

$$V' = x\, V_o \quad .$$

The problem is now reduced to the form where a relationship between V and Ω can be found, and their respective boundary conditions can be made identical.

Let,

$$\Omega = - \frac{H_o}{V_1} \frac{L_2}{L_1} V' \qquad \text{(A-21)}$$

$$\Omega_o = \frac{H_o}{V_1} \frac{L_2}{L_1} V_o$$

and the linear relationship between the mine and tank coordinates be:

$$x(\text{mine}) = \frac{L_2}{L_1} X_1(\text{tank}), \quad y = \frac{L_2}{L_1} Y_1(\text{tank}) \qquad \text{(A-22)}$$

$$z(\text{mine}) = \frac{L_2}{L_1} Z_1(\text{tank})$$

The transformed boundary conditions defining the situation in terms of Equation(A-21) will be:

at the level of the top electrode $(Z_1 = 0)$

$$\left.\begin{array}{ll} V' = 0 & \text{outside the excavated area,} \\ V' = \frac{V_1}{H_o} \frac{L_1}{L_2} \Omega_o = V_o & \text{within the excavated area where closure is complete,} \\ \frac{\partial V'}{\partial Z_1} = - \frac{V_1}{H_o} \left(1 + B \frac{Y_1}{L_1}\right) & \text{within the excavated area where closure is not complete} \end{array}\right\} \qquad \text{(A-23)}$$

and at infinity $(Z_1 = \infty)$

$$V' = x\, V_o \; .$$

In the Equations (A-21) and (A-22), H_o is the depth of the tank at any chosen origin.

Equation (A-20) defines the boundary conditions for V' derived from the tank and Equation (A-23) defines the boundary conditions derived from the mining problem. If the two sets of boundary conditions are made identical, the tank will correctly simulate the mining problem. On observing the Equations (A-20) and (A-23) this seems to be the case on the plane ($Z_1 = 0$) except in the area where closure is not complete. However, the condition in that zone can be identical, provided

$$\frac{V_1}{H_1(Y_1)} = \frac{V_1}{H_o}\left(1 + B\,\frac{Y_1}{L_1}\right)$$

or

$$H_1(Y_1) = \frac{H_o}{1 + B\,\dfrac{Y_1}{L_1}} \qquad \text{(A-24)}$$

Equation (A-24) defines the position of the curved bottom electrode (Figure A-2) and also satisfies the condition imposed by Equation (A-18).

From Equations (A-19) and (A-21), it follows that the function Ω at the $z = Z_1 = 0$ plane is related to the potential in the tank in the following form:

$$\Omega = -\frac{H_o}{V_1}\,\frac{L_2}{L_1}\,V \qquad \text{(A-25)}$$

provided, $$V_o = \frac{V_1}{H_o}\,\frac{L_1}{L_2}\,\Omega_o \qquad \text{(A-26)}$$

and $$H_1(Y_1) = \frac{H_o}{1 + B\frac{Y_1}{L_1}} \qquad \text{(A-27)}$$

The finite depth of the tank is the only discrepancy between two sets of boundary conditions defining V', but such an error can be kept at a minimum by arranging that the tank depth is large in comparison to the dimensions of the modelled mining area. These requirements will be discussed in the chapter dealing with the construction of the tank.

In simulating a horizontal deposit in the tank, the depth $H_1(Y_1)$ given by the Equation (A-27) is constant and equal to H_o, the maximum depth of the tank.

The curvature of the bottom electrode in case of inclined deposits is convex upwards (31) and not concave as published earlier (29).

Thus, the preceeding discussion has shown that the function Ω can be obtained experimentally in terms of the potential V. Equation (A-15) can now be expressed in terms of the potential V and the required formula in the simplest form (31) is

$$\delta_w = - NS_o \iint_{EA} V(x_1,y_1)\, z_o \left[\frac{2(2-\mu)z_o^2 + (1-2\mu)r^2}{(r^2 + z_o^2)^{5/2}} \right] dx_1 dy_1 \qquad \text{(A-28)}$$

where $N = \frac{S(1 + \mu)}{2\pi E V_1} H' = \text{constant}$

V_1 = the applied voltage to the bottom electrode

S = scale factor

E = Modulus of elasticity of the rock mass

μ = Poisson's ratio

S_o = Normal component of the field stress

$r^2 = (x_o - x_1)^2 + (y_o - y_1)^2$

and H' = distance between top and bottom electrode at the centre.

The above integral may be evaluated by dividing the plane into small grid squares and performing the following simple summation:

$$\delta_w = - NS_o \Sigma V \{\bar{k}\} \qquad \text{(A-29)}$$

where V and $\bar{k}$ are the values at the centre of the grid square. The necessary information regarding the solution of Equation (A-28) or (A-29) is explained in Appendix B-I, and the diagramatic representation of the analogue is shown in Figure 2-3 (see Chapter II).

APPENDIX B-I

The necessary kernels (or functions) to predict the displacements in the solid rock surrounding the mine excavations in an isotropic homogeneous elastic (infinite) medium have been summarized by Ortlepp (31) and are given below.

$$\delta_u (= \mathbb{K}_u) = [2(1 + \mu)z^2 - (1 - 2\mu)r^2]x$$

$$\delta_v (= \mathbb{K}_y) = [2(1 + \mu)z^2 - (1 - 2\mu)r^2]y$$

$$\delta_w (= \mathbb{K}_w) = [2(2 - \mu)z^2 + (1 - 2\mu)r^2]z$$

where $\mathbb{K}_u$, $\mathbb{K}_v$ and $\mathbb{K}_w$ are the components of displacement induced by the normal component, S_o, of the field stress in x,y and z directions respectively.

These functions (or $\mathbb{K}$'s) together with the data obtained from the electric analogue by simulating mine openings, completes the solution for the determination of the displacement components. The simple summation will thus take the form:

$$(\text{Displacement})_{S_o} = - NS_o \Sigma \frac{V\mathbb{K}}{(r^2 + z^2)^{5/2}}$$

where $$N = \frac{(1 + \mu)}{E} \frac{H'S}{V_1 2\pi} = \frac{(1 + \mu)}{E} M \frac{S}{2\pi} ,$$

the factor $M(= H'/V_1)$ is called the analogue constant and S the scale factor.

The mean depth H' is calculated by the Equation (A-27), V_1 is the voltage applied to the bottom electrode and V is the spot voltage at each grid point. The limits on the summation will depend on the grid. For example, if we have a 75 unit square (75 x 75) grid the total summation for each point of reference will be 75 x 75 = 5625 times.

The scale factor S, is a linear relationship between the mine co-ordinates and the tank coordinates. Suppose the mine plan is made 500' to an inch scale and this plan will be accommodated say within the working area, then the scale factor will be 500 x 12:1. In otherwords one unit on the tank will be equal to 6000 times that in mine. If L is the unit mine length and ℓ be the unit tank length, then the scale factor L/ℓ will be 6000/1 or 6000.

The analogue stress constant H'/V_1 is calculated as follows:

Let the applied voltage to the bottom electrode be 10 volts or 10,000 millivolts, and the actual depth, H', between the electrodes of the tank at the centre be 1.35 ft. or 1.35 x 304.8 mm, then

$$M = \frac{H'}{V_1} = \frac{1.35 \times 304.8}{1000} = 0.412$$

Note: 1.) The supply voltage of 10 volts or 10,000 milli-volts to the bottom electrode normally produces values greater than 1.0 volt in the working area and it is convenient to write these into data sheets as 100 mV instead of 1000 mV. Thus for calculation purposes the value of V_1 is 1000 and not 10,000. This is called the apparent supply voltage.

2.) The displacements computed from the analogue data are in terms of milli-meters because all the linear measurements of the tank are in terms of milli-meters and V_1 in milli-volts.

APPENDIX B-II

It has been shown in detail (27) that by making use of relations between displacement, strain and Hooke's law, the elementary strain and stress components can be calculated from displacement components induced by normal closure and by ride. The ride components are considered only in y-direction (dip), assuming that the mining geometry remains unaltered along an axis.

The stress kernels (or functions) for an isotropic homogeneous and elastic medium are given below in the simplified form (31).

1) Due to the normal stress components S_o,

$$K\sigma_x = 3x^2[(1-2\mu)r^2 - 2(2+\mu)z^2] + (r^2 + z^2)x$$

$$x\ [(-1+4\mu)r^2 + (2-2\mu)z^2]$$

$$K\sigma_y = 3y^2\ [(1-2\mu)r^2 - (2+\mu)z^2] + (r^2 + z^2)x$$

$$x\ \ [(-1+4\mu)r^2 + (2-2\mu)z^2]$$

$$K\sigma_z = r^4 + 8r^2z^2 - 8z^4$$

$$K\tau_{xy} = 3xy\ [r^2\ (1-2\mu) - 2z^2\ (2+\mu)]$$

$$K\tau_{yz} = -\ 3yz\ [r^2-4z^2\ ]$$

$$K\tau_{zx} = -\ 3zx\ [r^2-4z^2\ ]$$

2) Due to the shear stress component S_t'

$$K\sigma'_x = -3yz[(r^2 + z^2)(1 - 2\mu) - 5x^2]$$

$$K\sigma'_y = -3yz\,[(r^2 + z^2) - 5y^2]$$

$$K\sigma'_z = -3yz\,[(r^2 + z^2) - 5z^2]$$

$$K\tau'_{xy} = -3xz\,[(r^2 + z^2) - 5y^2)]$$

$$K\tau'_{yz} = (r^2 + z^2)[(r^2 + z^2) + (r^2 + z^2 - 3x^2)] - 15y^2z^2$$

$$K\tau'_{zx} = 3xy\,[(r^2 + z^2) - 5z^2]$$

The sample summation formulae are:

$$(\text{Stress})_{S_o} = M_1 S_o \;\Sigma\; \frac{V\,K}{(r^2 + z^2)^{7/2}}$$

$$(\text{Stress})_{S_t'} = M_1 S_t' \;\Sigma\; \frac{V\,K'}{(r^2 + z^2)^{7/2}}$$

where $M_1 = \dfrac{H'}{V_1\ 2\pi}\ \dfrac{XX}{\ell}$ (XX being grid size, i.e. whether 60,75 or 90, depends on the size of the working area) and ℓ is the total length of the square working area in mm.)

$\frac{H'}{V_1}$ has been defined previously as analogue stress constant equal to M, thus

$$M_1 = \frac{1}{2\pi} \frac{XX}{\ell} M .$$

The calculations of the displacements or stresses require the normal and shear stress components (S_o and S'_t) of the pre-mining stress field oriented to the reef plane. This is achieved by the following formulae or by Mohr circle, provided the constant σ_z , the dip of the reef, i, and the k are known.

$$S_o = \sigma_z (k \sin^2 i + \cos^2 i)$$

$$S'_t = \sigma_z (1-k) \sin i \cos i .$$

APPENDIX B-III

Calculation of Induced Principal Stresses:

The principal stresses can be calculated from the stress components by solving the following cubic equation. The detailed analysis of the stresses in three-dimensions is given elsewhere (72,73).

$$\text{Let } \sigma_x = (\sigma_x)_p + (\sigma_x)_Q$$

$$\sigma_y = (\sigma_y)_p + (\sigma_y)_Q$$

$$\sigma_z = (\sigma_z)_p + (\sigma_y)_Q$$

$$\tau_{xy} = (\tau_{xy})_p + (\tau_{xy})_Q$$

$$\tau_{yz} = (\tau_{yz})_p + (\tau_{yz})_Q$$

$$\tau_{zx} = (\tau_{zx})_p + (\tau_{zx})_Q$$

where the subscript P and Q stand for the stress components induced by S_o and S'_t respectively.

Therefore,

$$\sigma^3 - (\sigma_x + \sigma_y + \sigma_z)\sigma^2 + (\sigma_x\sigma_y + \sigma_y\sigma_z + \sigma_z\sigma_x - \tau^2_{xy} - {}^2_{yz} - \tau^2_{zx})\sigma -$$

$$- (\sigma_x\sigma_y\sigma_z - \sigma_x\tau^2_{yz} - \sigma_y\tau^2_{zx} - \sigma_z\tau^2_{xy} + 2\,\tau_{xy}\tau_{yz}\tau_{zx}) = 0 .$$

The roots of this cubic equation are real and are the principal stresses $\sigma_1 \cdot \sigma_2$ and σ_3. The planes on which the principal stresses act are the principal planes. For each value of σ the direction cosines are found by solving the following equations.

$$\cos(\sigma_i, x) = \frac{A_i}{\sqrt{A_i^2 + B_i^2 + C_i^2}}$$

$$\cos(\sigma_i, y) = \frac{B_i}{\sqrt{A_i^2 + B_i^2 + C_i^2}}$$

$$\cos(\sigma_i, z) = \frac{C_i}{\sqrt{A_i^2 + B_i^2 + C_i^2}}$$

where $A_i = (\sigma_y - \sigma_i)(\sigma_z - \sigma_i) - \tau_{zy}\tau_{yz}$

$B_i = (\tau_{yz}\tau_{xz} - \tau_{xy}(\sigma_z - \sigma_i)$

$C_i = \tau_{xy}\tau_{yz} - \tau_{xz}(\alpha_y - \sigma_i)$

and i stands for the three roots of the cubic equation.

Since the principal stresses on the principle planes remain unaltered by changes in coordinate systems, therefore the coefficients of the cubic equation are invariants which will remain constant under any transformation of the coordinate system (72).

Thus the three-invariants of the six cartesian components of stress are,

$$I_1 = \sigma_x + \sigma_y + \sigma_z$$

$$I_2 = \sigma_x\sigma_y + \sigma_y\sigma_z + \sigma_z\sigma_x - \tau^2_{xy} - \tau^2_{yz} - \tau^2_{zx}$$

$$I_3 = \sigma_x\sigma_y\sigma_z - \sigma_x\tau^2_{yz} - \sigma_y\tau_{zx} - \sigma_z\tau^2_{xy} + \tau_{xy}\tau_{yz}\tau_{zx} \quad .$$

The cubic equation can now be written in a more general form as

$$\sigma^3 - I_1\,\sigma^2 + I_2\,\sigma - I_3 = 0.$$